European Organisation for Astronomical Research in the Southern Hemisphere

Programme: VLT

Project/WP: 15000 VLT Interferometer (VLTI)

Interface Control Document between VLTI and its Instruments (Part I)

Document Number: ESO-045686

Document Version: 7

Document Type: Interface Control Document (ICD)

Released On: 2022-04-06

Document Classification: ESO Internal [Confidential for Non-ESO Staff]

Prepared by: Schuhler, Nicolas

Validated by: Stephan, Christian

Approved by: Kaufer, Andreas

Name

Authors

Name	Affiliation
Nicolas Schuhler	DoO – MSE - SAO

Change Record from previous Version

Affected Section(s)	Changes / Reason / Remarks

Contents

1. Introduction

1.1 Scope

This document describes the interfaces offered by the VLTI infrastructure in the VLTI complex and to the VLTI instruments. In some cases, the instruments may be interfaced to the VLTI in other locations than in the VLTI complex. In those cases, dedicated documents exist.

The SW interface between the VLTI and its instruments is also described in a specific document, AD7.

1.2 Definitions, Acronyms and Abbreviations

This document employs several abbreviations and acronyms to refer concisely to an item, after it has been introduced. The following list is aimed to help the reader in recalling the extended meaning of each short expression:

ACP	Alarm Connection Point
ARAL	ARtificial source and ALignment
ASM	Astronomical Site Monitor
AT	Auxiliary Telescope
BC	Beam Compressor
CAS	Central Alarm System
CCL	Combined Coudé Laboratory
DL	Delay Lines
DDL	Differential Delay Lines
EMC	ElectroMagnetic Compatibility
IC	Interferometric Complex
ISS	Interferometer Supervisor Software
IT	Information Technology
LAN	Local Area Network
OBE	Operating Basis Earthquake
OPD	Optical Path Difference
OPL	Optical Path Length
MLE	Maximum Likely Earthquake
NTP	Network Time Protocol
PSD	Power Spectral Density
RMN	Reflective Memory Network
SCP	Service Connection Point
TBC	To Be Clarified
TBD	To Be Defined
TIM	Time Interface Module
TMP	Turbo Molecular Pump
UPS	Uninterruptible Power Supply
UT	Unit Telescope
UTC	Coordinated Universal Time
VCM	Variable Curvature Mirror
VIBMET	VIBration METrology
VLTI	Very Large Telescope Interferometer

2. Related Documents

2.1 Applicable Documents

The following documents, of the exact version shown, form part of this document to the extent specified herein. In the event of conflict between the documents referenced herein and the content of this document, the content of this document shall be considered as superseding.

AD references shall be specific about which part of the target document is the subject of the reference.

AD1 VLTI Combined Coude Lab Layout;

ESO-324805 Version 2 / CAD-117412 Version 8

AD2 VLT Environmental specification;

ESO-038327 Version 6

AD3 Service Connection Point Technical Specification;

ESO-222131 Version 5

AD4 Technical Specification Electrical and electronics design;

ESO-044295 Version 4

AD5 Paranal Instrument Interface Document;

ESO-043721 Version 4

AD6 VLT Paranal Network / Computers / Consoles – Design Description;

ESO-043663 Version 11

AD7 ICD between the VLTI Supervisor Software and VLTI Instrumentation Software;

ESO-045837 Version 7

AD8 Time Interface Module Hardware Manual;

ESO-041682 Version 3

AD9 Change Control Board;

ESO-216822 Version 2

AD10 VLTI 2nd Generation Interferometer Supervisory Software Design;

ESO-266537 Version 1

AD11 Vacuum and Cryogenics Standards Components;

ESO-046147 Version 5

2.2 Reference Documents

The following documents, of the exact version shown herein, are listed as background references only. They are not to be construed as a binding complement to the present document.

RD1 *Astronomical Site Monitor Data User Manual;*
ESO-281474 Version 3

RD2 *VLT Time Reference System Specification;*
ESO-222615 Version 1

RD3 *VLT Central Time Standard, Manual;*
ESO-041621 Version 3

RD4 *Implementation of an Alarm System for the Paranal Observatory;*
ESO-044519 Version 1

RD5 *VLTI Laser Interlock System;*
ESO-276858 Version 1

RD6 *VLTI Supervisor Software – User and Maintenance Manual;*
ESO-285966 Version 3

RD7 *STS-AT #1 STS Commissioning Test Report;*
ESO-262932 Version 1

RD8 *Image Scale and Pupil Size AT1;*
VLTI-105

RD9 *VLTI PRIMA Star Separator Control Software System Design Description;*
ESO-047588 Version 4

RD10 *VLTI Complex and UT Coudé Oxygen Sensor Network;*
ESO-325005 Version 1

3. Interface definition and overview

3.1 Interface definition

The interface specified in this document is located between the VLTI infrastructure and the VLTI instruments inside the VLTI complex (Section 3.4). Some instruments might be interfaced to the VLTI infrastructure in some other locations like the Auxiliary Telescopes or the Unit Telescope coudé room. In those cases, other dedicated documents specify the interfaces.

This document considers the following types of interfaces:

- Environmental interfaces describing:
  - The atmospheric conditions one can expect when observing with the VLTI
  - The seismic conditions the instrument is exposed to in Paranal
  - The conditions such as temperature, humidity and pressure that the instrument will be exposed to inside the VLTI complex.
- Mechanical interfaces defining:
  - The different locations in the VLTI complex and the volumes allocated for visitor instruments. The layout of these locations is described in AD1.
- Fluid interfaces defining:
  - The type and location of the connections to the cooling liquid distribution system and the characteristics of the coolant.
  - The type and location of the connections to the compressed air distribution system and the characteristics of the air.
- Electrical interfaces defining:
  - The type and location of the connections to the power distribution system.
  - The characteristics of the distributed power.
- Communication interfaces defining:
  - The type of the connections to the Local Area Network (LAN)
  - The type of the connections to and the characteristics of the two distributed time network
  - The type of the connections and the characteristics of the Reflective Memory Network (RMN)
  - The type, location and usage of the connections to the VLTI complex optical fibre network infrastructure.
- Interfaces to the cable routing infrastructure defining:
  - The location and usage of the feedthroughs between different rooms.
  - The location and usage of the cable tray network existing in each room.
- Optical interfaces defining:
  - The position and characteristics of the beams delivered by the VLTI inside the VLTI laboratory.

- Interfaces to the safety systems defining:
  - The type, location and usage of the connections to the Central Alarm System (CAS).
  - The type, location and usage of the connections to the VLTI Laser Interlock System.
- Software interfaces defining:
  - The communication to the Interferometer Supervisor Software (detailed in a dedicated document, AD7).
  - The usage of the Reflective Memory Network.

3.2 Interface management

All the interfaces defined in this document are under the responsibility of the VLTI Paranal System Engineer. Any change must be first discussed and approved by the VLTI Paranal System Engineer and VLTI Paranal System Scientist prior to be submitted to the Paranal Change Control Board, AD9.

3.3 u, v, w coordinate system

A Cartesian coordinate system with the UV plane defined by the telescope platform on Paranal, the U-axis parallel to the rails of the delay lines and the zero-point (located between UT1 and UT2) measured in WGS84 coordinates:

- Latitude: 24.62743941° S
- Longitude: 70.40498689° E
- Height above geoid: 2669 m

This coordinate system is used to position all the VLTI elements such as mirrors, optical tables, telescope stations, …

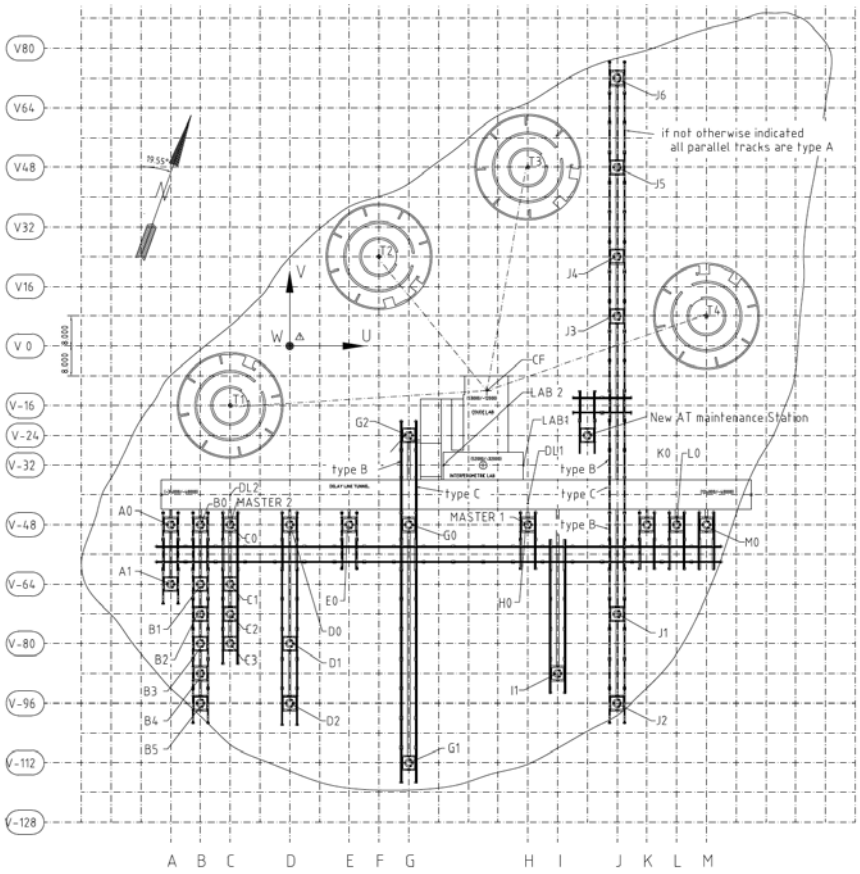

Figure 1: Paranal site layout in the uvw reference coordinate system. The origin of the coordinate system is indicated between UT1 and UT2.

3.4 VLTI complex

The VLTI complex is located at the centre of the Paranal platform. The rooms with a scientific purpose are all located underground. In this document we will consider:

- the VLTI Laboratory (IC108).
- the VLTI Tunnel (IC109).
- the Combined Coude Laboratory (IC107).
- the VLTI Storage room (IC104).
- the VLTI Computer room (IC102).

Figure 2: Paranal platform - the VLTI complex is shown in red, it includes the tunnel in red dashed line.

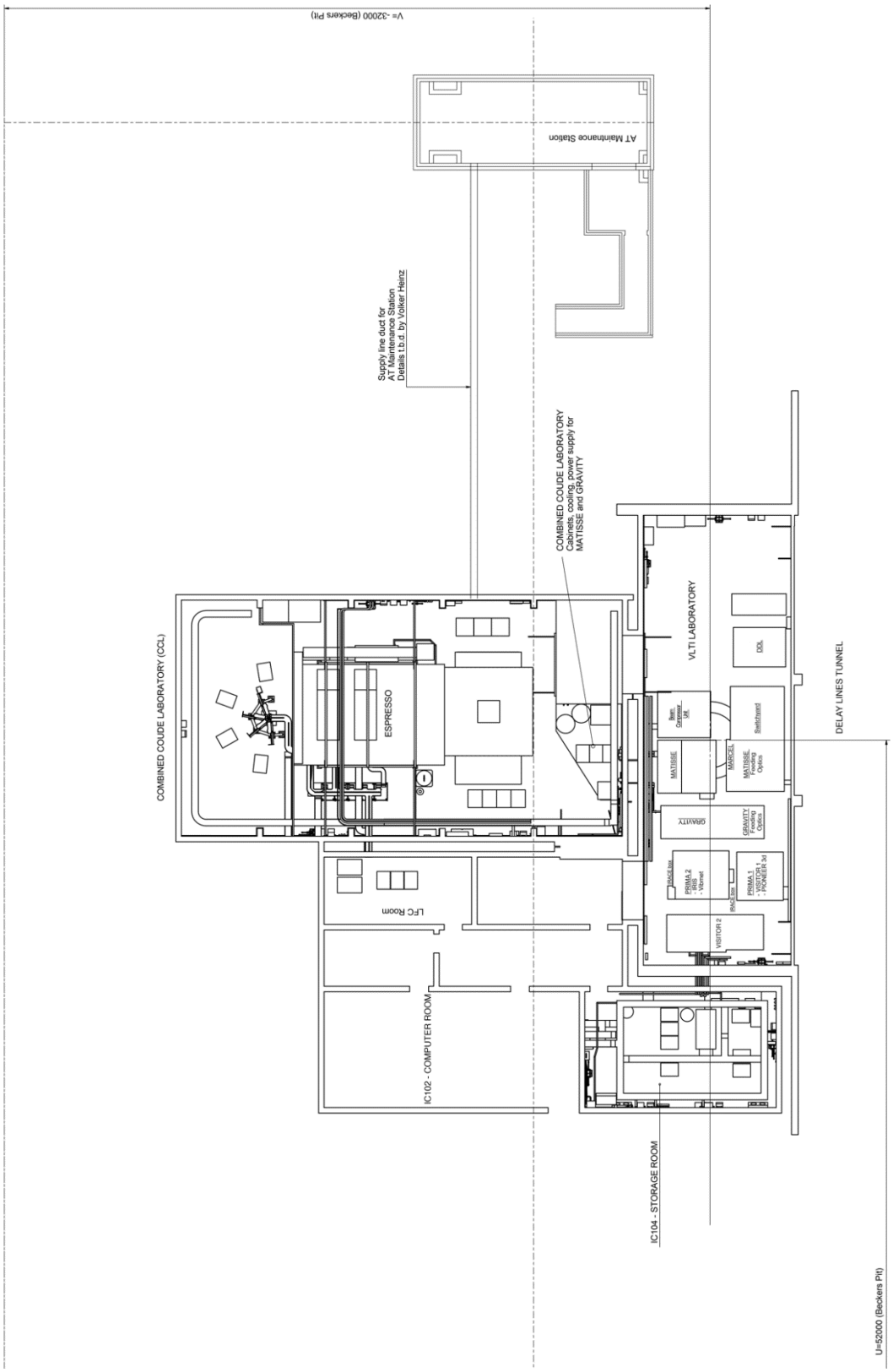

Figure 3: layout of the VLTI Complex basement level.

4. Interface between the VLTI complex environment and the instruments

4.1 Site seismic conditions

There are two main aspects of seismicity to be considered by the VLTI instruments:

1. The micro seismicity in terms of intensity and frequency of occurrence, related to:

   a. Design requirements which have to be defined for all instruments in order to assure a low sensitivity to the frequent micro-seismic events.

   b. Disturbances during observation (e.g. OPD jitter) produced mainly by the responses of the telescope structures to the micro seismic noise.

2. The frequent earthquakes which instruments are required to withstand without damage.

4.1.1 Micro seismicity

The seismicity of the Paranal site is best characterized by the Gamma-Frequency law, as shown in the following .

This plot shows the frequency of occurrence of seismic events at Paranal as characterized by the level of ground acceleration they generate. The parameter Γ is the average level of the PSD of the ground acceleration in the frequency range [10-50 Hz]. The Y-axis is the number of events, recorded during the 125 hours of the test period, which exceeded the value Γ. Note that the departure from the straight line at Γ < 100 nano-g/(Hz)$^{1/2}$ is due to the non-completeness of the sample.

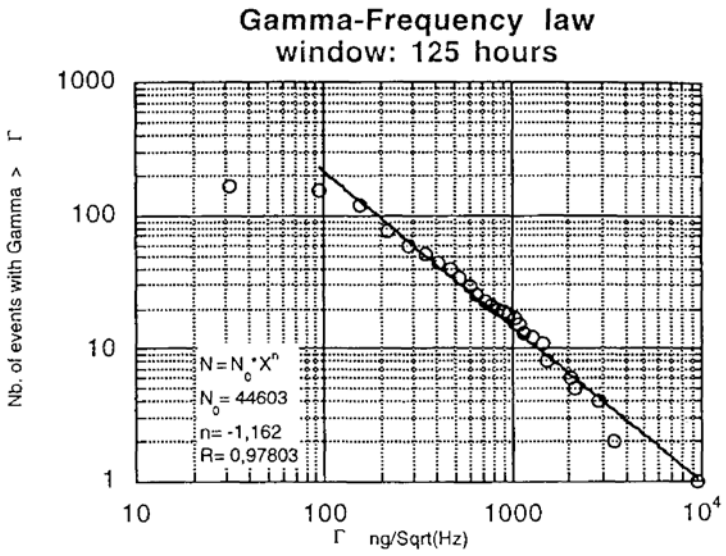

Table 1: gamma-frequency law.

4.1.2 Earthquakes

Two earthquake types are defined:

1. Operating Basis Earthquake (OBE): moderate earthquakes of a magnitude up to Mg 7.75 (Richter scale) with a high probability of occurrence in the lifetime of the observatory.
2. Maximum Likely Earthquake (MLE): an earthquake of large amplitude but with lower probability of occurrence during the lifetime of the observatory.

The characteristics of these earthquakes are summarized in the following table.

	OBE	MLE
Peak horizontal acceleration [g]	0.24	0.34
Probability of exceeding [%]	50	10
Repetition period [years]	25	100
Magnitude [Richter scale]	7.75	8.5
Hypocentral distance [km]	100	150
Duration [s]	65	200

Table 2: characteristics of the Operating Basis Earthquake and of the Maximum Likely Earthquake.

The type and frequency of Earthquakes are given in more detail in AD2.

4.2 Paranal atmosphere

The Paranal observatory is equipped with a set of tools to characterize the environmental conditions and atmosphere at the observatory, RD1. We summarize in this section statistics of the most important parameters.

4.2.1 Ambient temperature

Statistics of the ambient air temperature measured at 2 m above the platform level are given in Table 3. The time series is plotted in Figure 4 and the histogram and cumulative histogram distribution in Figure 5. The statistics have been obtained over 3 years of data.

A histogram of the gradient of the temperature in ° Celsius per hour is given in Figure 6.

	Temperature (° C)		Gradient (° C/ hour)
	Day	Night	
Mean	14.3	12.7	0.0
Std	2.8	2.8	0.7
1 % Quantile	6.1	4.5	-1.8
5 % Quantile	9.2	7.5	-1.1
50 % Quantile	14.6	13.1	0
95 % Quantile	18.3	16.6	1.1
99 % Quantile	20.2	18.2	1.7

Table 3: statistics of the ambient air temperature 2 m above the platform.

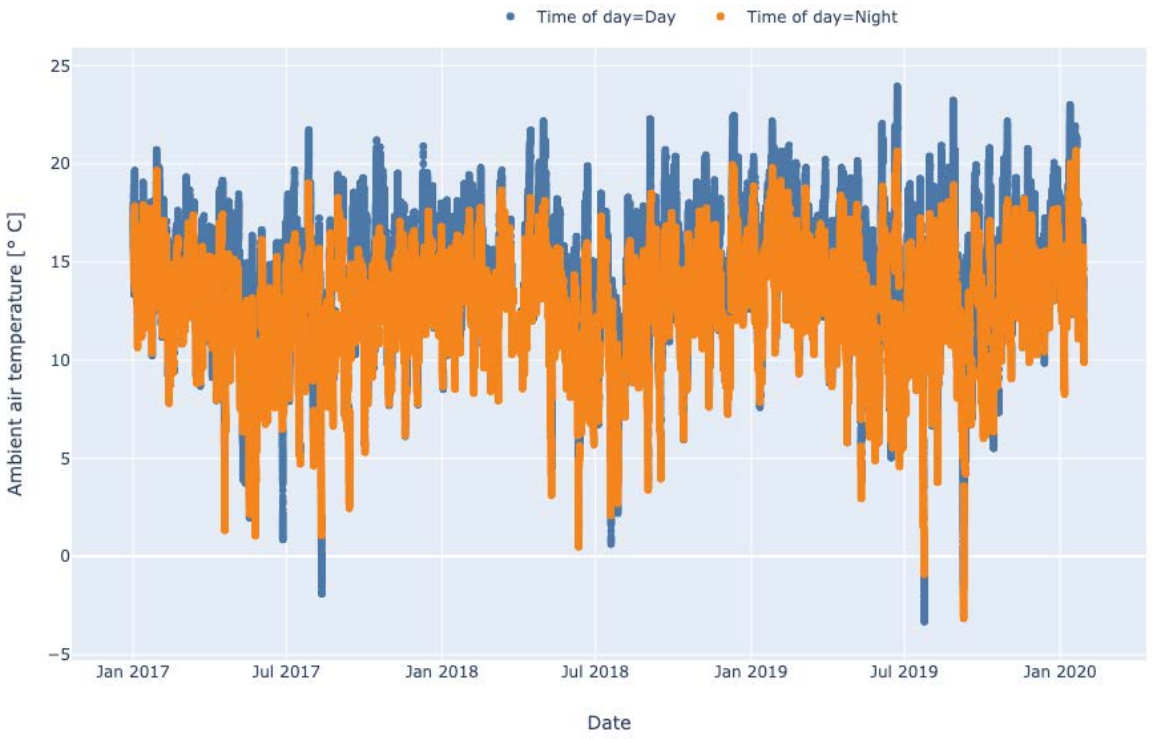

Figure 4: ambient air temperature 2 m over the platform.

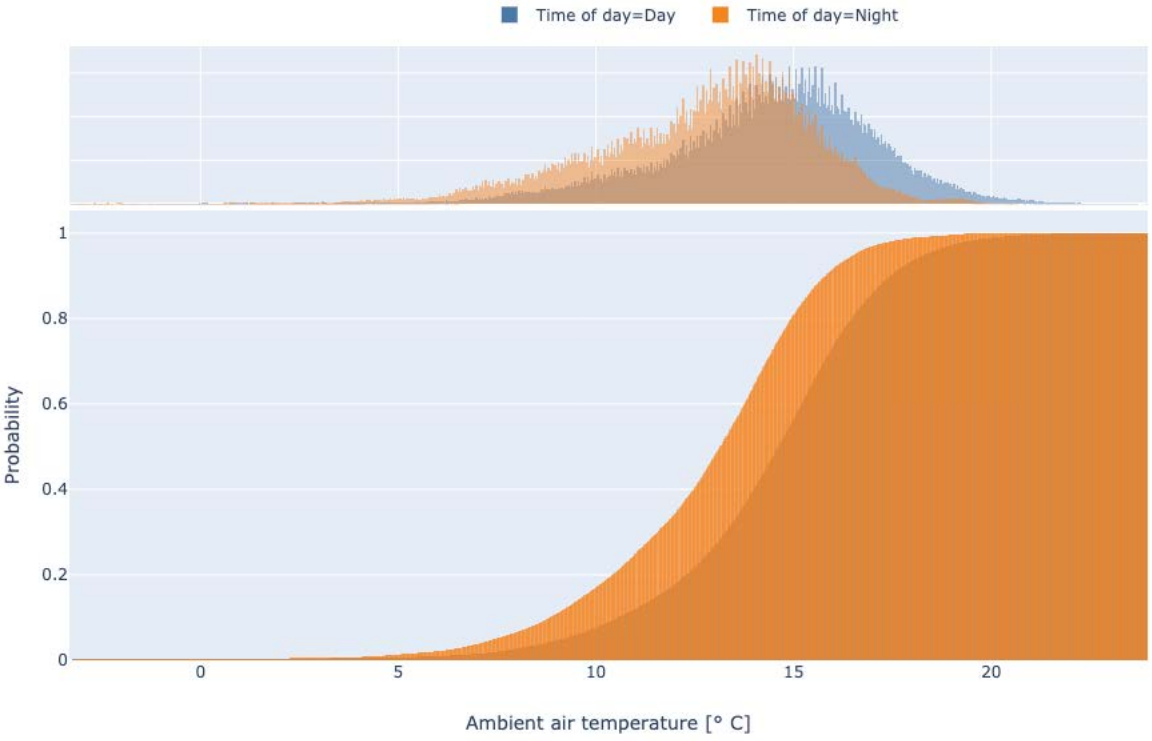

Figure 5: histogram (top) and cumulative histogram (bottom) of the ambient air temperature over three years of data.

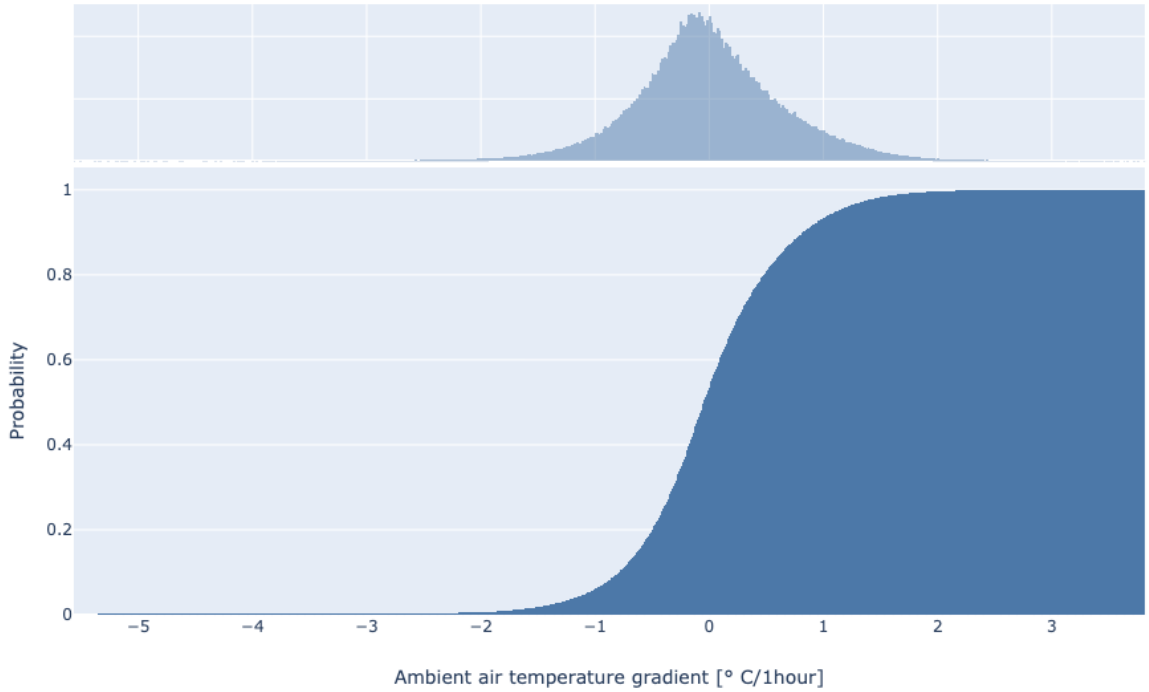

Figure 6: histogram (top) and cumulative histogram (bottom) of the distribution of the gradient of the ambient air temperature (during day or night).

4.2.2 Pressure

Statistics of the atmospheric pressure measured by the ASM are given in **Error! Reference source not found.**. The time series is plotted in Figure 7 and the histogram and cumulative histogram in Figure 8. The statistics have been obtained over 3 years of data.

	Pressure (hPa)		Gradient (hPa / hour)
	Day	Night	
Mean	744.1	743.9	0
Std	2.2	2.2	2.4
1 % Quantile	740.5	740.2	-0.7
5 % Quantile	741.7	741.4	-0.5
50 % Quantile	744.1	744.0	0.0
95 % Quantile	746.2	746.0	0.5
99 % Quantile	747.2	746.9	0.7

Table 4: statistics of the atmospheric pressure measured by the ASM.

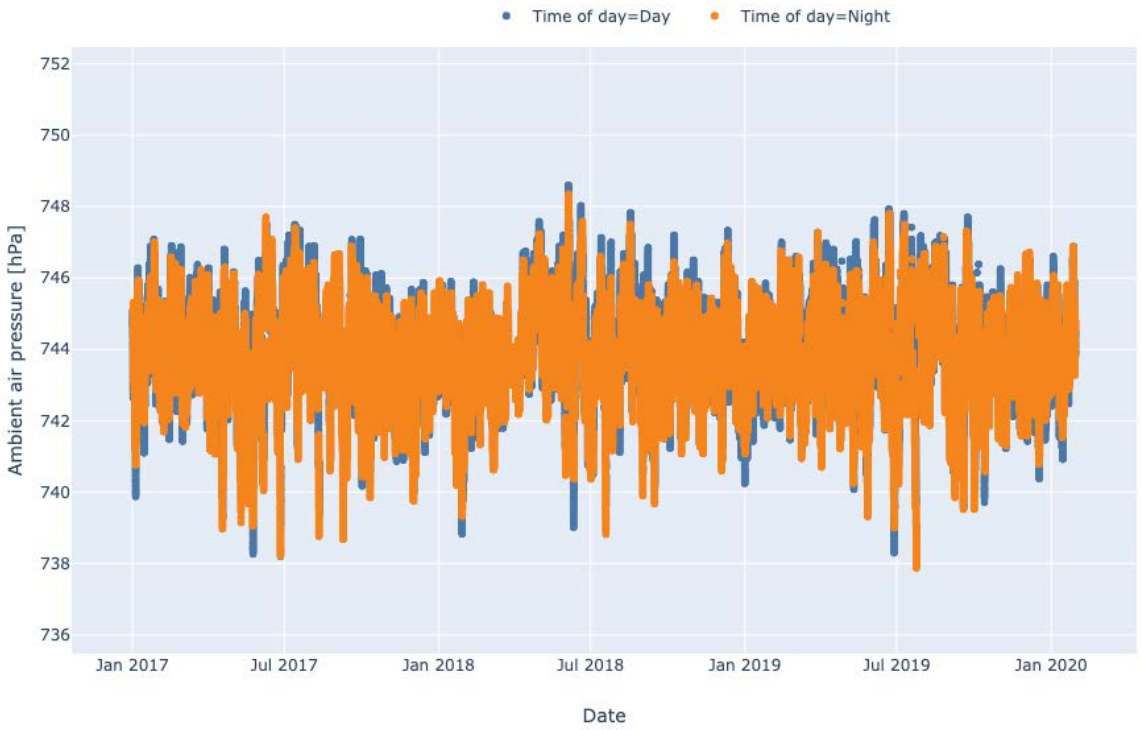

Figure 7: ambient air pressure measured by the ASM.

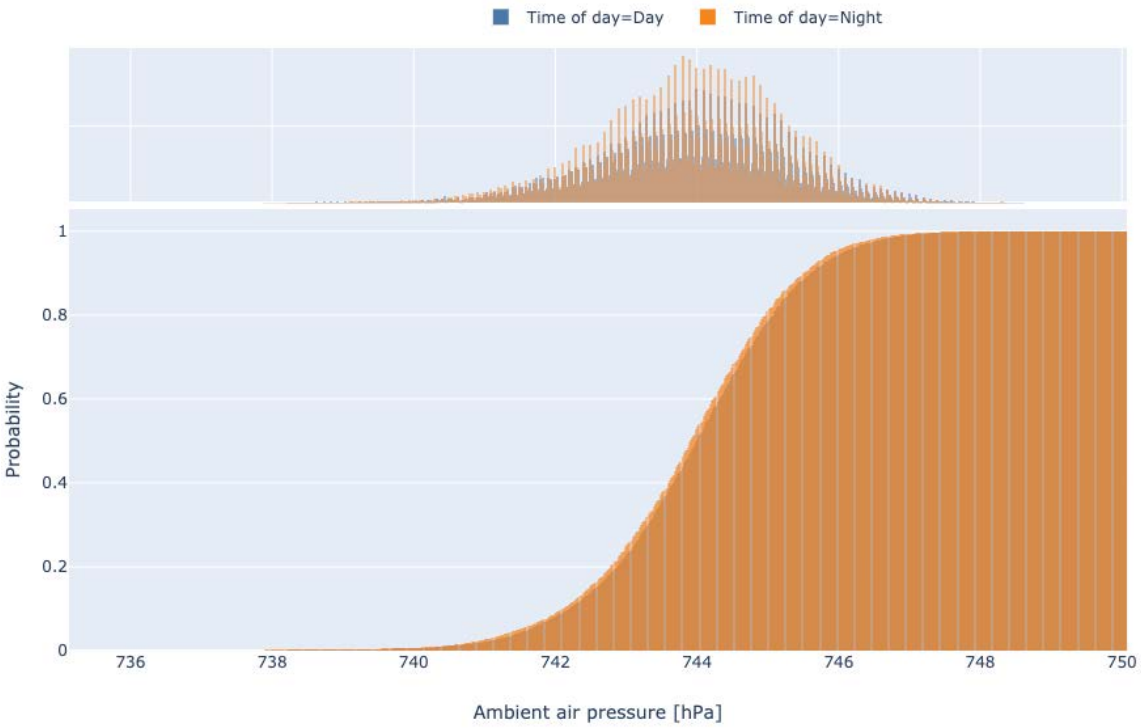

Figure 8: histogram (top) and cumulative histogram (bottom) of the ambient air temperature.

4.2.3 Relative humidity

Statistics of the atmospheric relative humidity measured at 2 m above the platform level are given in Table 5. The time series over 3 years is plotted in Figure 9.The histogram and cumulative histogram are plotted in Figure 10.

A histogram of the gradient of the temperature in ° Celsius per hour is given in Figure 11.

	Relative humidity (%)		Gradient (% / hour)
	Day	Night	
Mean	17.5	16.0	0.03
Std	13.8	13.7	3.7
1 % Quantile	3.0	3.0	-11.5
5 % Quantile	4.0	3.0	-5.5
50 % Quantile	13.0	11.5	0.0
95 % Quantile	48.0	45.5	5.5
99 % Quantile	67.0	66.5	11.5

Table 5: statistics of the relative humidity 2 m above the platform level.

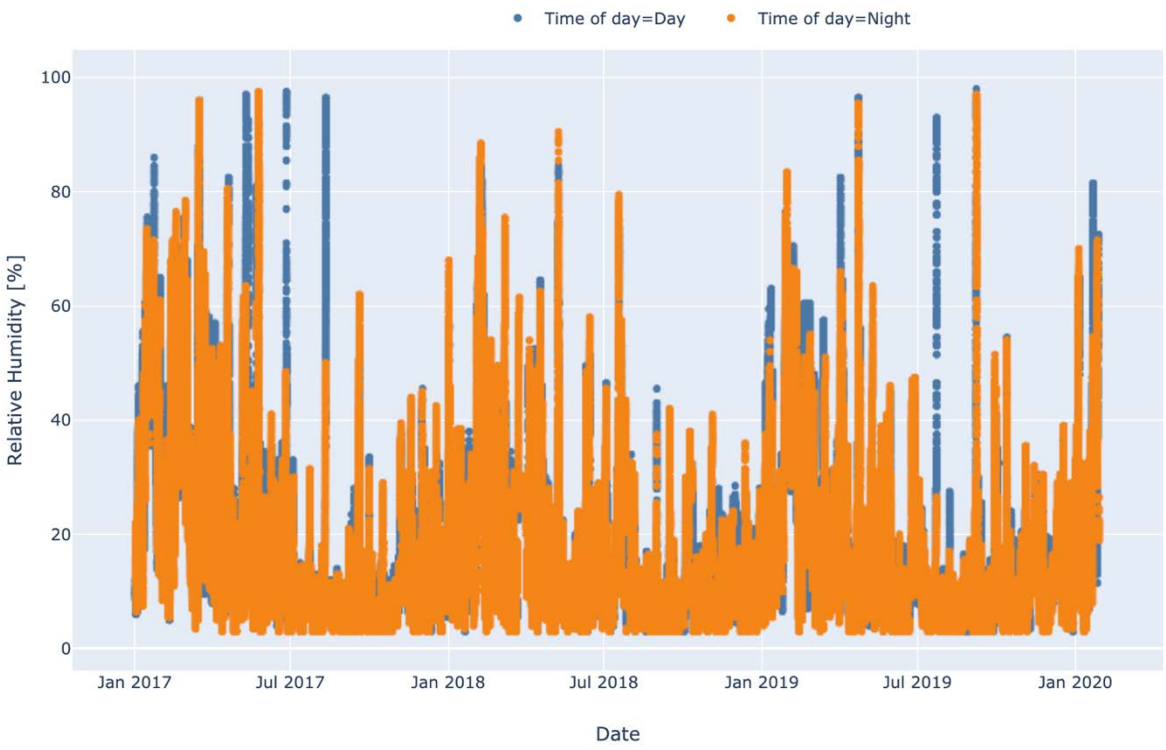

Figure 9: ambient air relative humidity at 2 m above the platform as measured by the ASM.

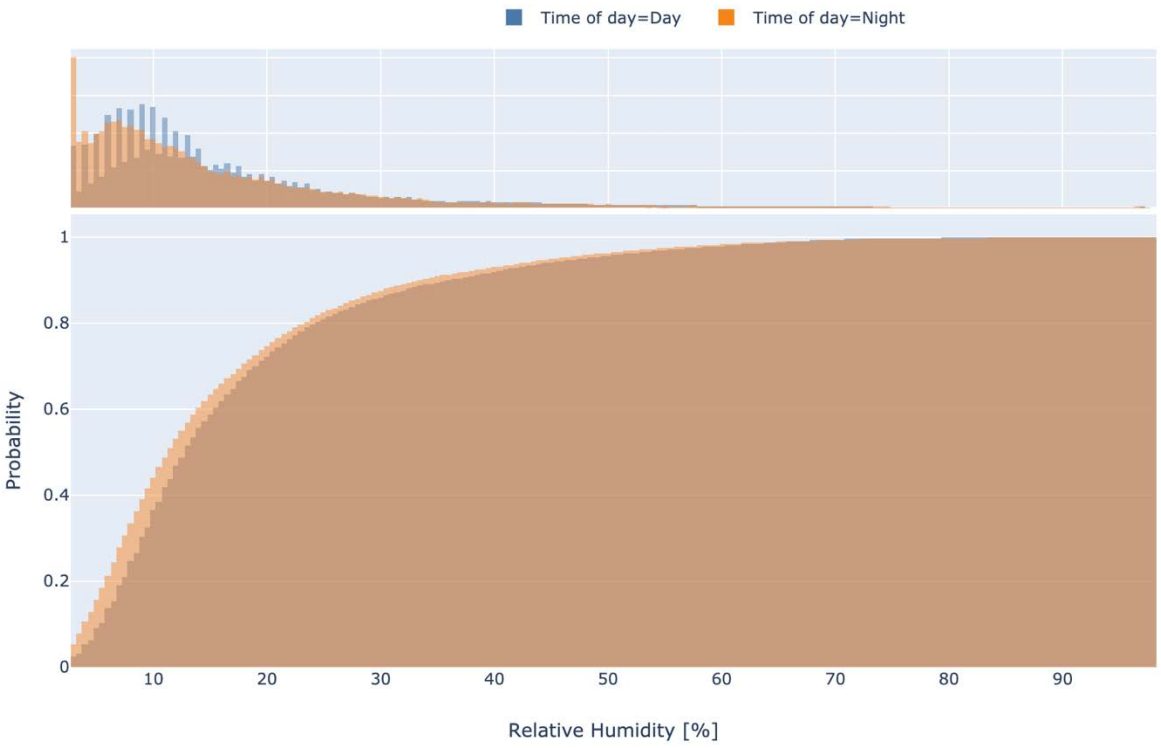

Figure 10: histogram (top) and cumulative histogram (bottom) of the ambient relative humidity content.

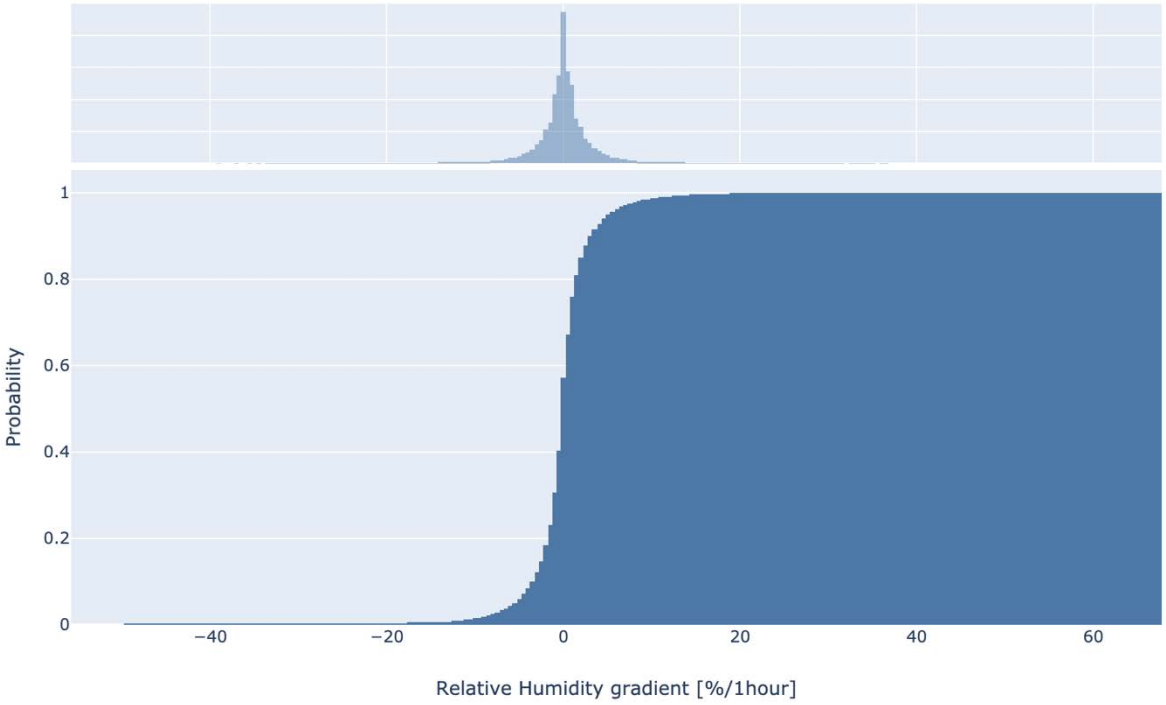

Figure 11: histogram (top) and cumulative histogram (bottom) ambient air relative humidity gradient over one hour.

4.2.4 Wind speed and wind direction

Statistics of the wind speed (1 minute average) measured by the ASM at 10 m above the platform level are given in Table 6. The times series over three years is plotted in Figure 12. The distribution and cumulative histogram are plotted in Figure 13.

The distribution of the wind direction is plotted in Figure 14.

	Wind speed (m / s)	
	Day	Night
Mean	7.1	6.8
Std	4.1	4.2
1 % Quantile	0.85	0.5
5 % Quantile	1.85	1.3
50 % Quantile	6.18	6.0
95 % Quantile	15.3	14.8
99 % Quantile	19.4	18.77

Table 6: statistics of the wind speed measured 10 m above the platform level.

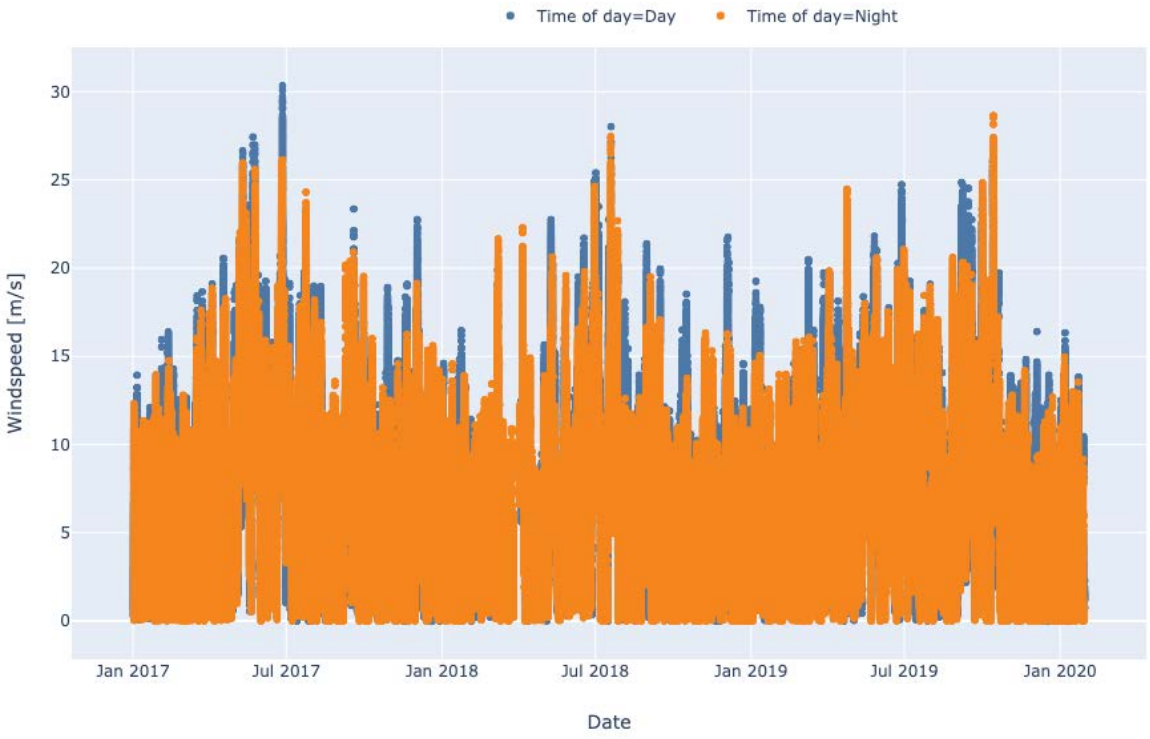

Figure 12: time series of the windspeed (average over 1 minute) measured 10 m above the platform by the ASM.

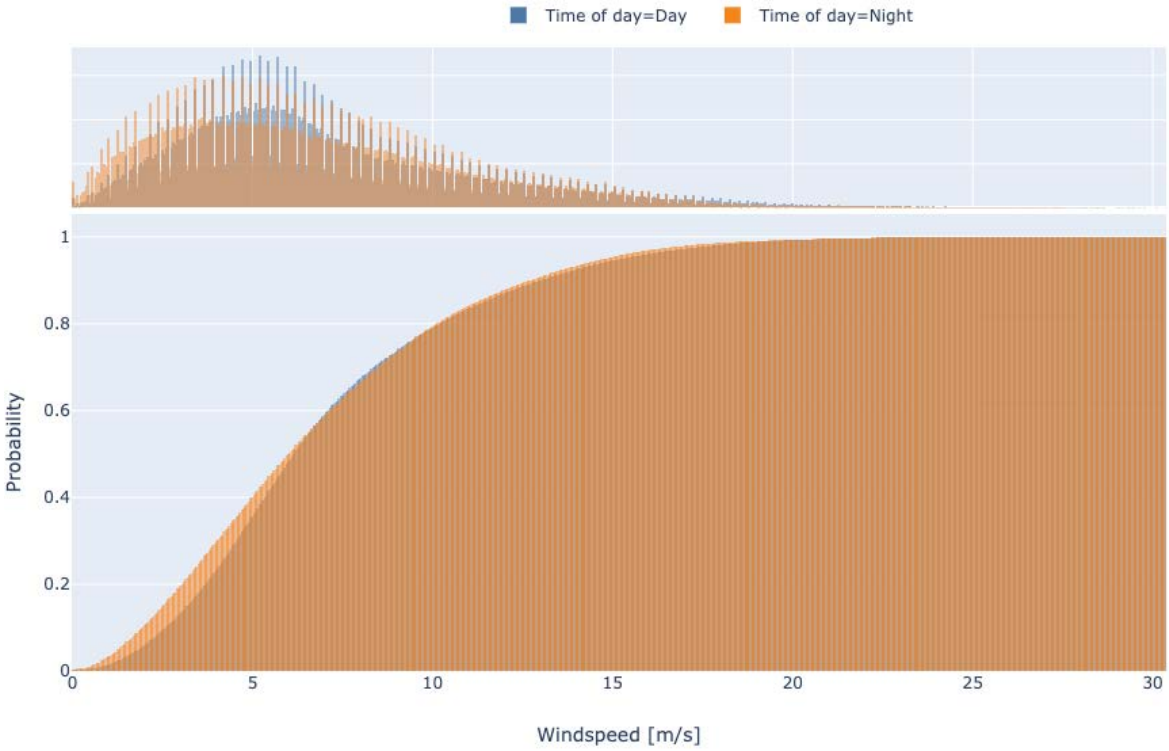

Figure 13: histogram and cumulative histogram of the windspeed (average over 1 minute) measured 10 m above the platform by the AMS.

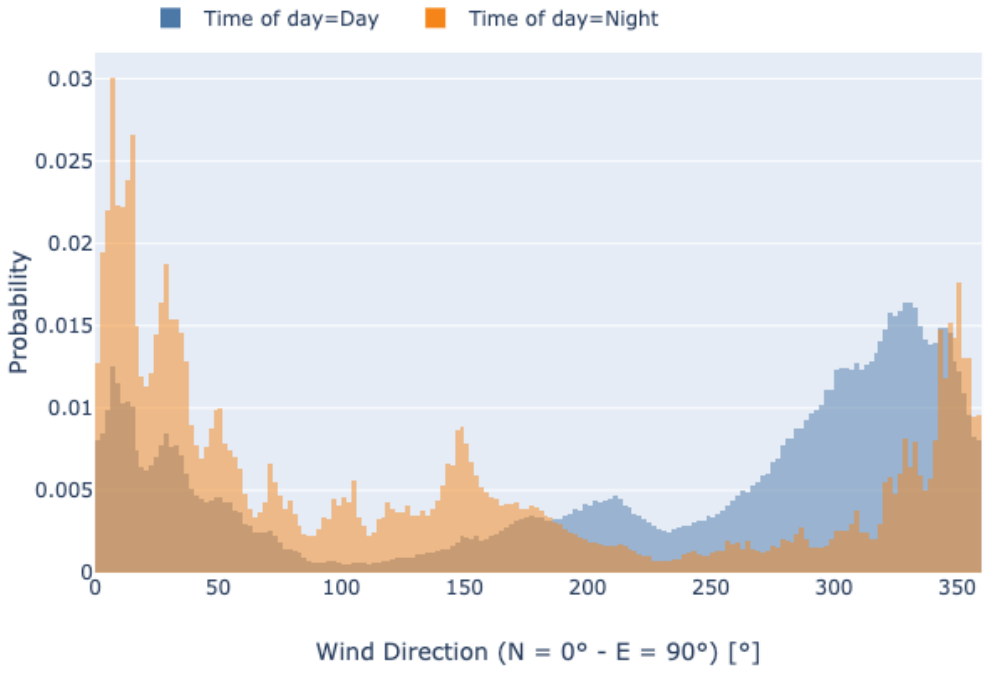

Figure 14: distribution of the wind direction measured 10 m above the platform level by the ASM.

4.2.5 Seeing

Statistics of the of the seeing of the atmosphere over Paranal as measured by the DIMM (see RD1) at 500 nm at zenith are given in Table 7. The distribution is plotted in Figure 16.

	Seeing (arcsec)
	Day
Mean	0.89
Std	0.55
1 % Quantile	0.32
5 % Quantile	0.4
50 % Quantile	0.73
95 % Quantile	1.92
99 % Quantile	3.18

Table 7: statistics of the seeing as measured by the DIMM at 500 nm at zenith.

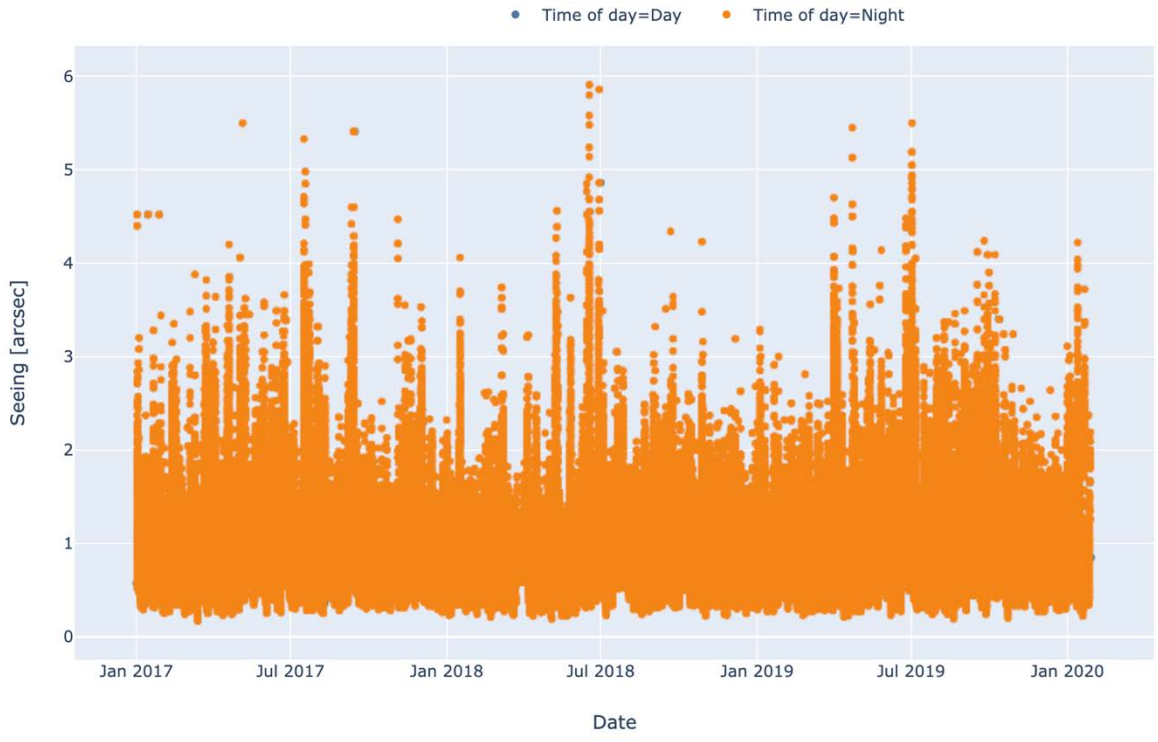

Figure 15: timeseries of the seeing measured by the DIMM over three years.

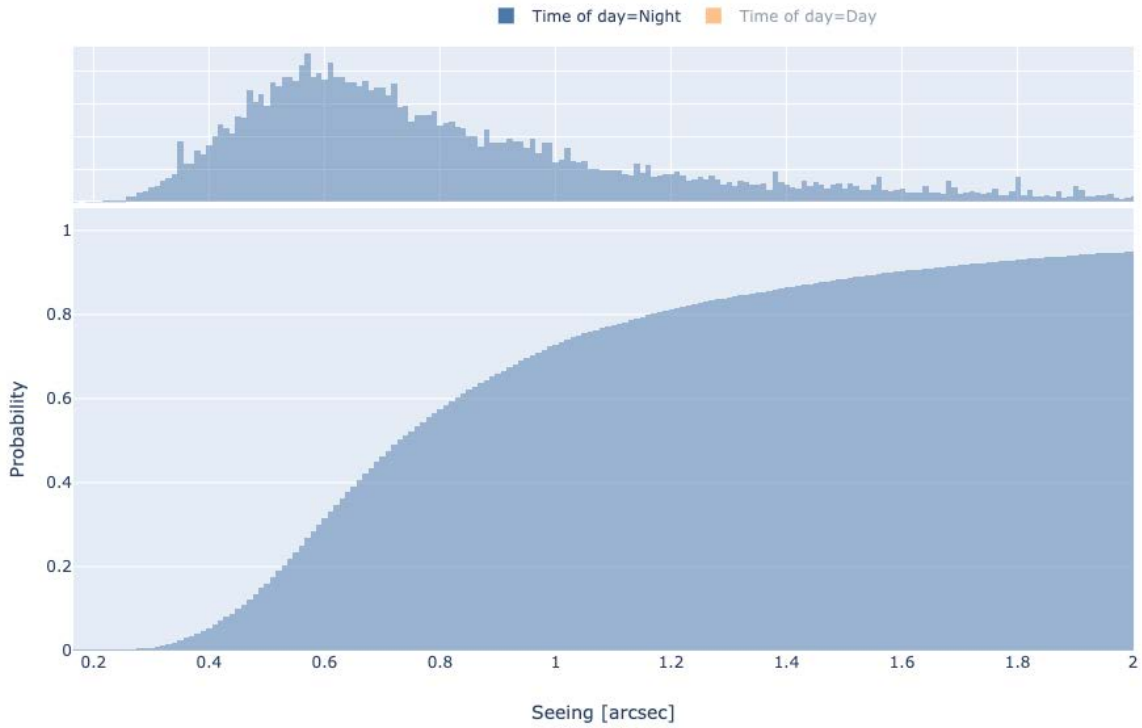

Figure 16: histogram (top) and cumulative histogram (bottom) of the seeing measured by the DIMM (over three years).

4.2.6 Coherence time

Statistics of the of the coherence time of the atmosphere over Paranal as measured by the MASS and the DIMM (see RD1) at 500 nm at zenith are given in Table 8. The distribution is plotted in Figure 18.

	Coherence time (ms)
Mean	5.0
Std	3.3
1 % Quantile	0.8
5 % Quantile	1.3
50 % Quantile	4.1
95 % Quantile	12.3
99 % Quantile	17.4

Table 8: statistics of the coherence time as measured by the MASS and the DIMM at 500 nm at zenith.

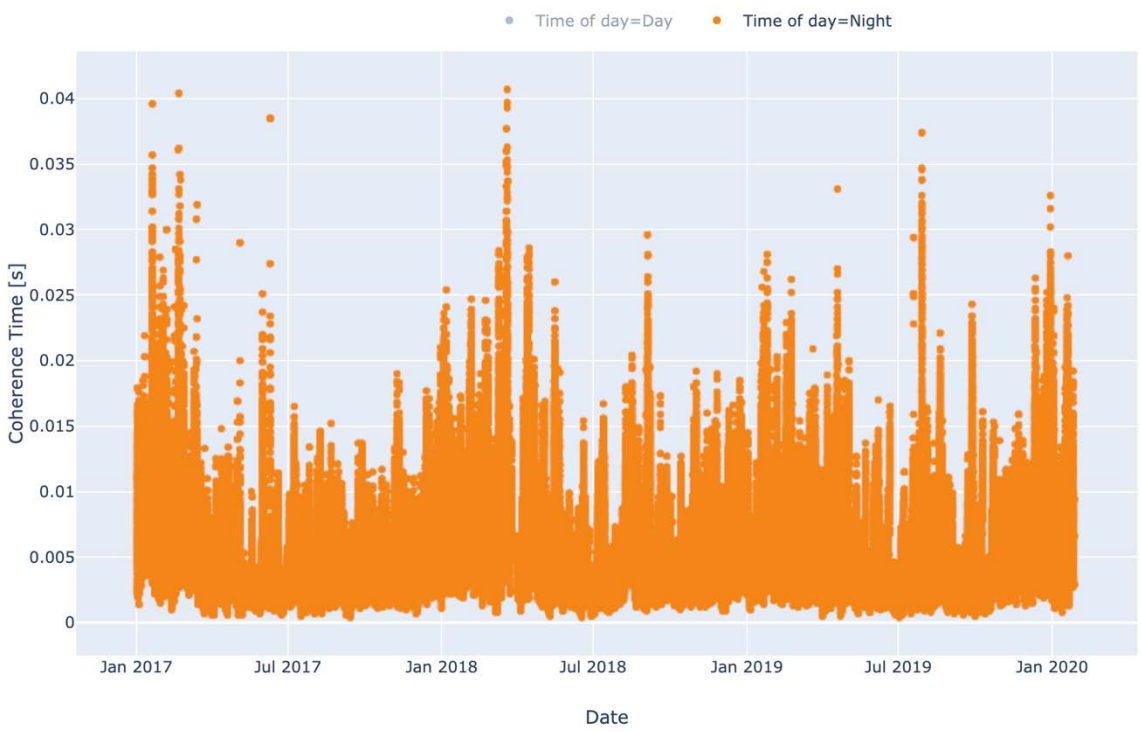

Figure 17: timeseries of the coherence time measured by the DIMM.

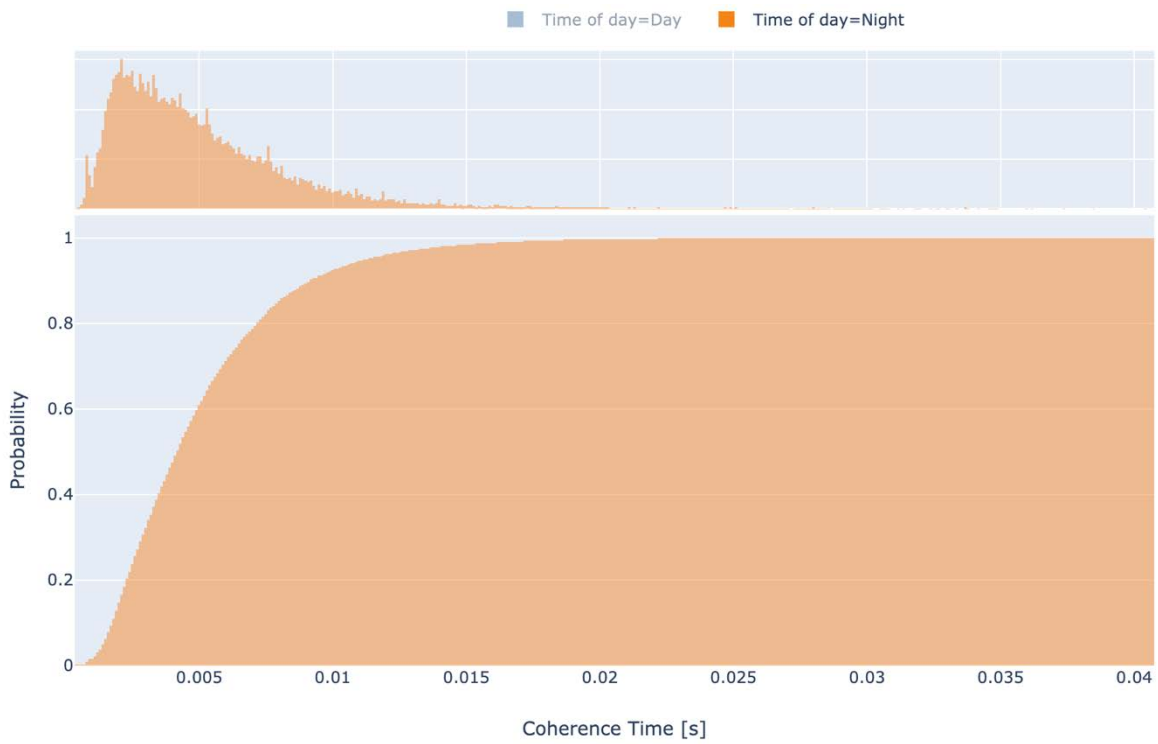

Figure 18: histogram (top) and cumulative histogram (bottom) of the coherence time measured by the DIMM (over three years).

4.3 VLTI Laboratory (IC108)

The VLTI Tunnel is not equipped with any air conditioning or air handling unit.

4.3.1 Laboratory ambient temperature

Statistics of the VLTI laboratory ambient temperature measured on the eastern wall are given in Table 9. The time series is plotted in Figure 19 and the distribution and cumulative probability are plotted in Figure 20. The distribution of the gradient over one hour is plotted in Figure 21. The statistics have been obtained over 3 years of data.

	Temperature (° C)		Gradient (° C/ hour)
	Day	Night	
Mean	14.9	14.7	0
Std	1.2	1.3	0.05
1 % Quantile	12.4	12.5	-0.1
5 % Quantile	12.7	12.7	-0.05
50 % Quantile	15.0	14.7	0.00
95 % Quantile	16.6	16.5	0.1
99 % Quantile	17.1	16.9	0.2

Table 9: statistics of the ambient temperature of the VLTI laboratory.

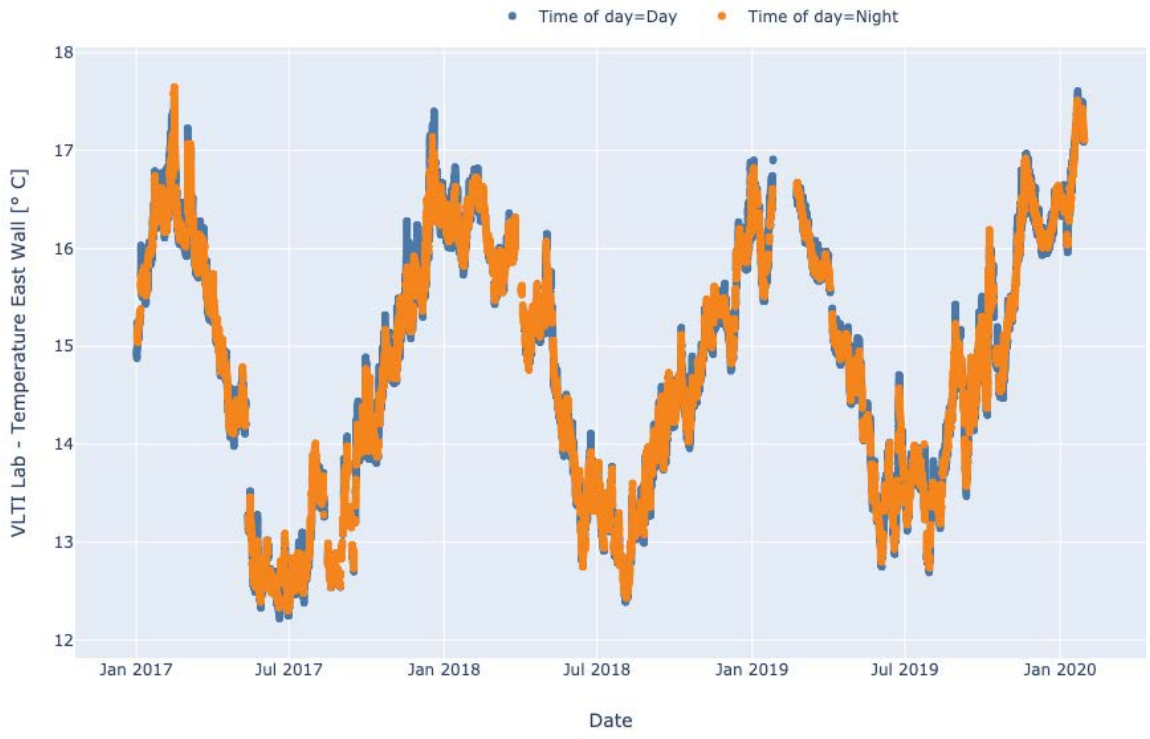

Figure 19: VLTI laboratory temperature close to the East wall.

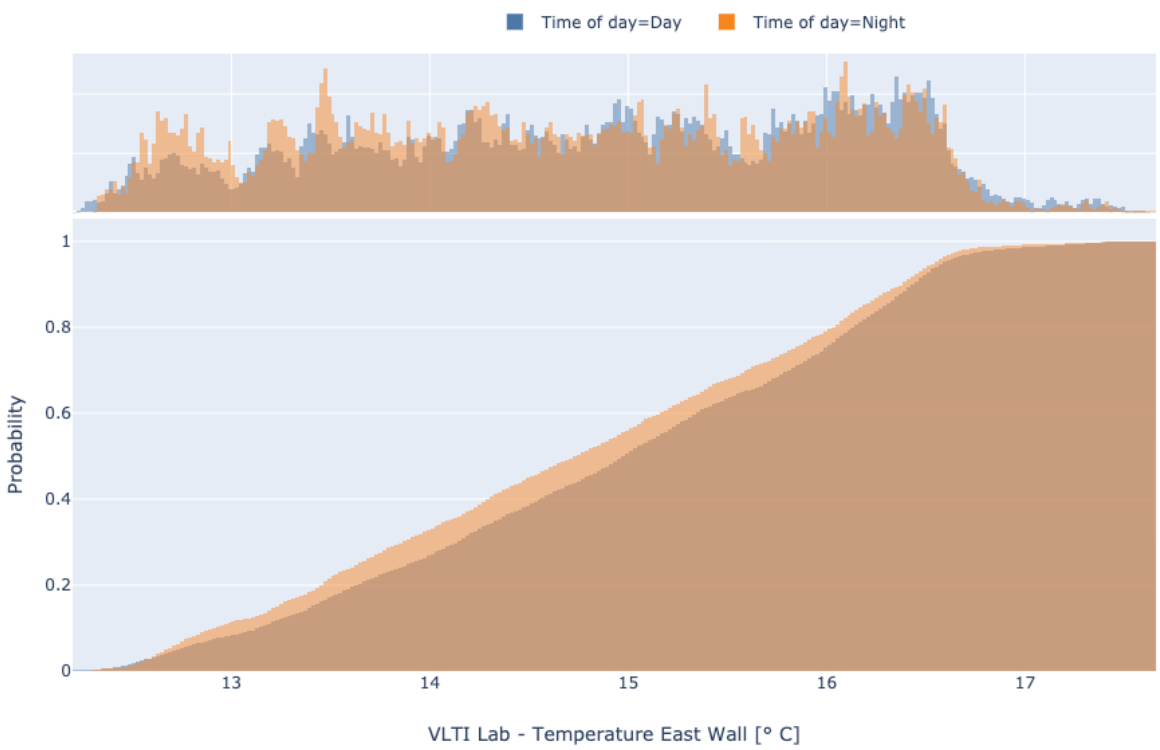

Figure 20: histogram (top) and cumulated histogram (bottom) of the temperature distribution in the VLTI laboratory close the East wall.

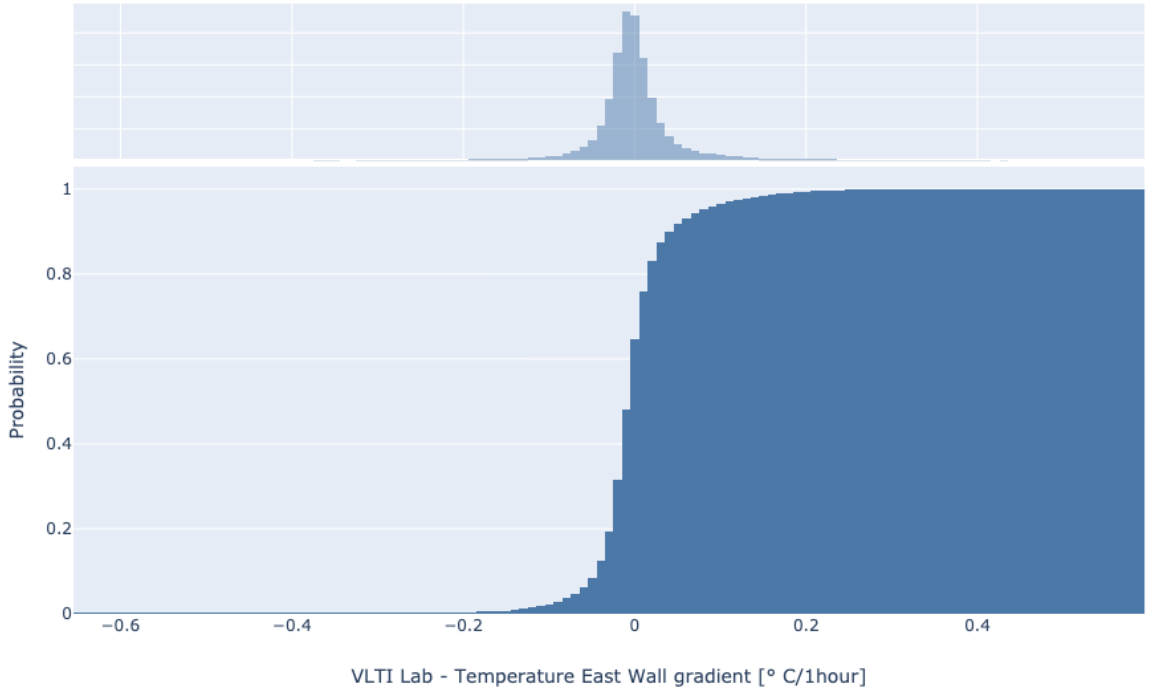

Figure 21: histogram (top) and cumulative histogram (bottom) of the temperature gradient in the VLTI Laboratory close to East wall.

4.3.2 Relative humidity

Statistics of the VLTI laboratory ambient air relative humidity are given in Table 10. The statistics have been obtained over 1 year. The time series is plotted in Figure 22. The histogram and cumulative histogram are plotted in .

	Relative humidity (%)		Gradient (% / hour)
	Day	Night	
Mean	18.5	17.4	0.0
Std	9.1	8.7	0.9
1 % Quantile	5.4	4.9	-3.0
5 % Quantile	7.8	7.1	-1.4
50 % Quantile	16.9	15.7	0.0
95 % Quantile	36.8	34.8	1.3
99 % Quantile	49.0	46.9	2.6

Table 10: statistics of the ambient air relative humidity of the VLTI laboratory.

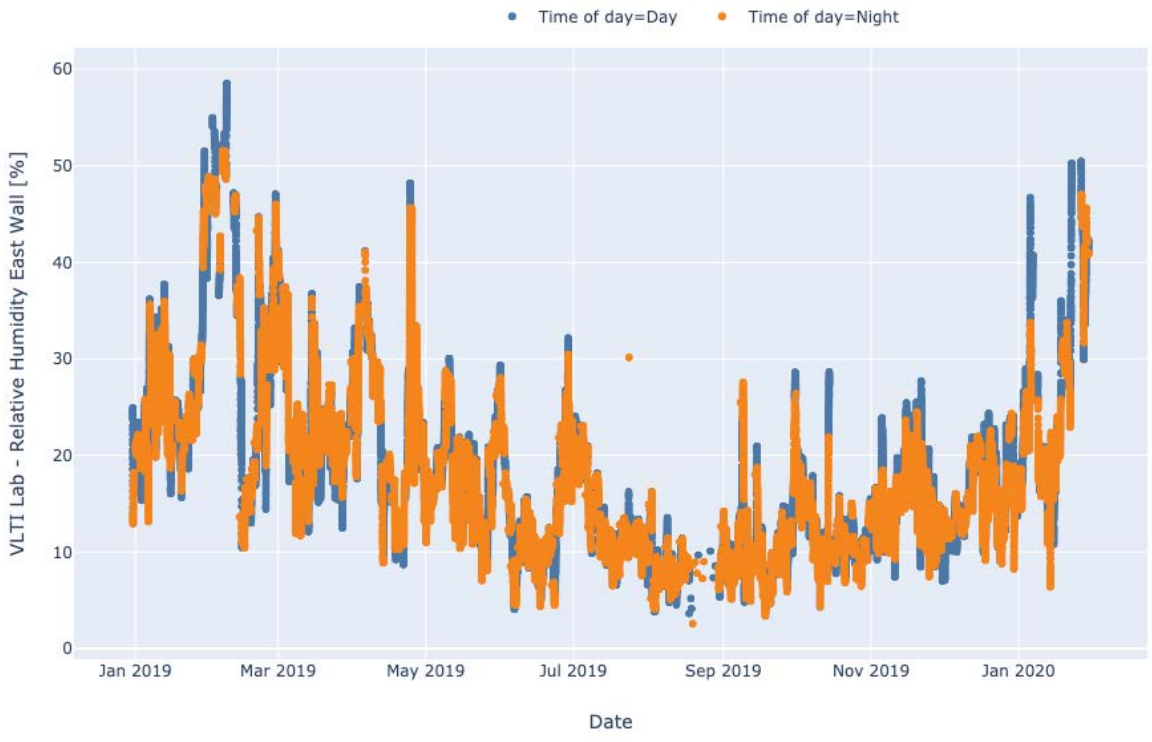

Figure 22: VLTI laboratory relative humidity over 1 year.

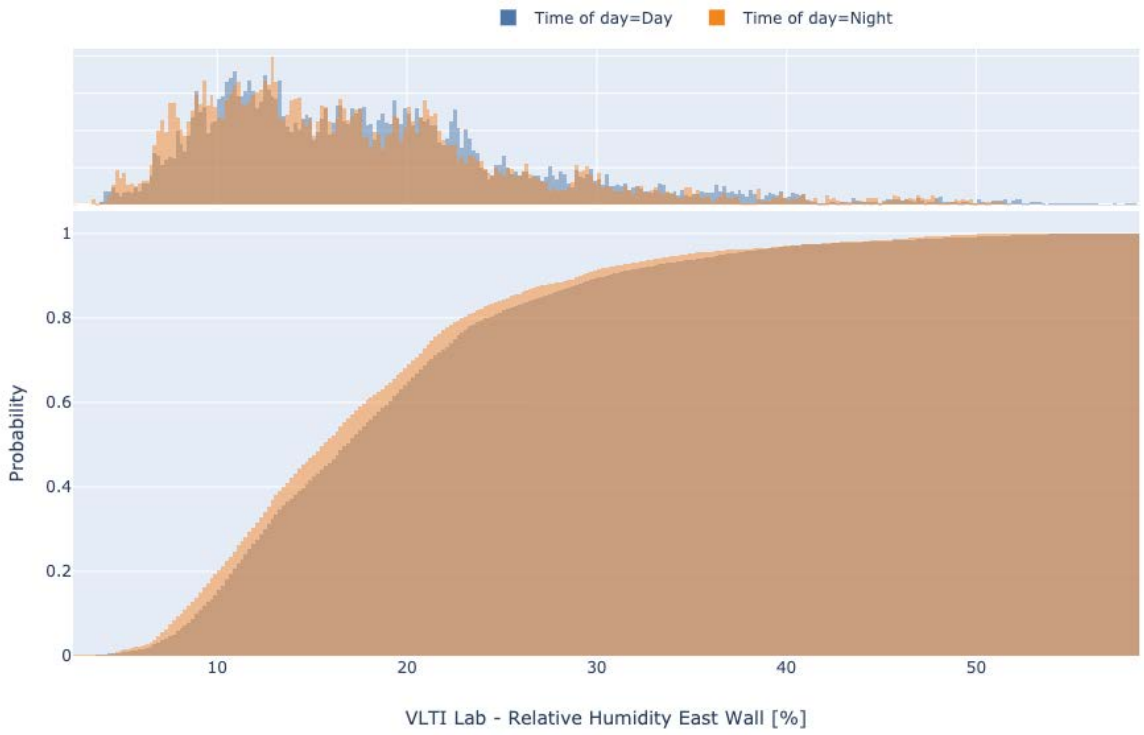

Figure 23: histogram (top) and cumulative histogram (bottom) of the air relative humidity in the VLTI laboratory (data obtained over 1 year).

4.3.3 Acoustic noise

To be completed in a future version of the document.

4.3.4 Air cleanliness

A particle counter was installed in the VLTI laboratory on the Differential Delay Lines table from September 10th to October 8th 2018. The results are plotted in the next three figures, Figure 24, Figure 25 and Figure 26. The VLTI laboratory can be considered a clean room of class 100,000 (ISO8).

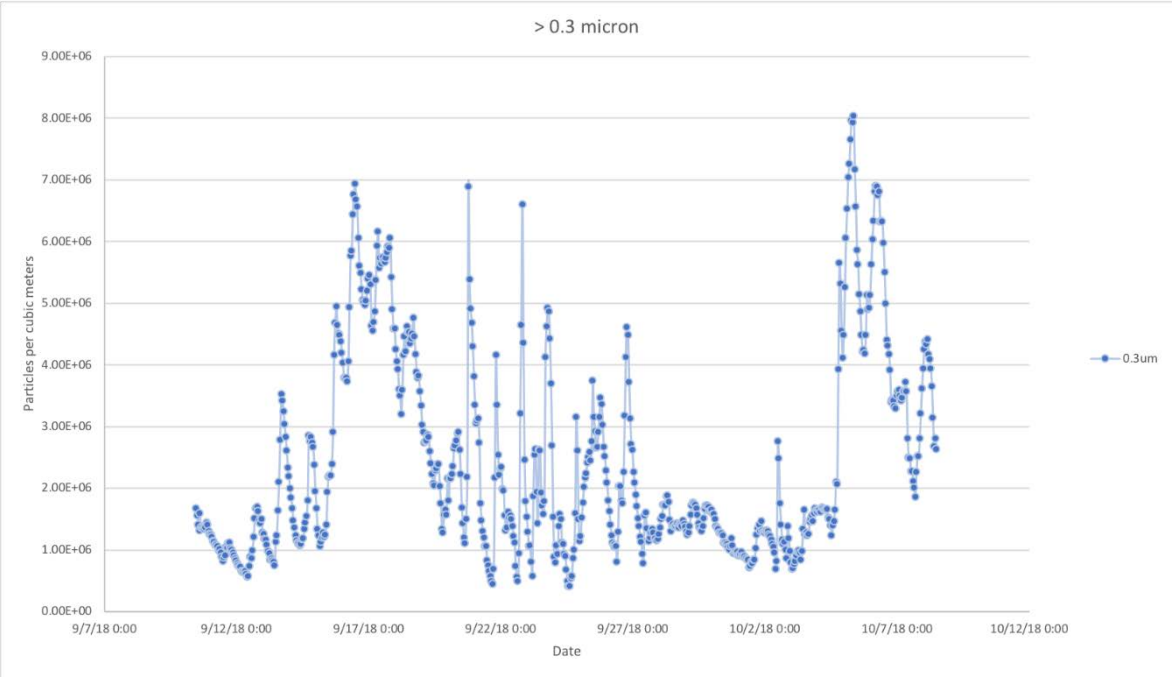

Figure 24: concentration of particles with diameter > 0.3 μm in the VLTI laboratory.

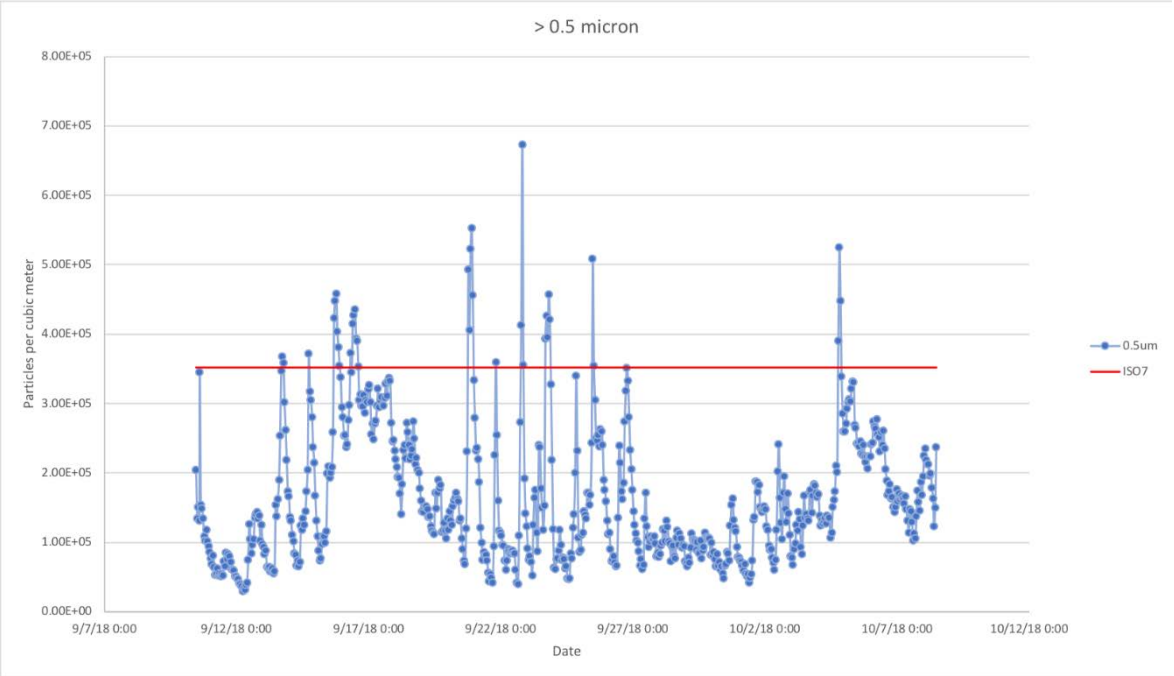

Figure 25: concentration of particles with diameter > 0.5 μm in the VLTI laboratory.

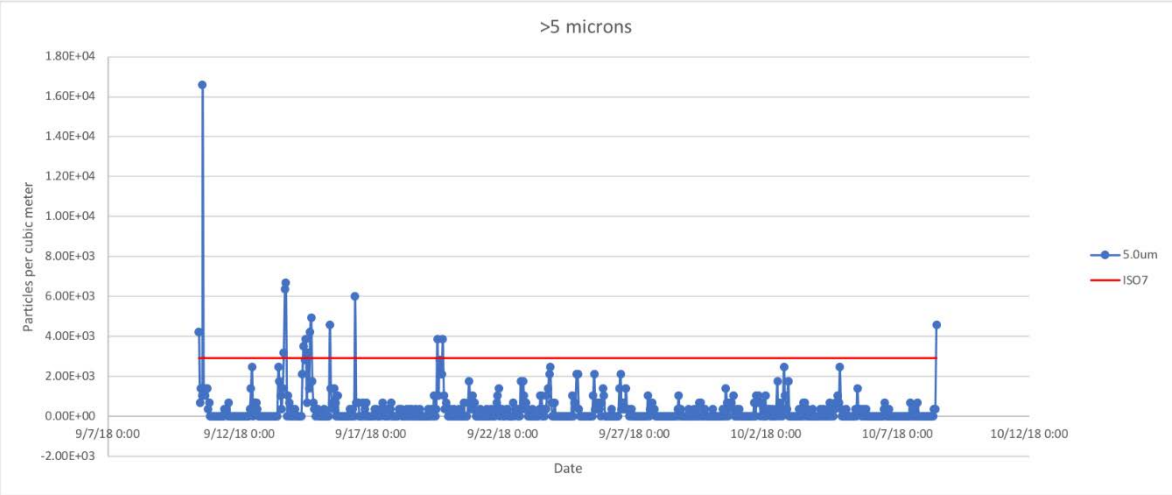

Figure 26: concentration of particles with diameter > 5 μm in the VLTI laboratory.

4.4 VLTI Tunnel (IC109)

The VLTI Tunnel is not equipped with any air conditioning or air handling unit. It therefore follows the yearly variations, Figure 28.

4.4.1 Ambient temperature

	Relative humidity (%)		Gradient (% / hour)
	Day	Night	
Mean	15.4	15.14	0.00
Std	1.54	1.58	0.05
1 % Quantile	12.45	12.37	-0.11
5 % Quantile	12.97	12.69	-0.05
50 % Quantile	15.62	15.07	0.00
95 % Quantile	17.51	17.44	0.05
99 % Quantile	17.84	17.78	0.11

Figure 27: statistics over 3 years of the ambient air temperature at the centre of the Delay Lines tunnel.

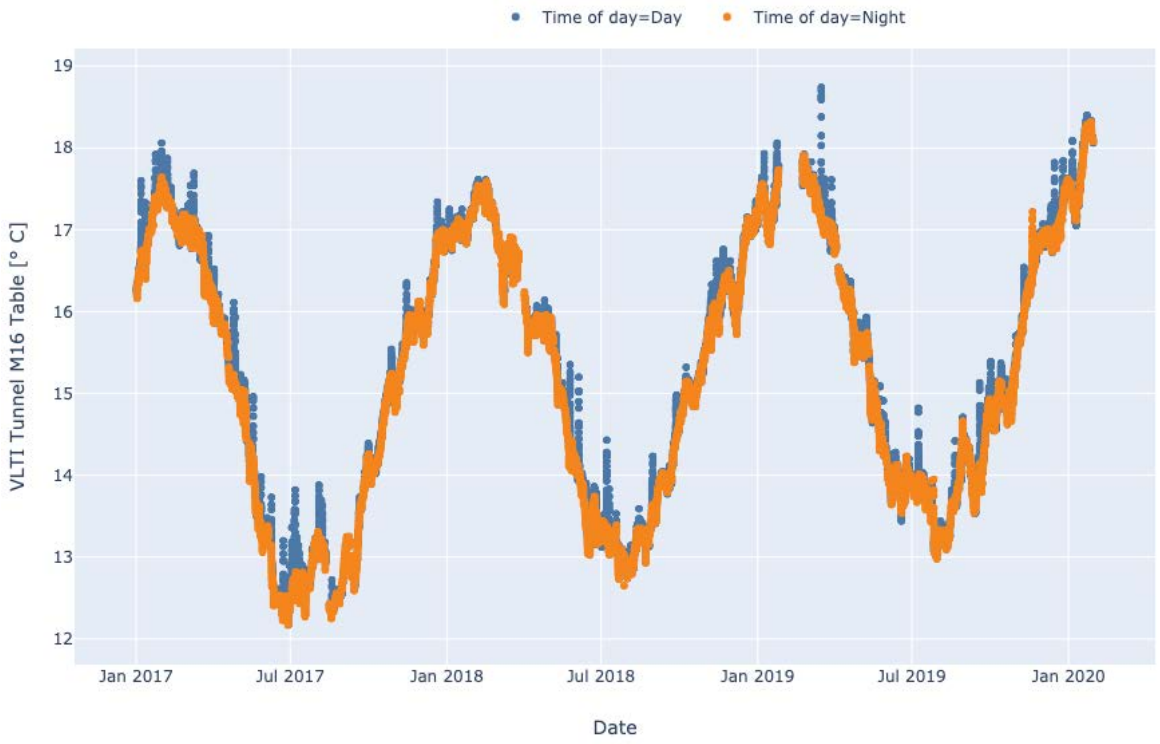

Figure 28: temperature (° C) at the centre of the VLTI delay lines tunnel.

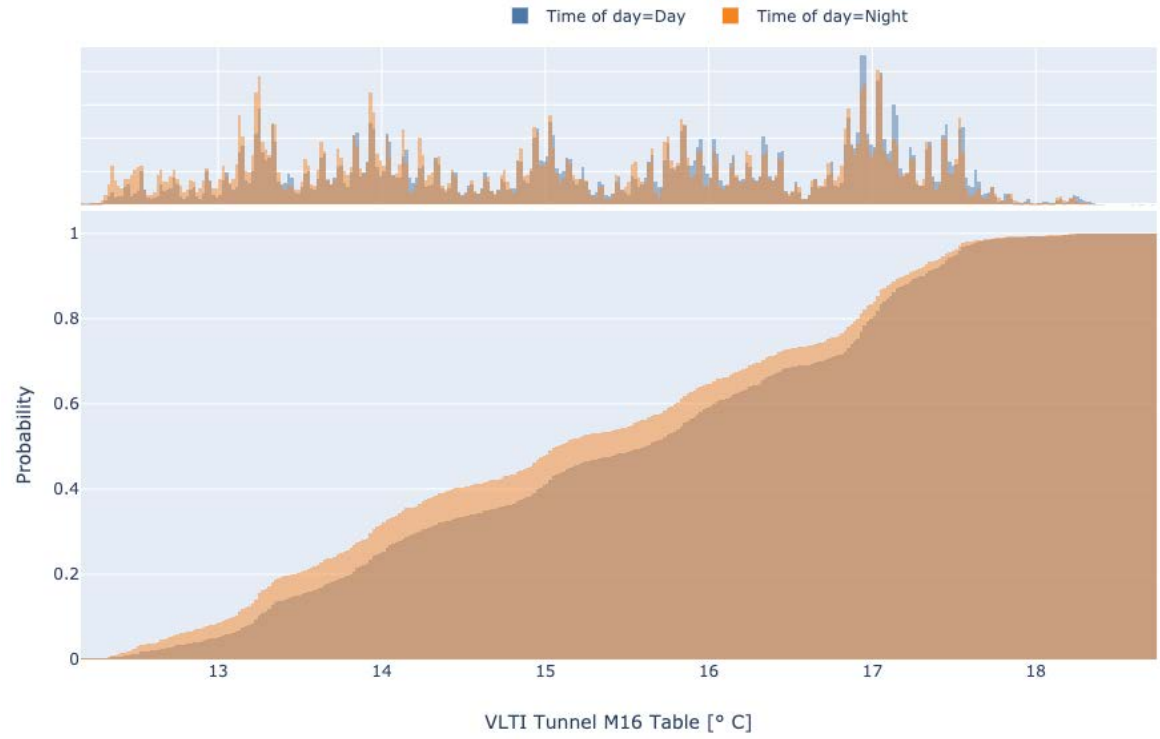

Figure 29: distribution of temperature (° C) measured at the centre of the VLTI delay lines tunnel during day and night (over ~ 3 years of data).

4.4.2 Relative humidity

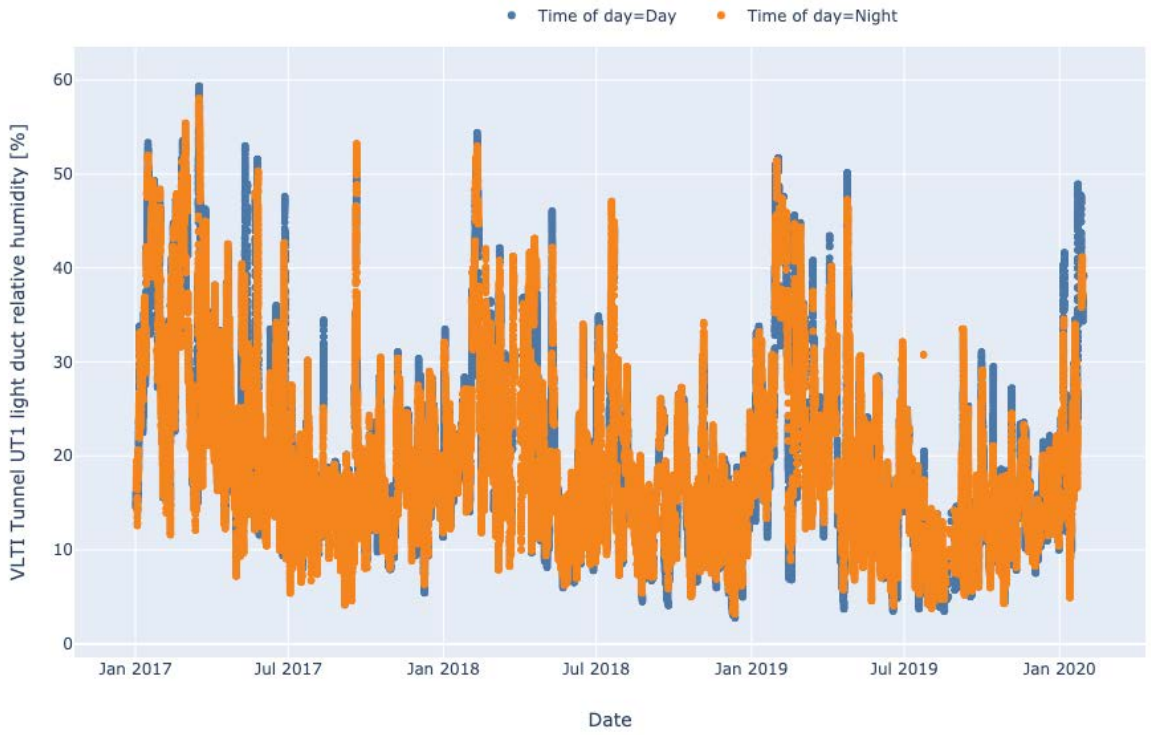

Figure 30: relative humidity (%) at the level of the UT1 light duct in the Delay Lines tunnel.

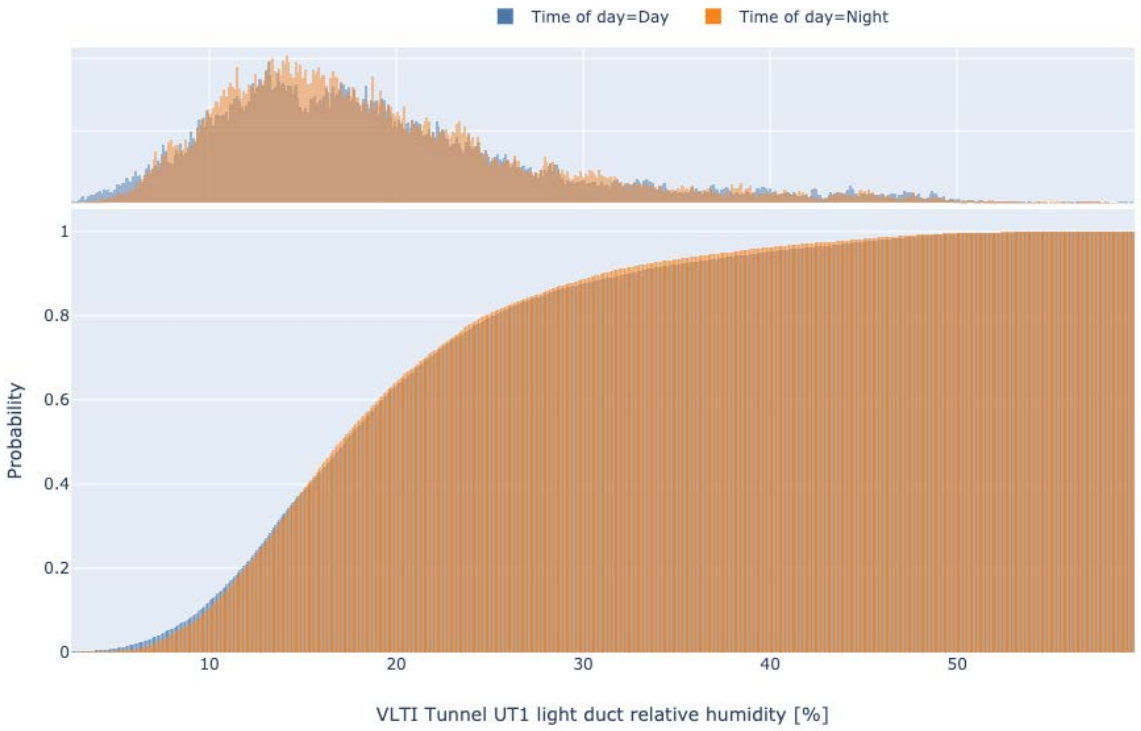

Figure 31: histogram (top) and cumulative histogram (bottom) of the relative humidity (%) at the level of the UT1 light duct in the Delay Lines tunnel (data obtained over three years).

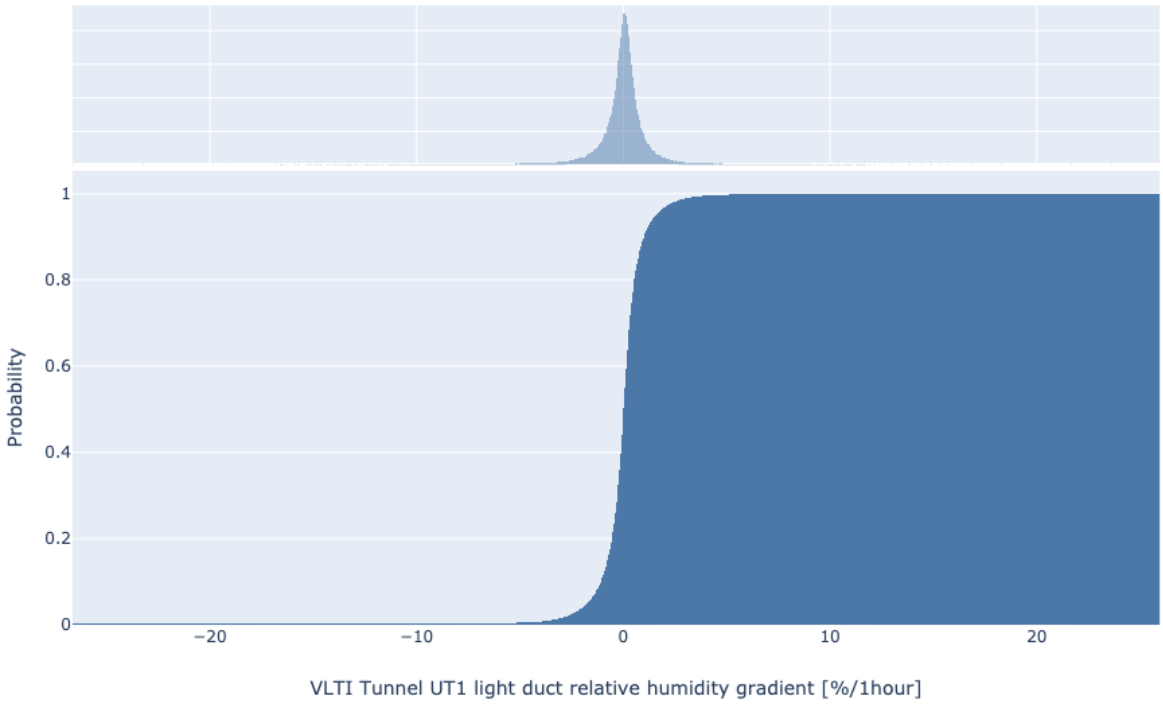

Figure 32: histogram (top) and cumulative histogram (bottom) of the ambient air relative humidity gradient at the level of the UT1 light duct in the Delay Lines tunnel.

4.5 Combined Coude Laboratory (IC107)

The Combined Coude Laboratory is not equipped with any air conditioning or air handling unit.

4.5.1 Ambient temperature

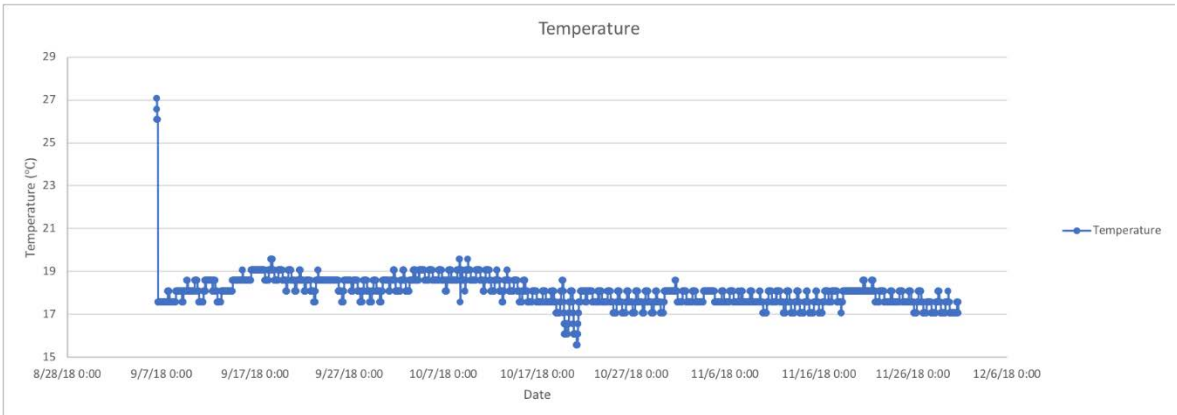

Figure 33: temperature in the CCL measured from September to November 2018.

4.5.2 Relative humidity

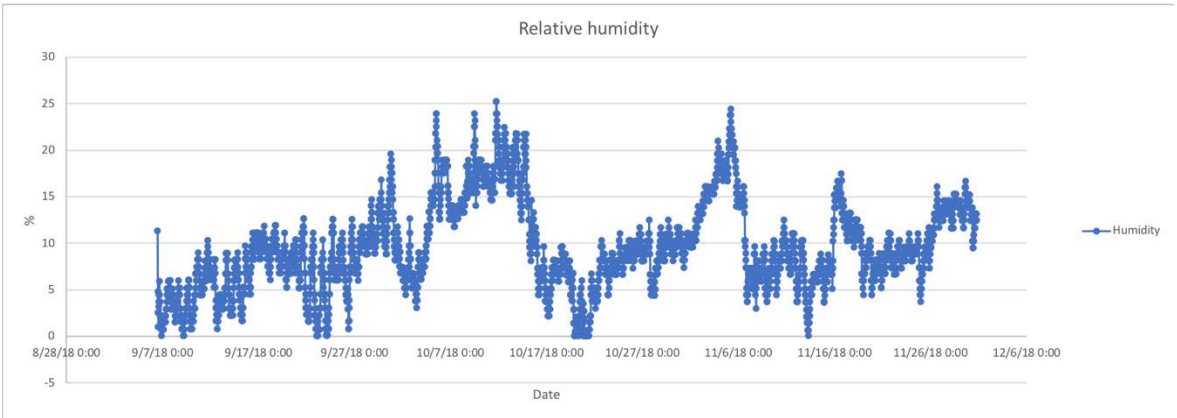

Figure 34: relative humidity in the CCL measured from September to November 2018.

4.6 VLTI Storage room (IC104)

The VLTI Storage room is equipped with two air handling units.

4.6.1 Ambient temperature

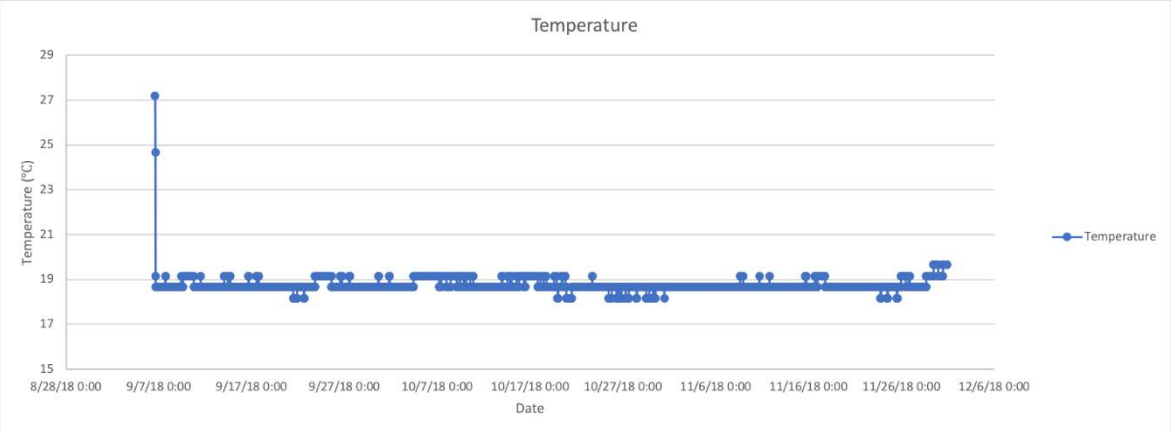

Figure 35: temperature in the IC-104 measured from September to November 2018.

4.6.2 Relative humidity

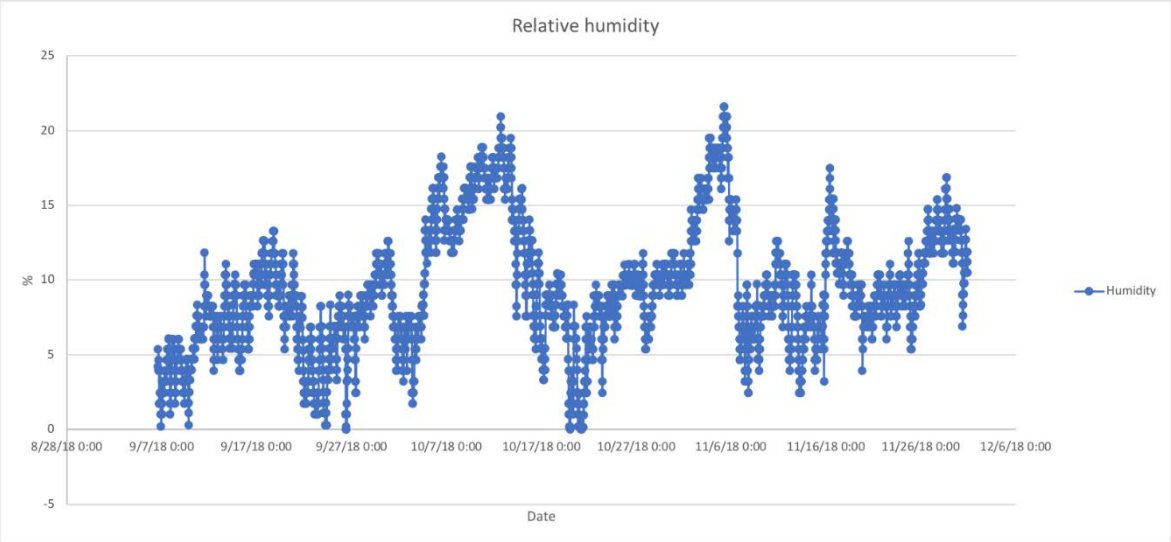

Figure 36: relative humidity in the IC-104 measured from September to November 2018.

4.7 VLTI Computer room (IC102)

The VLTI Computer room is equipped with an air conditioning system. Temperature and humidity have been measured over 3 months. Data are available in Figure 37 and Figure 38.

4.7.1 Ambient temperature

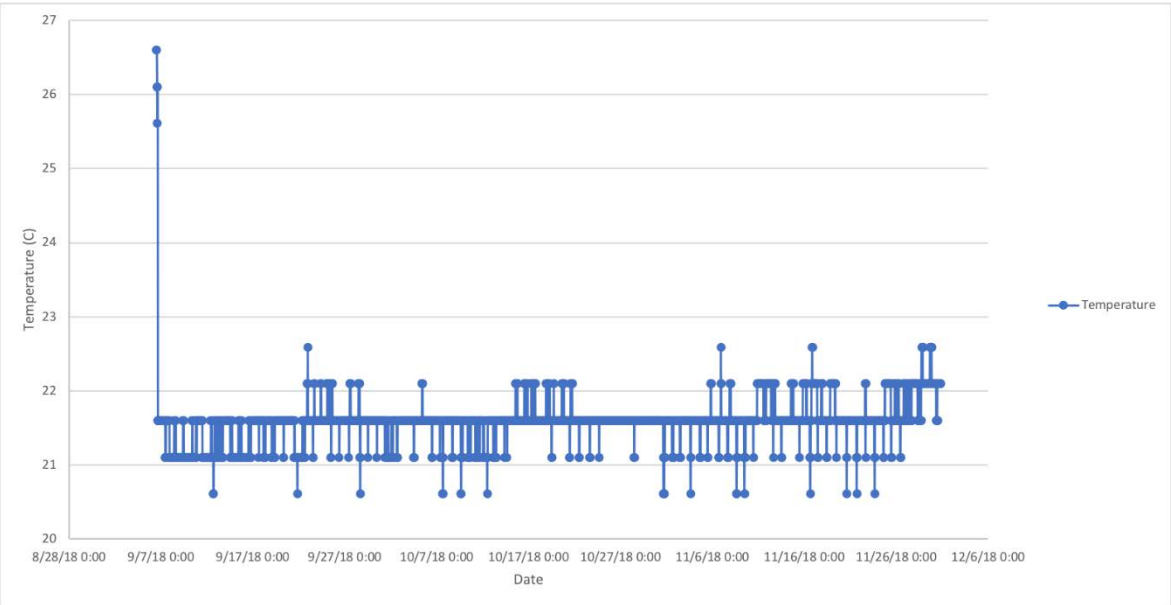

Figure 37: temperature in the IC-102 measured from September to November 2018.

4.7.2 Relative humidity

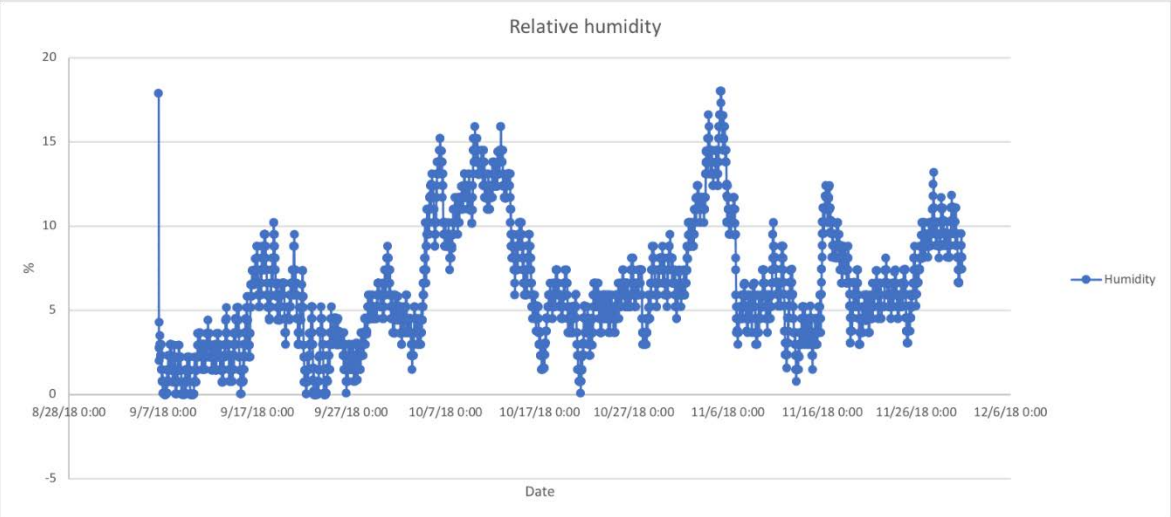

Figure 38: relative humidity in the IC-102 measured from September to November 2018.

5. Mechanical interfaces between the VLTI infrastructure and the instruments

5.1 VLTI Laboratory (IC108)

5.1.1 Room characteristics

	Values
Size U x V (m x m)	20.4 x 6.7
Access width x height (m x m)	2.7 x 2.08
Maximum usable height (m)	2.201

Table 11: VLTI Laboratory room characteristics.

5.1.2 Volumes

Layout of the room and its usage by the different subsystems are defined in the drawing AD1. Envelope volumes are allocated for possible visitor instruments.

5.1.2.1 VISITOR 1:

Two volumes are allocated to the VISITOR1:

- VI1A: 200 x 80 x 55 (U x V x W, cm^3) over the PRIMA1 table. The footprint over the table is defined in AD1.
- VI1B: small volume (to be defined) on the side for a cable tray leading down the cables.

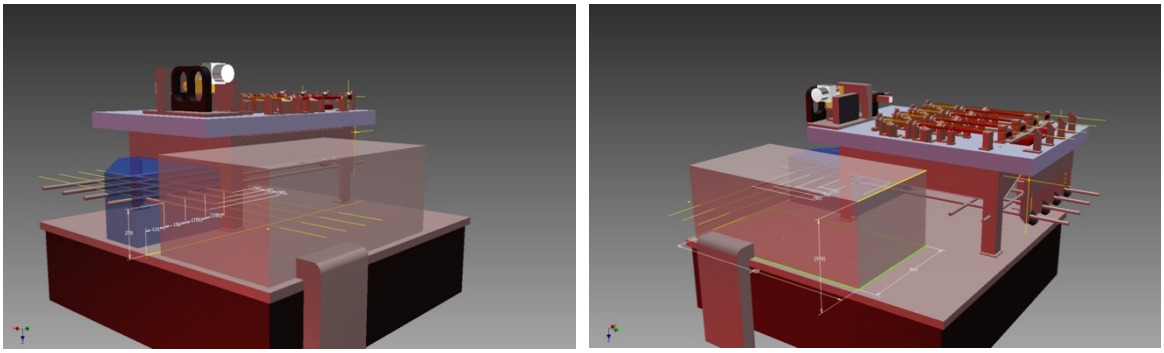

Figure 39: in red - volume V1A and V1B allocated for a visitor instrument on the PRIMA1 table. In blue – volume allocated for the feeding optics for a visitor instrument. The PIONIER instrument can be seen on the mezzanine.

5.1.2.2 VISITOR 2:

Two volumes are allocated to the VISITOR2:

- VI2A: 150 x 420 x 80 (U x V x W, cm^3) over the VISITOR2 table top surface (defined in Table 12).
- VI2B: small volume (to be defined) on the side for a cable tray leading down the cables.

5.1.3 Table interface

Table Name	Width (m)	Length (m)	Thick-ness (mm)	Table Height[1] (mm)	Beam Height[2] (mm)	Table Mass (kg)	Load mass assumed for frequency (kg)	First resonance frequency[3] (Hz)
Switchyard	2.10	2.10		116.8	292			
Beam Compressor	2.10	2.40	457	1348	112	950	400	> 130 Hz
MATISSE FO	1.20	2.40	457?	1168	292	570	250	160
GRAVITY FO	1.20	1.50	457	1168	292[4]	360		
MATISSE	2.00	1.50	610	1260		740	750	> 160
VISITOR2	1.50	4.20	610	1260	200[5]	1360	500	130
VISITOR1	2.10	2.10	457	1190	270	< 1200	400	> 130

[1] The upper surface of the table to the nominal height will be +/-0.2 mm
[2] The actual beam height will be +/-0.2 mm
[3] From Newport specification
[4] Ref.: Ldv Mechanical Design – VLT-SPE-MEU-15810-2000 – Issue 1.0 – 13/7/99
[5] Ref.: AMBER Hardware Interface Control Document– VLT-ICD-AMB-15830-0001– Issue 1.0 – 15/11/00

IRIS	2.10	2.30	457	1190	270	< 1315	400	> 130

Table 12: characteristics of the optics tables installed inside the VLTI laboratory.

5.1.4 False floor

The VLTI Laboratory is equipped with a false floor to allow routing of cables and hoses in cable trays at the level of the floor. The details of the false floor implementation are given in AD1. The cable trays are described in Section 10.1.

5.2 VLTI Tunnel (IC109)

5.2.1 Room characteristics

	Values
Size u x v (m x m)	161.9 x 6.675
Access width x height (m x m)	1.47 x 2.06
Maximum usable height (m)	2

5.2.2 Volumes

The volume PIO2 is defined for the electronics cabinet of PIONIER.

PIO2: 61 x 61 x 185 (U x V x W, cm^3) over the floor surface.

5.3 Combined Coude Laboratory (IC107)

5.3.1 Room characteristics

	Values
Size u x v(m x m)	10.7 x 20
Access width x height (m x m)	2.585 x 1.995 via elevator
Maximum usable height (m)	2.78

5.3.2 Volumes

The volumes used by the different subsystems are defined in AD1.

5.4 VLTI Storage room (IC104)

5.4.1 Room characteristics

	Values
Size u x v(m x m)	8.675 x 5.25
Access width x height (m x m)	0.8 x 1.975
Maximum usable height (m)	2.40

Table 13: VLTI Storage room characteristics.

5.4.2 Volumes

Layout of the room and its usage by the different subsystems are defined in the drawing AD1. Envelope volumes are allocated for possible visitor instruments.

5.4.2.1 VISITOR1

VIS1C is allocated for the installation of equipment belonging to the system installed on the VISITOR1 table.

VIS1C: 150 x 80 x 235 (U x V x W, cm^3) above the floor.

5.4.2.2 VISITOR2

VIS2C is allocated for the installation of equipment belonging to the system installed on the VISITOR2 table.

VIS2C: 30 x 80 x 215 (U x V x W, cm^3) + 245 x 80 x 235 (U x V x W, cm^3) above the floor.

5.5 VLTI Computer room (IC102)

5.5.1 Room characteristics

	Values
Size U x V(m x m)	11.5 x 5.25
Access width x height (m x m)	0.8 x 1.98
Maximum usable height (m)	2.36

Table 14: VLTI Computer room characteristics

5.5.2 Volumes

The volumes used by the different subsystems are defined in AD1.

5.5.2.1 Delay Lines

This volume contains all the Delay Lines electronics.

DLA: 80 x 242 x 200 (U x V x W, cm^3)

5.5.2.2 VLTI Control Electronics

This volume contains the VLTI control electronics.

CTR: 80 x 320 x 195 (U x V x W, cm^3)

5.5.2.3 VLTI Network Infrastructure

This volume contains the patch panels for the VLTI fibre network, the TIM distribution module and other IT equipment. This volume is under the responsibility of the Paranal IT group.

NET: 80 x 480 x 195 (U x V x W, cm^3)

5.5.2.4 VLTI Workstations

This volume contains various workstations for VLTI subsystems or instruments. This volume is under the responsibility of the Paranal IT group.

WS: 107 x 420 x 220 (U x V x W, cm^3)

6. Thermal interfaces between the VLTI complex and the instruments

6.1 Interface to the liquid cooling distribution system

The VLTI is equipped with a liquid cooling distribution system derived from the UT liquid cooling distribution system. VLTI distribution has its own heat exchanger and pump. The characteristics of the distributed cooling liquid are detailed in Table 15.

Clients are either directly connected to the distribution circuit or use one of the provided Service Connection Point. The type of connectors used at the SCP are defined in Table 19. The position of the connections points are given per room from 6.3 to 6.7.

6.1.1 Cooling liquid characteristics

Characteristics	Values
Coolant	HVAC-50-MA by Biochemical, monoethylene glycol 50% with additives against corrosion and algae, Freezing point -34°C. Data sheet in Section 19 Annex F.
Supply temperature	8 ° C +\- 0.3 ° C

Table 15: liquid cooling general characteristics.

6.1.2 Connections

6.1.3 Direct Connections

Gravity has its own cooling distribution panel which is connected directly to the liquid cooling distribution network. The connection is done in the CCL on the Western wall, see Table 25. Connectors types are defined in Table 16.

Side		Connector
Entrance	Distribution system outlet	Parker Rectus Type 75
	Equipment connector inlet	Parker Rectus Type 75
Return	Equipment connector outlet	Parker Rectus Type 75
	Distribution system inlet	Parker Rectus Type 75

Table 16: characteristics of the connectors for the direct connection of Gravity to the liquid cooling distribution system

MATISSE has its own cooling distribution panel which is connected directly to the liquid cooling distribution network. The connection is done in the CCL on the Southern wall, see Table 25. Connectors types are defined in Table 17.

Side		Connector
Entrance	Distribution system outlet	Parker Rectus Type 74
	Equipment connector inlet	Parker Rectus Type 74
Return	Equipment connector outlet	Parker Rectus Type 74

	Distribution system inlet	Parker Rectus Type 74

Table 17: characteristics of the connectors for the direct connection of MATISSE to the liquid cooling distribution system

6.1.4 Service Connection Point

Characteristics	Value
Nominal supply pressure (bar)	6
Supply differential pressure (bar)	Minimum = 0.8 Maximum = 2
Maximum flow rate per SCP (l/min)	15

Table 18: cooling flow characteristics at the SCP.

Side		Connector
Entrance	Distribution system outlet	Quick coupling Parker SH6-63-BSPP ¾" male
	Equipment connector inlet	Quick coupling Parker SH6-62-BSPP ¾" female
Return	Equipment connector outlet	Quick coupling Parker SH6-63-BSPP ¾" male
	Distribution system inlet	Quick coupling Parker SH6-62-BSPP ¾" female

Table 19: characteristics of the connectors for a connection to a Service Connection Point of the liquid cooling distribution system

6.2 Interface to the compressed air distribution system

The VLTI is equipped with a compressed air distribution system. The characteristics of the distributed air are detailed in Table 20. The type of connectors provided by the distribution system are defined in Table 21. The position of the connections point are given per room from 6.3 to 6.7.

6.2.1 Compressed air characteristics

Characteristics	Values
Supply pressure (bars)	7 < P < 8
Water	30 % relative humidity at 15 ° C at local atmospheric pressure.
Oil	> 1 mg/m^3

Table 20: compressed air characteristics for the VISTA telescope as measured during an external audit. UT compressed air is assumed to have the same characteristics (since the ambient conditions and type of Kaeser compressor are the same).

6.2.2 Service Connection Point

	Connector

Distribution system outlet (provider)	Rectus type 25 NW 7.8 male
Equipment connector (client)	Rectus type 25 NW 7.8 female

Table 21: compressed air distribution system connectors

6.3 VLTI Laboratory (IC108) connections points

Ref. #	Room	Approx. U coord. (m)	Approx. V coord. (m)	Port 1 (l/min)	Port 2 (l/min)	Port 3 (l/min)	Port 4 (l/min)	Port 5 (l/min)
34	Interferometric Laboratory	42.0	-32.5	DL3, > 3.5	DL4, > 3.5	Allocated to VI2	PIONIER, > 2	Allocated to VI2
35	Interferometric Laboratory	48.5	-29.0	Gravity Cab #1, > 4	Allocated to VI1	Allocated to VI1	IRIS IRACE, > 4	Gravity TMP, > 1.5
36	Interferometric Laboratory	59.5	-29.0	-	-	-	-	DDL, > 2.5

Table 22: position of the cooling SCP in the VLTI Laboratory and usage of their outlets.

6.4 VLTI Tunnel (IC109) connections points

Ref. #	Room	Approx. U coord. (m)	Approx. V coord. (m)	Port 1 (l/min)	Port 2 (l/min)	Port 3 (l/min)	Port 4 (l/min)	Port 5 (l/min)
34	VLTI Tunnel	62.5	-32.5	DL1, >3	DL2, >3	-	DL6, >3	DL5, >3

Table 23: position of the cooling SCP in the VLTI Tunnel and usage of their outlets.

6.5 Combined Coude Laboratory (IC107) connections points

Ref. #	Room	Approx. U coord. (m)	Approx. V coord. (m)	Port 1 (l/min)	Port 2 (l/min)	Port 3 (l/min)	Port 4 (l/min)	Port 5 (l/min)
43	Combined Coudé Laboratory	58.5	-17.0	DDL Cab 3, >2.0	DDL Cab 2, >2.0	-	DDL Cab 1, >2.0	ESPRESSO AC, >4.0

Table 24: position of the cooling SCP in the Combined Coudé Laboratory and usage of their outlets.

System	Approx U coord. (m)	Approx V coord. (m)	Flow (l/min)
MATISSE – Cooling panel #2 for electronics cabinet	53.0	-28.0	> 14.0

MATISSE – Cooling panel #1 for compressors	53.0	-28.0	> 16.0
Gravity – Cooling panel	48.0	-23.5	> 23.0

Table 25: Direct connections to the cooling distribution system in the CCL.

6.6 VLTI Storage room (IC104) connections points

Ref. #	Room	Approx. U coord. (m)	Approx. V coord. (m)	Port 1 (l/m)	Port 2 (l/m)	Port 3 (l/m)	Port 4 (l/m)	Port 5 (l/m)
31	Storage Room	39.5	-35.0	-	Metrology #1, > 3.5	-	VIBMET, > 3.5	Air Handling Unit 2, > 3.5
33	Storage room	35.5	-29.5	-	-	-	Air Handling Unit 1, > 3	-

Table 26: position of the SCP in the Combined Coudé Laboratory and usage of their outlets.

6.7 VLTI Computer room (IC102) connections points

System	Approx U coord. (m)	Approx V coord. (m)	Flow (l/min)
Air conditioning unit – Uniflair #1	40.0	-14.5	> 80.0

Table 27: Direct connections to the cooling distribution system in the Computer Room (IC102).

7. Interface to the cryogenics line and exhaust system

7.1 Cryogenics lines

Three Cryogenics lines with two outputs are permanently installed between the IC104 room and the VLTI laboratory, see AD1. They are terminated by Johnston DN6 or DN20 male interfaces, see Table 28 and AD11.

Line number	Position in the Laboratory	Interfaces	Allocated
1	Above VISITOR2 table, AD1.	Johnston DN6 male / Johnston DN6 male	VISITOR1

2	Above VISITOR2 table, AD1.	Johnston DN6 male / Johnston DN6 male	VISITOR2
3	Western wall behind VISITOR2 table	Johnston DN6 male / Johnston DN6 male	VISITOR2

Table 28: Allocated Cryogenics lines between IC104 and IC108.

The MATISSE and Gravity instruments implemented their own cryogenics lines between the IC107 Combined Coude Laboratory and the IC108 VLTI Laboratory, see AD1.

7.2 Exhaust lines

An exhaust system is implemented in the VLTI complex to evacuate gaseous nitrogen out of the building and reduce risk of suffocation. It has interfaces in the IC104 room and in the IC107 room, see AD1. The interface is made of Johnston DN20 male interfaces, AD11.

Exhaust lines are also permanently installed between the IC108 VLTI Laboratory and the IC104, see Table 29 and AD11.

Line number	Position in the Laboratory	Interfaces	Allocated
1	Above VISITOR2 table	Johnston DN6 male / Johnston DN6 male	VISITOR1
2	Above VISITOR2 table	Johnston DN6 male / Johnston DN6 male	VISITOR2
3	Western wall behind VISITOR2 table	Johnston DN6 male / Johnston DN20 male	VISITOR2

Table 29: Allocated exhaust lines between IC108 and IC104.

Matisse and Gravity instruments gas heaters are connected to the exhaust system in the IC107 Combined Coude Laboratory, see AD1.

7.3 Safety – Oxygen Sensors Network

A network of oxygen sensors is deployed in the VLTI Complex and UT coudé room to reduce the risk of suffocation due to a quick release of nitrogen in confined spaces. It is described in RD10.

8. Electrical Interfaces between the VLTI complex and the instruments

The VLTI electrical distribution system is connected to the Paranal one which is itself connected to the Chilean power distribution grid. The delivered power quality is described in Section 8.1. Systems can be connected directly:

- To the SCP sockets
- To the SCP terminal blocks
- Directly to terminal blocks in the power distribution cabinet

The type of connections provided by the SCP are defined in Section 8.2.1. Connections to the distribution cabinets are defined in Section 8.2.2. The position of the SCPs and distribution cabinets along with their usage are given per room from Section 8.3 to 8.6.

8.1 Power quality

Paranal is connected to the Chilean power grid via a power conditioning system to clean the quality of the delivered power. Paranal also offers for critical components an Uninterruptable Power Supply.

8.1.1 Non-UPS

The quality of the non-ups power is given by the specifications of the Power Conditioning System installed at Paranal which aims at cleaning the quality of the power delivered by the Chilean power grid. The Power Conditioning System uses a 1250 kVA 400 V 50 Hz MTU Engine from EURO-DIESEL The technical specifications are given in Annex A: Power Conditioning System Technical Specifications.

8.1.2 UPS

The UPS is using a 300 kVA (6 impulse) system from Liebert. The quality of the power distributed by this system is given in the technical specifications of the system available in Annex B: UPS Technical Specifications.

The UPS delivers power for at least 90 minutes after the failure of the main power.

8.2 Connections to the power distribution system

8.2.1 Connections to the SCP

Different sockets outlets are available for the temporary connection equipment:

- 400 VAC, 50 Hz (One connector: red-colour coded panel socket outlet; three-phases, neutral and earthing contact at the 6h position; rated current 16A, as per CENELEC document HD 196 S1 (1978)/IEC 309/CEE-el 17.
- 230 VAC, 50 Hz, (Two connectors: white or light grey coloured panel socket outlet; phase, neutral and earthing contact; rated current 10/16A, as per CEE-el 7/VII (Schuko).
- 230 VAC Uninterruptible Power Supply (UPS), 50 Hz, (Two connectors: blue-colour coded panel socket outlet, single-phase, neutral and earthing contact at the 6h position, rated current 16A, as per CENELEC document HD 196 S1 (1978)/IEC 309/CEE-el 17.

In addition to the socket outlets, power connection to normal or UPS power may also be via direct connection to terminal blocks inside the SCP. Details of the internal electrical connections are given in AD3.

Equipment connected to the SCP electrical socket-outlets shall conform to the following requirements:

- The peak electrical current drawn from one SCP must not exceed 16A per phase for the normal electrical supply, and 16A total for the UPS supply.
- The total average electrical power taken from the UPS outlets by instruments shall not exceed 2 kW per SCP. The total average non-UPS electrical power shall not exceed 6 kW per SCP without the written agreement of ESO.

- Electrical equipment connected to the SCP must respect the EMC requirements for susceptibility and emissions given in AD4.
- The requirements for the design and implementation of electronic equipment contained in AD4 shall be applicable to all equipment connected to the SCP.
- All fuses, circuit breakers and residual current detectors required for the protection of the instrument, supply cables or operator shall be incorporated in the instrument concerned.

8.2.2 Connections to the distribution cabinets

The distribution cabinets contain breakers and differential breakers as described in the following sections (from section 8.3 to 8.6). When not specified otherwise the brand of the breakers is ABB.

8.3 VLTI Laboratory (IC108) connections points

Ref. #	Room	Approx. U coord. (m)	Approx. V coord. (m)
34	Interferometric Laboratory	42.0	-32.5
35	Interferometric Laboratory	48.5	-29.0
36	Interferometric Laboratory	59.5	-29.0
37	Interferometric Laboratory	62.5	-32.5

Table 30: position of the SCP in the VLTI Laboratory and usage.

Distribution cabinet	Approx U coord. (m)	Approx V coord. (m)
UPS – 11B	61.3	-29.0

Table 31: Position of the UPS cabinet of the power distribution system in the VLTI Laboratory.

Reference	System	Breaker description
QF1	DDL Optics table	DDA 202AC AP-R 0.03A, S202M C10
QF2	FSU FE	DDA 202AC AP-R 0.03A, S202M C6
QF3	FSU IRACE	DDA 202AC AP-R 0.03A, S202M C6
QF4	Laser Interlock	DDA 202A 0.5A, S202M C6
QF5	DDL Cabinet 3	DDA 202AC AP-R 0.03A, S202M C10
QF6	DDL Cabinet 2	DDA 202AC AP-R 0.03A, S202M C10
QF7	DDL Cabinet 1	DDA 202AC AP-R 0.03A, S202M C6
QF8	-	DDA 202AC AP-R 0.03A, S202M C16
QF9	-	DDA 202AC AP-R 0.03A, S202 C10
QF10	-	DDA 202AC AP-R 0.03A, S202 C10

QF11	Gravity Cabinet 1	DDA 202AC AP-R 0.03A, S202 C10
QF12	-	DDA 202AC AP-R 0.03A, S202 C10
QF13	Plug AMBER	DDA 202AC AP-R 0.03A, S202M C16
QF14	Plug PRIMA1 FINITO	DDA 202AC AP-R 0.03A, S202M C16
QF15	Plug PRIMA2	DDA 202AC AP-R 0.03A, S202M C16
QF16	Plug VINCI	DDA 202AC AP-R 0.03A, S202M C16
QF17	Plug MIDI	DDA 202AC AP-R 0.03A, S202M C16
QF18	Plug MIDI FO	DDA 202AC AP-R 0.03A, S202M C16
QF19	Plug LEONARDO MARCEL	DDA 202AC AP-R 0.03A, S202M C16
QF20	Plug Switchyard	DDA 202AC AP-R 0.03A, S202M C16
QF21	Plug Beam Compressor	DDA 202AC AP-R 0.03A, S202M C16
QF22	Plug DDL	DDA 202AC AP-R 0.03A, S202M C16
QF23	VI1	DDA 202AC AP-R 0.03A, S202M C16
QF24	VI1	DDA 202AC AP-R 0.03A, S202M C16
QF25	VI2	DDA 202AC AP-R 0.03A, S202M C16
QF26	VI2	DDA 204AC AP-R 0.03A, S204M C16
QF27	-	DDA 204AC AP-R 0.03A, S204M C10
QF28	-	DDA 202A AP-R 0.03A, S202M C10
QF29	-	DDA 202A AP-R 0.03A, S202M C10
QF30	-	DDA 202A AP-R 0.03A, S202M C10

Table 32: usage of the VLTI Laboratory UPS – 11B cabinet. QF23 and QF24 have been pre-allocated to the visitor focus VI1. QF25 and QF26 have been pre-allocated to the visitor focus VI2.

8.4 Combined Coude Laboratory (IC107) connections points

Ref. #	Room	Approx. U coord. (m)	Approx. V coord. (m)
43	Combined Coudé Laboratory	58.5	-17.0

Table 33: position of the SCP in the Combined Coudé Laboratory.

Distribution cabinet	Approx U coord. (m)	Approx V coord. (m)
UPS – 11E	48.0	-19.5
Non-UPS - 41	48.0	-25.0

Table 34: Position of the cabinets of the power distribution system in the Combined Coudé Laboratory.

Reference	System	Breaker description
QF1	-	DDA202 AC AP-R 30 mA, S202M C16
QF2	Gravity - Cabinet 2	DDA202 AC AP-R 30 mA, S202M C16
QF3	Gravity - Cabinet 3	DDA202 AC AP-R 30 mA, S202M C16
QF4	Gravity - Cabinet 4	DDA202 AC AP-R 30 mA, S202M C16
QF5	Gravity - Cabinet 5	DDA202 AC AP-R 30 mA, S202M C16
QF6	Gravity - Cabinet 6	DDA202 AC AP-R 30 mA, S202M C16
QF7	-	DDA202 AC AP-R 30 mA, S202M C16
QF8	MATISSE - WOP Cabinet	DDA202 AC AP-R 30 mA, S202M C16
QF9	MATISSE - LM Cabinet	DDA202 AC AP-R 30 mA, S202M C16
QF10	MATISSE - N Cabinet	DDA202 AC AP-R 30 mA, S202M C16
QF11	MATISSE – Cryo controller	DDA202 AC AP-R 30 mA, S202M C16
QF12	-	DDA202 AC AP-R 30 mA, S202M C16
QF13	-	DDA202 AC AP-R 30 mA, S202M C16
QF14	-	DDA202 AC AP-R 30 mA, S202M C16
QF15	-	DDA202 AC AP-R 30 mA, S202M C16
QF16	-	DDA202 AC AP-R 30 mA, S202M C16
QF17	ESPRESSO	(Merlin Gerin) S272 C63
QF18	I2	(Merlin Gerin) Multi9 vigi C60SI, Multi 9 C60N C25

Table 35: usage of the Combined Coudé Laboratory UPS – 11E cabinet

Reference	System	Breaker description
QF1	New I2 station	DDA 204A 0.3A, S204M C63
QF2	-	DDA 204A AP-R 0.03A, S204M C25
QF3	MATISSE compressor LM band	DDA 204A AP-R 0.03A, S204M C25
QF4	MATISSE compressor N band	DDA 204A AP-R 0.03A, S204M C25
QF5	WOP cabinet	DDA 204A AP-R 0.03A, S204M C16
QF6	LM band cabinet	DDA 204A AP-R 0.03A, S204M C16
QF7	N band cabinet	DDA 204A AP-R 0.03A, S204M C16
QF8	-	DDA 204A AP-R 0.03A, S204M C16
QF9	-	DDA 204A AP-R 0.03A, S204M C16
QF10	-	DDA 204A AP-R 0.03A, S204M C16

QF11	-	DDA 204A AP-R 0.03A, S204M C16
QF12	-	DDA 204A AP-R 0.03A, S204M C16
QF13	-	DDA 202A AP-R 0.03A, S202 C10
QF14	Gravity cabinet 2	DDA 202A AP-R 0.03A, S202 C16
QF15	Gravity cabinet 3	DDA 202A AP-R 0.03A, S202 C16
QF16	Gravity cabinet 4	DDA 202A AP-R 0.03A, S202 C16
QF17	Gravity cabinet 5	DDA 202A AP-R 0.03A, S202 C10
QF18	Gravity cabinet 6	DDA 202A AP-R 0.03A, S202 C16
QF19	Compressor cabinet	DDA 202A AP-R 0.03A, S202 C16
QF20	Enchufes auxiliaries ESPRESSO	DDA 202A AP-R 0.03A, S202 C16
QF21	-	DDA 202A AP-R 0.03A, S202 C16
QF22	-	DDA 202A AP-R 0.03A, S202 C16
QF23	-	DDA 202A AP-R 0.03A, S202 C16
QF24	-	DDA 202A AP-R 0.03A, S202 C16
QF25	-	DDA 202A AP-R 0.03A, S202 C16
QF26	-	DDA 202A AP-R 0.03A, S202 C10
QF27	-	DDA 202A AP-R 0.03A, S202 C10
QF28	-	DDA 202A AP-R 0.03A, S202 C16
QF29	-	DDA 202A AP-R 0.03A, S202M C16
QF30	-	DDA 202A AP-R 0.03A, S202M C16
QF31	-	DDA 202A AP-R 0.03A, S202M C16
QF32	-	DDA 202A AP-R 0.03A, S202M C16
QF33	-	DDA 202A AP-R 0.03A, S202M C16
QF34	-	DDA 202A AP-R 0.03A, S202M C16
QF35	-	DDA 202A AP-R 0.03A, S202M C16
QF36	-	DDA 202A AP-R 0.03A, S202M C16
QF37	-	DDA 202A AP-R 0.03A, S202 C10
QF40	ESSPRESSO line 1	S804B C80
QF41	ESSPRESSO line 1	S804B C80

Table 36: usage of the Combined Coudé Laboratory Non-UPS – 41 cabinet

Reference	System	Breaker description
QF1	DDL Table	DDA 202A AP-R 0.03A, S202M C10
QF2	DDL Cabinet 3	DDA 202A 0.5A, S202M C10
QF3	DDL Cabinet 2	DDA 202A 0.5A, S202M C10

QF4	DDL Cabinet 1	DDA 202A 0.5A, S202M C10
QF5	-	DDA 202AC AP-R 0.03A, S202M B10
QF6	-	DDA 202AC AP-R 0.03A, S202M B10

Table 37: normal power DDL

8.5 VLTI Storage room (IC104) connections points

Ref. #	Room	Approx. U coord. (m)	Approx. V coord. (m)
31	Storage Room	39.5	-35.0
33	Storage room	35.5	-29.5

Table 38: position of the SCP in the Combined Coudé Laboratory.

Distribution cabinet	Approx U coord. (m)	Approx V coord. (m)
UPS – 11C	37.6	-26.0
Non-UPS – 21B	37.1	-26.0

Table 39: position of the cabinets of the power distribution system in the Storage Room.

Reference	System	Breaker description
QF1	Metrology1	DS672 C10
QF2	VIBMET	DS672 C10
QF3	Metrology 3	DDA202 AC AP-R 0.03 A, S202 M C 6
QF4	Laser Interlock	DS672 C10
QF5	Oxygen monitor	DDA202 AC AP-R 0.03 A, S202 M C 6
QF6	-	DS672 C10
QF7	-	DS672 C10
QF8	VI1	DDA202 AC AP-R 0.03 A, S202 M C 16
QF9	VI1	DDA202 AC AP-R 0.03 A, S202 M C 16
QF10	VI2	DDA202 AC AP-R 0.03 A, S202 M C 16
QF11	VI2	DDA202 AC AP-R 0.03 A, S202 M C 16
QF12	VI2	DDA202 AC AP-R 0.03 A, S202 M C 16
QF13	VI2	DDA202 AC AP-R 0.03 A, S202 M C 16
QF14	-	DDA202 AC AP-R 0.03 A, S202 M C 16
QF15	-	DDA202 AC AP-R 0.03 A, S202 M C 16
QF16	-	DDA 204 AC AP-R 0.03 A, S204M C16

QF17	-	DDA 204 AC AP-R 0.03 A, S204M C10
QF18	-	DS672 C10
QF19	-	DS672 C10
QF20	-	DS672 C10

Table 40: usage of the Storage room UPS – 11C cabinet. QF8 and QF9 have been pre-allocated to the visitor focus VI1. QF10 to QF13 have been pre-allocated to the visitor focus VI2.

Reference	System	Breaker description
QF1	AIR #1	DDA202 30 mA S202M B10
QF2	AIR #2	DDA202 30 mA S202M B10
QF3	-	S202M C3
QF4	-	S202M C3
QF5	VI1	DDA202 50 mA S202M C10
QF6	VI2	DDA202 50 mA S202M C10

Table 41: usage of the Storage room Non-UPS – 21B cabinet. QF5 has been pre-allocated to the visitor focus VI1. QF6 has been pre-allocated to the visitor focus VI2.

8.6 VLTI Computer room (IC102) connections points

Distribution cabinet	Approx U coord. (m)	Approx V coord. (m)
UPS – 11A	35.0	14.0

Table 42: position of the cabinets of the power distribution system in the Computer room.

Reference	System	Breaker description
QF1	Sockets Cabinet 3	DDA 72 30 mA, S282 C16
QF2	Sockets Cabinet 4	DDA 72 30 mA, S282 C16
QF3	Sockets Cabinet 5	DDA 72 30 mA, S282 C16
QF4	Sockets Cabinet 6	DDA 72 30 mA, S282 C16
QF5	-	DS 672 C20, 30 mA
QF6	-	DDA 72 30 mA, S282 C16
QF7	Sockets Cabinet 9	DDA 72 30 mA, S282 C16
QF8	Sockets Cabinet 10	DDA 72 30 mA, S282 C16
QF9	Sockets Cabinet 11 (new APC rack)	DDA 72 30 mA, S282 C16
QF10	Sockets Cabinet 12 (new APC rack	DDA 72 30 mA, S282 C16
QF11	Sockets Cabinet 13 (new APC rack)	DDA 72 30 mA, S282 C16
QF12	Sockets Cabinet 14 (new APC rack)	DDA 72 30 mA, S282 C16

----	No name	C3, F202 AC
QF13	Sockets Cabinet 15 (new APC rack)	DDA 72 30 mA, S282 C16
QF14	Sockets Cabinet 16 (new APC rack)	DDA 72 30 mA, S282 C16
QF15	Sockets Cabinet 17	DDA 72 30 mA, S282 C16
QF16	Sockets Cabinet 18	DDA 72 30 mA, S282 C16
QF17	Sockets Cabinet 19	DDA 72 30 mA, S282 C16
QF18	Sockets Cabinet 20	DDA 72 30 mA, S282 C16
QF19	Sockets Cabinet 1 – Main Power DL1 and DL2	DDA 72 30 mA, S282 C16
QF20	Sockets Cabinet 2 – Main Power DL3 and DL4	DDA 72 30 mA, S282 C16
QF21	Access card reader VLTI Laboratory	DDA 72 30 mA, S282 C16
QF22	Estacion enchufes	DDA 72 30 mA, S282 C16
QF23	Cooling pump and refilling controllers	DDA 72 30 mA, S282 C16
QF24	Motion stop ATs	S272 C8
QF25	Sockets Cabinet 3 – Main Power DL5 and DL6	DDA 72 30 mA, S282 C16
QF26	M16 Units – tables 1 & 2	DDA 72 30 mA, S282 C16
QF27	M16 Units – tables 3 & 4	DDA 72 30 mA, S282 C16
QF28	IRIS	DDA 72 30 mA, S282 C16
QF29	Cabinete del VLTI	DDA 72 30 mA, S282 C16
QF30	EPOD webcam	DDA 72 30 mA, S282 C16
QF31	Rack 7	DDA 72 30 mA, S282 C16
QF32	PCI FIRE	DDA202 30 mA, S202M C16

Table 43: usage of the Computer room UPS – 11A cabinet

9. Interface between the VLTI complex data communication network and the instruments

The VLTI Control System provides three data communication channels to VLTI:

- Control Network (see AD6)
- Reflective Memory Network
- Two types of Time Bus

The LAN is used to convey commands from the Instrument Control Software to the VLTI Control Software and to transfer back replies and status reports. It is also used to bear the data traffic due to the access to the on-line database.

The VLTI Reflective Memory Network (RMN) is a dedicated high-speed data communication channel which carries real-time control data between computers, LCU or workstations.

Two different types of Time Bus distribute the UTC can be distributed to computing nodes of the VLTI Control System and instruments in order to synchronize real-time tasks.

The data communication network makes use of a network of optical fibers of different types. Connections are done on the SCP. SCP can be linked one to another thanks to patch panels located in the VLTI Computer Room. A list of SCP available and connection type is given by room from 9.4 to 9.7.

9.1 LAN

The VLT Control LAN is based on the latest mature industry standards for network technology (Fast Ethernet, Gigabit Ethernet), that supports the TCP/IP communication protocol. The VLTI Instrument Control System is connected to the VLTI Backbone through the VLT core devices to communicate to the rest of the VLTI.

An accurate description of the services and connection types available for ESO and Visitor instruments arriving to Paranal is given in AD5.

The address assignment and type of network interface for each instrument host are defined in AD6.

9.2 Time bus

The observatory reference time can be obtained through different protocols:

- ESO time bus for synchronization of VME LCU;
- IEEE 1588 v2 time for Beckhoff PLC, etc.
- NTP time for servers, etc.

9.2.1 ESO TIM

The VLTI Control System CPUs rely on the Time Reference System (TRS) to be synchronized to each other and to receive the UTC. The TRS gets the UTC from the GPS satellites and distributes it to all the LCUs using a dedicated Time Bus. The TRS is also available to the VLTI Instrument Control System through the SCPs. The Time Bus signal is split at the level of the VLTI Computer room to be sent to the different SCP using the network of fibers.

Each LCU requiring time synchronization better than 1 second shall be equipped with a Time Interface Module (TIM), AD8, a VME board developed by ESO, which is linked to the Time Bus and decodes the time signal to make it available to the other electronics within the LCU.

Channel 1	Channel 2	Channel 3	Channel 4

Board #3	SCP 42 P24 / Free	SCP 44 P24 / Lddl6	SCP 43 P07 / Free	TIM D0-1 in Cub 2
Board #4	SCP 31 P20 / Free	SCP 31 P19 / Free	TIM D1-1 In Cub 2	Cub 3 SP1 24 “Control Room”
Board #5	SCP 45 P24 / Free	SCP 30 P24 / Free	SCP 32 P24 / Free	SCP 33 P24 / Free
Board #6	SCP 36 P24 / Free	SCP 37 P24 / Free	SCP 40 P24 / Gravity TIM spare	SCP 41 P24 / Free
Board #7	Cub 3 SP4 P19 / C3 / (?)	SCP 30 P22 / Free	SCP 34 P24 / Free	SCP 35 P24 / Free
Board #8	Cub 3 SP5 P3 / C3 / (?)	Cub 3 SP5 P4 / C3 / (?)	SCP 31 P23 / Free	SCP 31 P24 / Free

Table 44: Cubiculo 1 B6, Rack “TIM D-2”

	Channel 1	Channel 2	Channel 3	Channel 4
Board #2	TIM 1 MATISSE SCP40 P17	TIM 1 MATISSE SCP40 P18	SCP 43 P08 / Free	Free
Board #3	Free	Free	Fiber #7 / lvibacq @Metrology #2	Fiber #8 / lvibpd / @Metrology #2
Board #4	Fiber #9 Spare @Metrology #2	Fiber #10 Spare @Metrology #2	SCP 44 P01 / Lddl4	SCP 44 P02 / Lddl2
Board #5	SCP 44 P03 / lddlhk	SCP 44 P04 / lddl8	SCP 44 P05 / Lddl3	SCP 44 P06 / Lddl1
Board #6	SCP 44 P07 / Fiber 13, To network Lddl6 (**)	Cub 18 Patch 3 F.O.8 / PRIMA TIM 5/3 / Lvgmon	SCP 45 P01 / Lariris	SCP 45 P03 / Ldlfacu

Table 45: Cubiculo 2 B5, Rack “TIME BUS PRIMA”

	Channel 1	Channel 2	Channel 3	Channel 4
Board #1	AT station C3 12	Test LCU3 (Cub 3, SP4, P24)	AT station J1 12	AT station I1 12
Board #2	AT station M0 12	AT station L0 12	AT station K0 12	AT station J6 12
Board #3	AT station J5 12	AT station J4 12	AT station J3 12	AT station J2 12

Board #4	SCP 30 P21 Free (weak)	Cub3 SP5 11 / C3 / (?)	Cub3 SP5 12 / C3 / (?)	Cub3 SP5 14 / C3 / (?)
Board #5	SCP 45 P06 / Free	TIM BUS NEW STATION	SCP 40 P23 / (?)	LGVREC

Table 46: Cubiculo 2 B5, Rack "TIM D-0"

	Channel 1	**Channel 2**	**Channel 3**	**Channel 4**
Board #3	AT station B4 12	AT station B5 12	AT station B2 12	AT station B3 12
Board #4	AT station C0 12	AT station C1 12	Cub3 SP3 13 / C3 / (?)	Free
Board #5	AT station D0 12	AT station D1 12	AT station D2 12	AT station H0 12
Board #6	AT station E0 12	AT station G0 12	AT station G1*12	AT station G2*12
Board #7	AT station B1 12	AT station B0 12	AT station A0*12	AT station A1*12
Board #8	Cub3 SP3 11 / C3 / (?)	Cub3 SP3 12 / C3 / (?)	Cub3 SP3 09 / C3 / (?)	Cub3 SP3 10 / C3 / (?)

Table 47: Cubiculo 2 B5, Rack "TIM D-1"

9.2.2 NTP time for servers

LCUs requiring less accuracy will synchronize their internal timers with the UTC via NTP over the network. The software interface to the TRS is provided by the LCC software.

9.2.3 IEEE 1588

Some newer standard components, Beckhoff PLCs for example, cannot use the ESO TIM bus for time synchronization and must rely on the IEEE1588 Time bus. For more information on the protocol, hardware and expected performance consult RD3.

In the VLTI complex, the IEEE1588 signal can be accessed from a switch installed in the Combined Coude Laboratory. Connection from the switch is made via Ethernet over copper cables.

Module ID	Output number	Usage
1	1	Gravity PLC (fibre)
	2	Gravity PLC (fibre)
2	1	Free
	2	Free
3	1	Free
	2	Free
4	1	Free
	2	Free

5	1	Gravity PLC (copper)
	2	Gravity PLC (copper)
6	1	Free
	2	Free
7	1	Free
	2	Free
8	1	Free
	2	Free
9	1	Free
	2	Free
10	1	Free
	2	Free

Table 48: IEEE 1588 VLTI distribution switch usage

9.3 Reflective Memory Network hardware interface

The Reflective Memory Network topology is a ring.

The nodes, LCU or workstation, are equipped with a dedicated electronic board which is interfaced to the other nodes by optical fibres, Table 49.

For one subsystem, nodes are connected locally together thanks to a patch panel to allow bypassing a whole subsystem easily. The different patch panels are connected to each other using the SCP and patch panels of the optical fibre infrastructure, **Error! Reference source not found.**.

The internal interfaces of the RMN ring are under the responsibility of the Paranal Information Technology (IT) group. The physical layout of the ring is under configuration control and described in AD6.

Node type	Model	Fibre type	Fibre connector type Rx / Tx
LCU	ABACO PMC5565PIORC	Multimode 62.5/125	LC / LC
Workstation	ABACO PCIE-5565PIORC	Multimode 62.5/125	LC / LC
Intermediate RMN patch panel	Custom made	Multimode 62.5/125	ST / ST

Table 49: hardware interface between the instrument and the RMN ring.

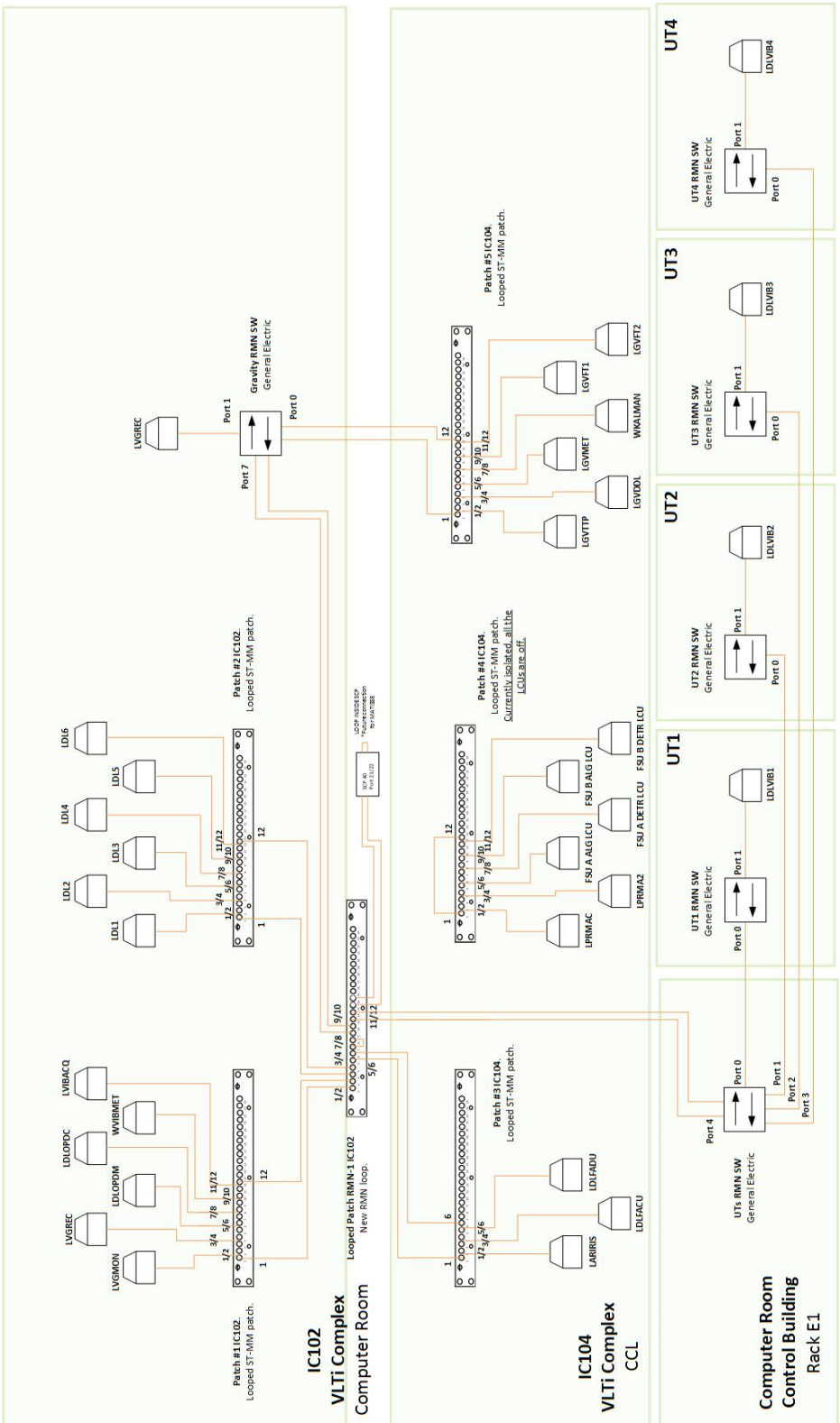

Figure 40: physical layout of the RMN ring as of July 2018. The physical layout is under configuration control by the Information Technology group and is described in AD6.

9.4 VLTI Laboratory (IC108) connections points

SCP #	Port #	Usage	Fibre type	Connector type	Approx. U coord. (m)	Approx. V coord. (m)
34	1 – 2	Xvg29	MM	ST – ST	42.0	-32.5
34	3 – 4	Pionier PLC Engineering	MM	ST – ST		
34	5 – 6	VI2 – VI2	MM	ST – ST		
34	7 – 8	VI2 – VI2	MM	ST – ST		
34	9 – 10	VI2 – VI2	MM	ST – ST		
34	11 – 12	VI2 – VI2	MM	ST – ST		
34	13 – 14	VI2 – VI2	MM	ST – ST		
34	15 – 16	VI1 – VI1	MM	ST – ST		
34	17 – 18	VI1 – VI1	MM	ST – ST		
34	19 – 20	VI1 – VI1	MM	ST – ST		
34	21 – 22	VI1 – VI1	MM	ST – ST		
34	23 – 24	VI1 – VI1	MM	ST – ST		
35	1 – 2	MATISSE Eth1	MM	ST – ST	48.5	-29.0
35	3 – 4	XAM1	MM	ST – ST		
35	5 – 6	Free – Free (was MATISSE ETH4)	MM	ST – ST		
35	7 – 8	Gravity Eth	MM	ST – ST		
35	9 – 10	Free – Free (was Matisse Eth2)	MM	ST – ST		
35	11 – 12	Free – Free (was Matisse Eth3)	MM	ST – ST		
35	13 – 14	Pionier	MM	ST – ST		
35	15 – 16	Pionier	MM	ST – ST		
35	17 – 18	Pionier RMN (To be removed)	MM	ST – ST		

35	19 – 20	Free - Free	SM	ST – ST		
35	21 – 22	Free - Free	SM	ST – ST		
35	23 – 24	TIM (Free) – TIM (Free)	MM	ST – ST		
36	1 – 2	Free – Free	MM	ST – ST	59.5	-29.0
36	3 – 4	Free – Free	MM	ST – ST		
36	5 – 6	Free – Free	MM	ST – ST		
36	7 – 8	Free – Free	MM	ST – ST		
36	9 – 10	Free – Free	MM	ST – ST		
36	11 – 12	Free – Free	MM	ST – ST		
36	13 – 14	Free – Free	MM	ST – ST		
36	15 – 16	Free – Free	MM	ST – ST		
36	17 – 18	Free – Free	MM	ST – ST		
36	19 – 20	Free – Free	MM	ST – ST		
36	21 – 22	Free – Free	MM	ST – ST		
36	23 – 24	Free – Free	MM	ST – ST		
37	1 – 2	Free – Free	MM	ST – ST	62.5	-32.5
37	3 – 4	Free – Free	MM	ST – ST		
37	5 – 6	Free – Free	MM	ST – ST		
37	7 – 8	Free – Free	MM	ST – ST		
37	9 – 10	Free – Free	MM	ST – ST		
37	11 – 12	Free – Free	MM	ST – ST		
37	13 – 14	Free – Free	MM	ST – ST		
37	15 – 16	Free – Free	MM	ST – ST		
37	17 – 18	Free – Free	MM	ST – ST		
37	19 – 20	Free – Free	MM	ST – ST		
37	21 – 22	Free – Free	MM	ST – ST		
37	23 – 24	Free – Free	MM	ST - ST		
MATISSE SCP	1A	MATISSE LH2RG	SM	LC – LC		
MATISSE SCP	1B	Free	SM	LC – LC		
MATISSE SCP	1C	Free	SM	LC – LC		

MATISSE SCP	2A	MATISSE AQCN2	SM	LC – LC		
MATISSE SCP	2B	Free	SM	LC – LC		
MATISSE SCP	2C	Free	SM	LC – LC		
MATISSE SCP	3A	MATISSE SPARE	SM	LC – LC		
MATISSE SCP	3B	Free	SM	LC – LC		
MATISSE SCP	3C	Free	SM	LC – LC		
MATISSE SCP	4A	MATISSE AQLN1	SM	LC – LC		
MATISSE SCP	4B	Free	SM	LC – LC		
MATISSE SCP	4C	Free	SM	LC – LC		
MATISSE SCP	5A	Free	SM	LC – LC		
MATISSE SCP	5B	Free	SM	LC – LC		
MATISSE SCP	5C	Free	SM	LC – LC		
MATISSE SCP	6A	Free	SM	LC – LC		
MATISSE SCP	6B	Free	SM	LC – LC		
MATISSE SCP	6C	Free	SM	LC – LC		
MATISSE SCP	7A	Free	SM	LC – LC		
MATISSE SCP	7B	Free	SM	LC – LC		
MATISSE SCP	7C	Free	SM	LC – LC		
MATISSE SCP	8A	Free	SM	LC – LC		
MATISSE SCP	8B	Free	SM	LC – LC		

MATISSE SCP	8C	Free	SM	LC – LC		
MATISSE SCP	9A	Free	SM	LC – LC		
MATISSE SCP	9B	Free	SM	LC – LC		
MATISSE SCP	9C	Free	SM	LC – LC		
MATISSE SCP	10A	Free	SM	LC – LC		
MATISSE SCP	10B	Free	SM	LC – LC		
MATISSE SCP	10C	Free	SM	LC – LC		
MATISSE SCP	11A	Free	SM	LC – LC		
MATISSE SCP	11B	Free	SM	LC – LC		
MATISSE SCP	11C	Free	SM	LC – LC		
MATISSE SCP	12A	Free	SM	LC – LC		
MATISSE SCP	12B	Free	SM	LC – LC		
MATISSE SCP	12C	Free	SM	LC – LC		

Table 50: data distribution network SCP usage in the VLTI Laboratory. TBC indicates that a fibre is connected to the port but the exact usage has to be confirmed. Ports of SCP 34 are pre-allocated to the visitor foci VI1 and VI2.

9.5 VLTI Tunnel (IC109) connections points

9.6 Combined Coude Laboratory (IC107) connections points

SCP #	Port #	Usage	Fibre type	Connector type	Approx. U coord. (m)	Approx. V coord. (m)
40	1 – 2	IEEE 1588	MM	ST – ST	47.5	-23.5
40	3 – 4	TBC - TBC	MM	ST – ST		
40	5 – 6	Free - T1 (TBC)	MM	ST – ST		

40	7 – 8	Free - T2 (TBC)	MM	ST – ST		
40	9 – 10	B 20 20 (TBC) - Free	MM	ST – ST		
40	11 – 12	Free – B 20-19 (TBC)	MM	ST – ST		
40	13 – 14	CAS BOX	MM	ST – ST		
40	15 – 16	Gravity CU DIODE (TBC) - Free	MM	ST – ST		
40	17 – 18	TIM MATISSE	MM	ST – ST		
40	19 – 20	Free - Free	MM	ST – ST		
40	21 – 22	RMN MATISSE	MM	ST – ST		
40	23 – 24	TIM (TBC) - TIM spare Gravity	MM	ST – ST		
41	Incoherent Combining Laboratory area				47.5	-15.0
42	Incoherent Combining Laboratory area				52.5	-8.0
43	1 – 2	Security Camera CCL	MM	ST – ST	58.5	-17.0
43	3 – 4	Free - Free	MM	ST – ST		
43	5 – 6	ESPRESSO ALPIQ	MM	ST – ST		
43	7 – 8	TIM (Available) – TIM (Available)	MM	ST – ST		
43	9 – 10	RMN DDL	MM	ST – ST		
43	11 – 12	Lddl2 LAN	MM	ST – ST		
43	13 – 14	Free – Free was Lddopdc LAN	MM	ST – ST		
43	15 – 16	Lddl4 LAN	MM	ST – ST		
43	17 – 18	lddlhkl LAN	MM	ST – ST		
43	19 – 20	Free - Free	MM	ST – ST		

43	21 – 22	Lddl3 LAN	MM	ST – ST		
43	23 – 24	Lddl1 LAN	MM	ST – ST		
44	1 – 2	Lddl4 TIM – lddl2 TIM	MM	ST – ST		
44	3 – 4	Lddlhk TIM – lddl8 TIM	MM	ST – ST		
44	5 – 6	Lddl3 TIM – lddl1 TIM	MM	ST – ST		
44	7 – 8	Lddl6 LAN	MM	ST – ST		
44	9 – 10	Lddl8 LAN	MM	ST – ST		
44	11 – 12	Free - Free	MM	ST – ST		
44	13 – 14	Free - Free	MM	ST – ST		
44	15 – 16	Free - Free	MM	ST – ST		
44	17 – 18	Free - Free	MM	ST – ST		
44	19 – 20	Free - Free	MM	ST – ST		
44	21 – 22	Free - Free	MM	ST – ST		
44	23 – 24	Free – TIM lddl6	MM	ST – ST		

Table 51: data distribution network SCP usage in the Combined Coudé Laboratory. TBC indicates that a fibre is connected to the port but the exact usage has to be confirmed.

9.7 VLTI Storage room (IC104) connections points

SCP #	Port #	Usage	Fibre type	Connector type	Approx. U coord. (m)	Approx. V coord. (m)
30	1 – 2	Free – Free	MM	ST – ST	40.5	-30.0
30	3 – 4	Free – Free	MM	ST – ST		
30	5 – 6	Lariris LAN	MM	ST – ST		
30	7 – 8	larics3 LAN	MM	ST – ST		
30	9 – 10	Free – Free	MM	ST – ST		
30	11 – 12	lariris 2nd ETH	MM	ST – ST		
30	13 – 14	Free - Free	MM	ST – ST		

30	15 – 16	Free – Free	MM	ST – ST		
30	17 – 18	Free – Free	MM	ST – ST		
30	19 – 20	Free - Free	MM	ST – ST		
30	21 – 22	Free – TIM (Available)	MM	ST – ST		
30	23 – 24	Free – TIM (Available)	MM	ST – ST		
31	1 – 2	Larics1 LAN	MM	ST – ST	39.5	-35.0
31	3 – 4	Free – Free (was lvnics1)	MM	ST – ST		
31	5 – 6	Free – Free (was lartccd)	MM	ST – ST		
31	7 – 8	Ldlfmu LAN	MM	ST – ST		
31	9 – 10	Ldlfadu LAN	MM	ST – ST		
31	11 – 12	Ldlfacu LAN	MM	ST – ST		
31	13 – 14	Larics2 LAN	MM	ST – ST		
31	15 – 16	FINITO patch	MM	ST – ST		
31	17 – 18	Ldlfadu 5576 RCV – ldlfacu 5576 xmit	MM	ST – ST		
31	19 – 20	TIM (Available) - TIM (Available)	MM	ST – ST		
31	21 – 22	Free - Free	MM	ST – ST		
31	23 – 24	TIM (Available) – TIM (Available)	MM	ST – ST		
32	1 – 2	XAM2	MM	ST – ST	35.5	-32.5
32	3 – 4	VI1 – VI1	MM	ST – ST		

32	5 – 6	VI1 – VI1	MM	ST – ST		
32	7 – 8	VI1 – VI1	MM	ST – ST		
32	9 – 10	VI1 – VI1	MM	ST – ST		
32	11 – 12	VI1 – VI1	MM	ST – ST		
32	13 – 14	VI1 – VI1	MM	ST – ST		
32	15 – 16	Vibmet lvibpd VCM virtual LAN	MM	ST – ST		
32	17 – 18	Lvibpd LAN	MM	ST – ST		
32	19 – 20	Lvibacq LAN	MM	ST – ST		
32	21 – 22	Vibmet RMN	MM	ST – ST		
32	23 – 24	Free – Free	MM	ST – ST		
33	1 – 2	VI2 – VI2	MM	ST – ST	35.5	-29.5
33	3 – 4	VI2 – VI2	MM	ST – ST		
33	5 – 6	VI2 – VI2	MM	ST – ST		
33	7 – 8	VI2 – VI2	MM	ST – ST		
33	9 – 10	VI2 – VI2	MM	ST – ST		
33	11 – 12	VLTI Laser Interlock SPARE	MM	ST – ST		
33	13 – 14	VLTI Laser Interlock UT1	MM	ST – ST		
33	15 – 16	VLTI Laser Interlock UT2	MM	ST – ST		
33	17 – 18	VLTI Laser Interlock UT3	MM	ST – ST		
33	19 – 20	VLTI Laser Interlock UT4	MM	ST – ST		
33	21 – 22	Free - Free	MM	ST – ST		
33	23 – 24	Free - Free	MM	ST – ST		
45	1 – 2	Lariris TIM - Free	MM	ST – ST		

45	3 – 4	Ldlfacu TIM - Free	MM	ST – ST		
45	5 – 6	Free – TIM (Available)	MM	ST – ST		
45	7 – 8	Free - Free	MM	ST – ST		
45	9 – 10	Free - Free	MM	ST – ST		
45	11 – 12	Free - Free	MM	ST – ST		
45	13 – 14	Free - Free	MM	ST – ST		
45	15 – 16	Free - Free	MM	ST – ST		
45	17 – 18	Free - Free	MM	ST – ST		
45	19 – 20	Free - Free	MM	ST – ST		
45	21 – 22	Free - Free	MM	ST – ST		
45	23 – 24	Free - Free	MM	ST – ST		

Table 52: data distribution network SCP usage in the Storage room. TBC indicates that a fibre is connected to the port but the exact usage has to be confirmed. Ports of SCP 31 and 33 are pre-allocated to the visitor foci VI1 and VI2.

10. Interface between the VLTI complex cable routing network and the instruments

The VLTI complex is equipped with a network cable trays and feedthrough to allow routing cables to and from almost any location.

10.1 Cable trays network

The layout of the network of cable trays is defined in AD1.

10.2 Feedthroughs

The characteristics and usage of the feedthroughs leading to the VLTI Laboratory are defined in Table 53.

Ref. #	From:	To:	Number and Shape	Approx. height wrt floor	Size (mm x mm, ∅ mm)	Detailed drawing	Usage	Wall thickness (mm)
1	VLTI Laboratory	Storage room	1 rectangular	115 mm	110*680	AD1	ARAL, VISITOR 1	1240
2	VLTI Laboratory	Storage room	1 rectangular	2355 mm	110 x 670	AD1	Reserved for cryogenics piping (IRIS and possibly VISITOR1 and 2)	1240

3	VLTI Laboratory	Storage room	8 circular	500 mm	150	AD1	3-1: VISITOR 2 3-2: VISITOR 2 3-3: IRIS cryo controller + 4 ARAL motor cables 3-4: VIBMET 3-5: VISITOR 2 3-6: VISITOR 2 3-7: MARCEL blackbody fiber + PRIMA FE Patch cord 3-8: VISITOR 2	1240
4	VLTI Laboratory	CCL	1 rectangular	100 mm	135 x 490	AD1	MATISSE LN2 refill and exhaust lines + cables	985
5	VLTI Laboratory	CCL	1 rectangular	2300 mm	640 x 130	AD1	GRAVITY LN2 refill + cables	985
6	VLTI Laboratory	CCL	1 circular	1460 mm	65	AD1	Free	985
7	VLTI Laboratory	CCL	1 circular	1175 mm	80	AD1	Free	985
8	VLTI Laboratory	CCL	1 circular	190 mm	200	AD1	GRAVITY flex-line	985
9	VLTI Laboratory	CCL	1 circular	210 mm	200	AD1	Free	985
10	VLTI Laboratory	CCL	1 circular	165 mm	200	AD1	Free	985
11	VLTI Laboratory	CCL	1 circular	2810 mm	200	AD1	MATISSE L band: - PTC flexline	985
12	VLTI Laboratory	CCL	1 circular	2810 mm	200	AD1	MATISSE N band: - PTC flexline	985
13	VLTI Laboratory	CCL	1 rectangular			AD1	GRAVITY exhaust flex line	985
14	VLTI Laboratory	VLTI Tunnel				AD1	PIONIER	
15	VLTI Laboratory	VLTI Tunnel				AD1	PIONIER	

Table 53: characteristics and usage of the feedthroughs leading to the VLTI Laboratory.

11. Optical interface between the VLTI and the instruments

11.1 Pupil

11.1.1 Pupil shape and diameter

In both AT and UT cases, the aperture stop is the M2.

The pupil diameter in the laboratory is the same when using ATs or UTs. Due to a non-conformity of AT1 STS optics, the pupil delivered by AT1 in the laboratory has a slightly larger diameter, RD7 and RD8.

Telescope	Pupil diameter (mm)	
	AT	UT
1	19.8 +/- 0.3	18.0 +/- 0.3
2	18.0 +/- 0.3	18.0 +/- 0.3
3	18.0 +/- 0.3	18.0 +/- 0.3
4	18.0 +/- 0.3	18.0 +/- 0.3

Table 54: pupil diameter in the laboratory.

11.1.2 Pupil position

11.1.2.1 Nominal position

The pupil is reimaged several times along the VLTI optical train. Their nominal position in the laboratory are defined in Table 55 and are identical when using ATs or UTs.

IP	U (m)	V(m)	W(m)
1	46.560	-34.215	-1.490
3	46.560	-33.975	-1.490
5	46.560	-33.735	-1.490
7	46.560	-33.495	-1.490

Table 55: nominal position of the pupil in the VLTI laboratory.

11.1.2.1.1 Case of Gravity

In the case of Gravity the pupil is positioned about 20 cm downstream of the nominal position due to the current location of the Beam Combiner Instrument.

IP	U (m)	V(m)	W(m)
1	46.360	-34.215	-1.490
3	46.360	-33.975	-1.490
5	46.360	-33.735	-1.490

7	46.360	-33.495	-1.490

Table 56: nominal position of the pupil in the VLTI laboratory for IP1, 3, 5 and 7 when used with Gravity.

11.1.2.2 Lateral position accuracy

Right after alignment on IRIS, the lateral position of the pupil is accurate within +/- 1 % of the pupil diameter.

Then, during operation, several contributions degrade the pupil position accuracy as defined in Table 57 for the ATs and Table 58 for the UTs.

The contribution of the DLs increases with the OPL of DL due to the increasing curvature of the VCM. The data in the table below are for the worst case, i.e the DL at the end of the rails. The DL unperfect rail shape generates instability at different spatial frequencies. The wobble is due to the carriage wheels and its period is 2.46 m OPL. The hysteresis appears when the carriage changes direction. The magnitude of the hysteresis is very different from one DL to another and depends on the temperature of the tunnel, i.e the time of the year. Statistics of the effects of the hysteresis on the pupil motion are given in Annex D: statistics of the pupil motion due to hysteresis.

The effect of turbulence in the light ducts and tunnel is neglectable compared to the motion introduced by the telescope and the DL.

	AT azimuth runout	AT derotator runout	DL rail shape + wobble	DL hysteresis
Pupil lateral position error (% of diameter)	< 5 %	< 5 %	< 5 %	< 20 %

Table 57: pupil lateral instability with the ATs

	UT azimuth runout	DL rail shape + wobble	DL hysteresis
Pupil lateral position error (% of diameter)	< 5 %	< 5 %	< 20 %

Table 58: pupil lateral instability with the UTs

11.1.2.3 Longitudinal position accuracy

The Variable Curvature Mirror (VCM) inside the delay line has the function to re-image the pupil at a desired location in the interferometric lab. In the current lab configuration, the VCM re-images the pupils at the locations defined in Table 55.

Currently, the pupil position can be blindly positioned with a precision of +/- 3 m before the Beam Compressors depending on the interferometer arm configuration. As the residual error for a given configuration (station + DL + input channel) is repeatable over time, the actual error after calibration can be reduced to +/- 250 mm before the Beam Compressor which corresponds to +/- 12.8 mm after the beam compressor.

	UT	AT
Longitudinal position error after the BC	+/- 12.8 mm	+/- 12.8 mm

Table 59: pupil longitudinal position error after the BC.

11.1.3 Pupil rotation

The pupil rotation is in general defined in a differential manner. The pupil rotation for any telescope position is the rotation angle which allows to superimpose the pupil as it is seen in this position to the pupil as seen when the telescope is in its reference position.

As it is not practical to have a differential definition, we defined it in an “absolute” way in the pupil plane located after the switchyard as being the angle of the Y axis of the M2 in the Paranal (V,W) reference frame.

The pupil rotation ν after the switchyard is given by:

$$\nu = \pm(a - A - 90°) + \Delta\nu + \theta_{rot}$$

With:

1. a telescope altitude angle,
2. A telescope azimuth angle,
3. $\Delta\nu$ angle in the (V,W) reference frame of the Y axis of the M2 imaged after the switchyard when the telescope is in its reference position,
4. θ_{rot} the angle of the derotator with respect to its reference position.

The $\Delta\nu$ sign depends on possible rotation between the telescope Coudé and the VLTI laboratory.

θ_{rot} is always 0 for the UTs since they do not use a derotator.

In the case of the ATs, θ_{rot} depends on the type of presets. Please see AD10 for more details.

	Reference position	Pupil rotation
AT on a Northern station	Atitude = 90 ° Azimuth = 0 ° Derotator = 0 °	$\nu = a - A + 12.98° + \theta_{rot}$
AT on a Southern station	Atitude = 90 ° Azimuth = 0 ° Derotator = 0 °	$\nu = a - A - 167.02° + \theta_{rot}$
UT	Atitude = 90 ° Azimuth = 0 °	$\nu = -a + A - 12.98°$

Table 60: pupil rotation after the switchyard.

The errors in the orientation of the pupil will be dominated by alignment errors of the mirrors in the complete optical train (e.g. M9 misalignment around the Azimuth axis). The expected pupil orientation errors is < ± 60 arcmin.

11.2 Wavefront

11.2.1 Field of view

11.2.1.1 At coude focus

The Field Of View (diameter) available at the coudé focus is as follows:

	UT	AT
Unvignetted FOV	> 120 arcsec	> 120 arcsec

Table 61: Field Of View (on the sky) at the coudé focus.

The guide star used by the adaptive optics system, CIAO or MACAO on UTs and NAOMI on the ATs, must be selected within this FOV.

11.2.1.2 In the VLTI laboratory

The Field Of View (diameter) available at the input of the instrument is as follows:

	UT	AT
Unvignetted FOV	> 2 arcsec	> 4 arcsec

Table 62: Field Of View (on the sky) at instrument input.

The STS allows to pick up 1 field of diameter as mentioned in Table 62 anywhere on a global Coudé field of view of 120 arcsec diameter.

11.2.2 Field of view orientation

The field rotation is in general defined in a differential manner. The field rotation for any telescope position is the rotation angle which allows to superimpose the field as it is seen in this position to the field as seen when the telescope is in its reference position (therefore field rotation is zero by definition when altitude = 90 deg, azimuth = 0 deg and derotator (in the case of ATs only) at 0 deg).

As it is not practical to have a differential definition, it is defined here in an “absolute” way after the switchyard as being the angle in the Paranal (V,W) reference frame of the North direction in the focal plane of an imaginary lens that would be placed after the switchyard.

The field rotation φ after the switchyard is given by:

$$\varphi = \pm(-p + a - A - 90) + \Delta\varphi - \varphi_{derot}$$

With:

1. p parallactic angle,
2. a the telescope altitude angle,
3. A the telescope azimuth angle (0º to the South and 90º to the East),
4. $\Delta\varphi$ angle in the (V,W) reference frame of the North direction after the switchyard when the telescope is in its reference position.
5. φ_{derot}, the derotator offset.

In the case of the UTs θ_{rot} is always 0 since there is no derotator.

In the case of the ATs, an optical derotator, located before the coudé focus, is used to compensate for the field rotation and apply an offset, called presetOffset, to the field

orientation. The value of this offset depends on the type of preset. Please refer to AD10 and RD9 for more details.

The results of the computation of the field rotation after the switchyard depend on

1. the type of telescope,
2. their location with respect to the VLTI tunnel,
3. the use of the DL in single or double pass.

Some results are given in Table 63. The value of the field rotation in the VLTI laboratory, using the same conventions, is published by the ISS in its database, AD10.

Telescope	Relay	Delay Line	Switchyard	Field rotation	
				North/DEC	East/RA
UT	STS	Simple	Compressed	+p-Alt+Az-12.98	-90
AT-N	STS	Simple	Compressed	-presetOffset-90	-90
AT-S	STS	Simple	Compressed	-presetOffset-90	-90
AT-N	STS	Double	Compressed	270+presetOffset	+90
AT-S	STS	Double	Compressed	270+presetOffset	+90

Table 63: field orientation in the VLTI laboratory.

11.2.3 Wavefront quality

This section will be updated in a future version.

11.2.4 Residual tip-tilt

This section will be updated in a future version.

11.3 Optical transmission

The transmission values given in this section are defined as the ratio of the number of photons after reflection on the switchyard over the number of photons incident on the telescope primary mirror. These transmission values are therefore specific to the VLTI configuration (telescope used, single or double feed) and to the waveband considered.

	V band	J band	H band	K band	L band	N band
AT	< 0.2 %	> 11 %	> 23 %	> 28 %	> 29 %	> 33 %
UT	< 0.2 %	> 6 %	> 12 %	> 18 %	> 19 %	> 21 %

Table 64: minimum transmission after the switchyard mirror.

For information only, the evolution of the infrared transmission as measured on IRIS over several years is given in Annex E: Infrared transmission monitoring.

11.4 Polarization

A measurement campaign is scheduled for 2021. This section will be updated with the results in another version.

12. Interface between the VLTI complex safety systems and the instruments

12.1 Central Alarm System

The Central Alarm System is described in RD4. In the VLTI complex, one Alarm Connection Point (ACP) box is available behind the Gravity cabinets. Its usage is summarized in Table 65.

CAS box input	System
1	Free
2	GRAVITY
3	Oxygen sensors
4	ESPRESSO liquid leakage
5	VLTI Nitrogen
6	MATISSE
7	ESPRESSO
8	Free
9	Free
10	Free
11	Free
12	Free
13	Free
14	Free
15	Free
16	Free

Table 65: usage of the CAS ACP located in the CCL.

CAS box input	System
1	ATx Fire
2	ATx Pre-Fire
3	ATx Temperature Signal Cabinet
4	ATx Temperature Altitude Cabinet
5	ATx CWP4 Stop
6	ATx ACS-LCM Chiller Fail
7	ATx Power Chiller Fail
8	ATx NAOMI General Alarm

9	ATx CAS Connection (External push button after relocation)
10	Free
11	Free
12	Free
13	Free
14	Free
15	Free
16	Free

Table 66: usage of the AT CAS ACP.

12.2 VLTI Laser interlock

The VLTI Laser Interlock System implementation and operation are described in RD5.

The subsystems connected to the VLTI Laser Interlock are:

1. Gravity safety shutters.
2. VIBMET laser.

13. Software interface between the VLTI and the instruments

The main software interface between an instrument and VLTI is the Interferometer Supervisor Software, Section 13.1. An instrument may also be interfaced via the reflective memory network, Section 13.2.

13.1 Interferometer Supervisor Software

Interfaces between the instrument and the Interferometer Supervisor Software are described in the dedicated document AD7.

13.2 Reflective Memory Network software interface

The physical interface to the RMN is described in Section 9.3. The software interface corresponds to the assignment of the memory addresses to the different subsystems writing on the RMN. This is handled by the rmassLayout.h file available in Annex C: rmassLayout.h.

14. Annex A: Power Conditioning System Technical Specifications

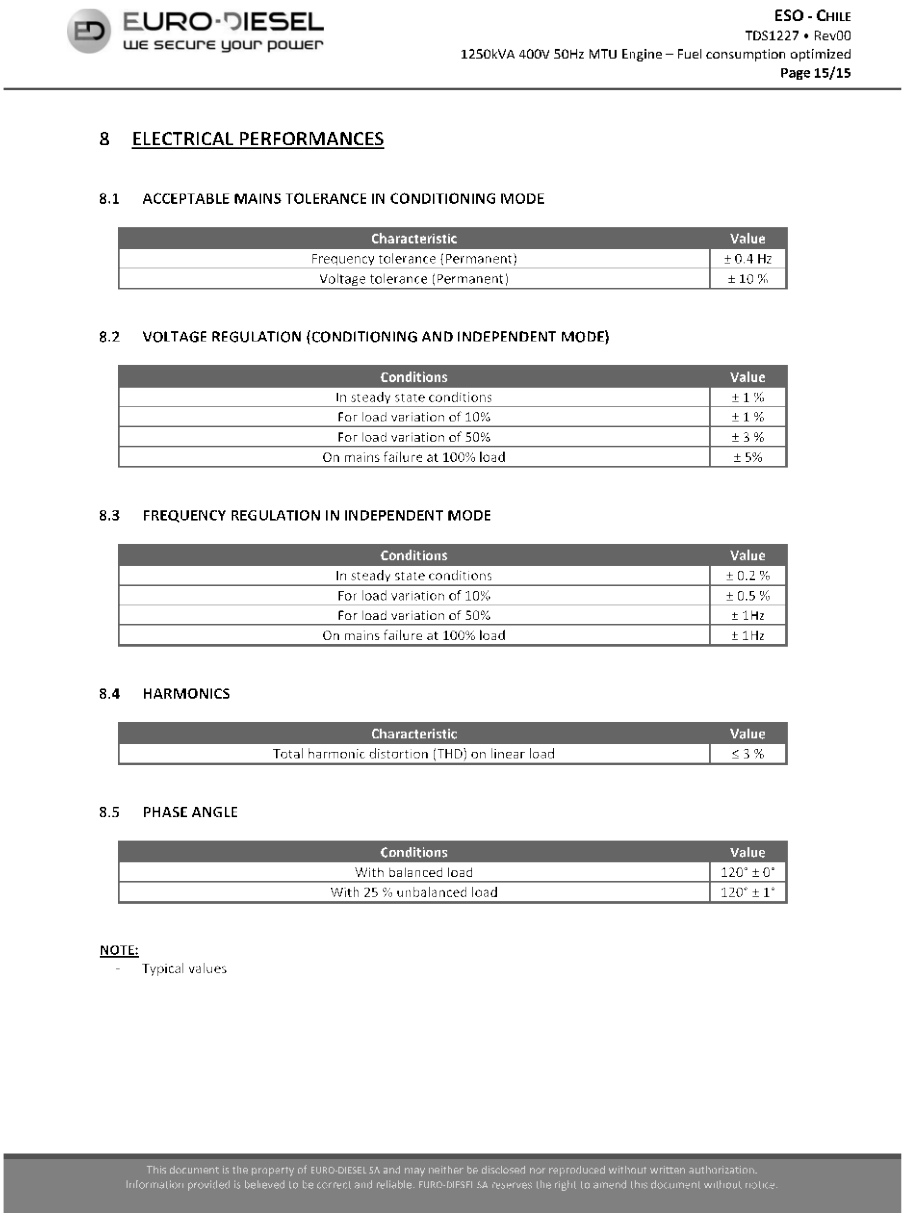

EURO-DIESEL
we secure your power

ESO - CHILE
TDS1227 • Rev00
1250kVA 400V 50Hz MTU Engine – Fuel consumption optimized
Page 15/15

8 ELECTRICAL PERFORMANCES

8.1 ACCEPTABLE MAINS TOLERANCE IN CONDITIONING MODE

Characteristic	Value
Frequency tolerance (Permanent)	± 0.4 Hz
Voltage tolerance (Permanent)	± 10 %

8.2 VOLTAGE REGULATION (CONDITIONING AND INDEPENDENT MODE)

Conditions	Value
In steady state conditions	± 1 %
For load variation of 10%	± 1 %
For load variation of 50%	± 3 %
On mains failure at 100% load	± 5%

8.3 FREQUENCY REGULATION IN INDEPENDENT MODE

Conditions	Value
In steady state conditions	± 0.2 %
For load variation of 10%	± 0.5 %
For load variation of 50%	± 1Hz
On mains failure at 100% load	± 1Hz

8.4 HARMONICS

Characteristic	Value
Total harmonic distortion (THD) on linear load	≤ 3 %

8.5 PHASE ANGLE

Conditions	Value
With balanced load	120° ± 0°
With 25 % unbalanced load	120° ± 1°

NOTE:
- Typical values

This document is the property of EURO-DIESEL SA and may neither be disclosed nor reproduced without written authorization.
Information provided is believed to be correct and reliable. EURO-DIESEL SA reserves the right to amend this document without notice.

Figure 41: Technical specifications of the power delivered by the Power Conditioning System.

15. Annex B: UPS Technical Specifications

Please consider the specifications of the LIEBERT TA 300 kVA 6 impulsos.

5.4 Características eléctricas del UPS (Rectificador de entrada).

tida.

❺= Coloque el puente en el tablero de control del rectificador (rápido o lento).

5.5 Características eléctricas del UPS (Circuito intermedio C.C.).

RLA y WET) y Ni-Cad con tensión y cargado de corriente constantes para unidades Europeas.

5.6 Características eléctricas del UPS (Salida del inversor)

or de la corriente de corte neutral donde las regulaciones locales lo permitan.

5.7 Características eléctricas del UPS (Red eléctrica de entrada del bypass)

al donde las regulaciones locales lo permitan.

Manual de instalación Sistema UPS único o "1+N" | Liebert Hipulse E | Capítulo 5 – "Especificación"

5.8 Características eléctricas del UPS (Prestación del sistema)

kW

			ro de entrada (4%)	24,8 con filtro de entrada (9%)	26,7 con filtro de entrada (4%)
Modo ECO		7.4	8.0	9.9	10.3

(07/04) Página 7

16. Annex C: rmassLayout.h

```
/*****************************************************************************
* E.S.O. - VLT project
```

```
*
* "@(#) $Id: rmassLayout.h 305507 2018-01-19 15:24:31Z rabuter $"
*
* who       when        what
* --------  ----------  ----------------------------------------------
* rabuter    2018-01-19  added defines for FTKSENS and modified type from DOUBLE to UINT32 for the
flag
* rdembet   2018-01-11  Fixed typos for MTLPIS and MTNPIS
* rdembet   2017-12-14  Clean up and merged VIBMET, GRAVITY & MATISSE areas
* smorel    2017-03-09  Added MATISSE areas
* tphan     2016-03-17  Commented out Matisse and PRIMA. Re-organise order of nodes.
* rdembet   2015-11-10  Add new items in GR OPDC table
* tphan     2015-08-23  Commented out wvgrmn
* tphan     2015-07-27  Added wmt.
* tphan     2015-06-30  Added wvgrmn.
* rabuter   2015-06-23  change lgvft3 to wgvkalm
* sg/ekw    2015-03-20  Adopt to new Metrology Design
*                       Date shift due to SVN confusions
* tphan     2015-03-22  Removed PRIMA LCUs from RMN ring.
* lb        2015-01-29  Corrected FDDL numbering
* rabuter   2015-01-29  Added TTP GRAVITY area
* tphan     2014-12-25  Updated GRAVITY layout.
* tphan     2014-07-10  Added RFM to DLs.
* tphan     2014-05-27  Added Matisse node ids. Moved rmassRMN_LAYOUT from rmassPublic.h.
* ekw       2014-05-12  Added lgvttp TTP_NODE
* rabuter   2013-05-02  Added Gravity node ids
* aramirez  2011-10-08  PPRS41845 Updated names in list of nodes, as per
*                       VLT-SPE-ESO-17100-3439
* swehner   2008-10-05  Created
*/

/************************************************************************
 *
 *----------------------------------------------------------------------
 */

#ifndef RMASS_LAYOUT_H
#define RMASS_LAYOUT_H

/************************************************************************
 * Contains the public global data and data type definitions
 * to be used in accessing the Reflective Memory in a safe way
 *----------------------------------------------------------------------
```

```
 */


/*
 ****************************************************************************
 * Header Files
 ****************************************************************************
 */

/* System Includes */

/*
 ****************************************************************************
 * Data Types
 ****************************************************************************
 */

#define rmassRfmBUFFER_LENGTH_DMA 128

/*
 * The rmassRMN_LAYOUT data structure will contain a list of all
 * data fields in the RMN window. It contains
 * - a _description_ in clear text
 * - a _token_, a short mnemonic string of max. 8 characters (has to be unique)
 * - the value's unit
 * - the frequency with which the data is provided (in Hertz)
 * - the data _type_ of the stored value
 * - and the _offset_ in the RMN window.
 *
 */
#define rmassTOKEN_LEN 8

typedef struct {
    char               description[70];
    char               token[rmassTOKEN_LEN+1];
    char               unit[12];
    double             period;
    rmassRMN_DATA_TYPE type;
    unsigned int       offset;
} rmassRMN_LAYOUT;

/*
 ****************************************************************************
```

```
 * List of nodes
 ******************************************************************************
 */

/*****************************************************************************
 * Contains the public global data and data type definitions
 * to be used in accessing the Reflective Memory in a safe way
 *----------------------------------------------------------------------------
 */

#define rmassOPDC_NODE        0x20
#define rmassOPDM_NODE        0x01

#define rmassIRIS_NODE        0x03

/* FINITO : ADU 0x4 ACU 0x5 */
#define rmassFSU_NODE         0x04
#define rmassFINITO_NODE      0x04

/* Delay Lines 1 to 8 */
#define rmassDL1_NODE         0x08
#define rmassDL2_NODE         0x09
#define rmassDL3_NODE         0x0A
#define rmassDL4_NODE         0x0B
#define rmassDL5_NODE         0x0C
#define rmassDL6_NODE         0x0D
#define rmassDL7_NODE         0x0E /* reserved in VLT-SPE-ESO-17100-343 */
#define rmassDL8_NODE         0x0F /* reserved */

/* DDL : dOPDC */
#define rmassDOPDC_NODE       0x10

/* PRIMA: LCU/WS re-used in the VIBMET project */
#define rmassVIBMET_ACQ       0x13
#define rmassVIBMET_WS        0x28

/* DDL 1 to 4 */
#define rmassDDL1_NODE        0x15
#define rmassDDL2_NODE        0x16
#define rmassDDL3_NODE        0x17
#define rmassDDL4_NODE        0x18 /* 0x19-0x1A reserved */
#define rmassDDL5_NODE        0x19
#define rmassDDL6_NODE        0x1A
```

```
#define rmassDDL7_NODE        0x1B
#define rmassDDL8_NODE        0x1C

/* RMN Recorder */
#define rmassRMNREC_NODE      0x1D

/* PRIMA: FSU A/B ACU's */
#define rmassPRIFSUA_ACU_NODE 0x1E
#define rmassPRIFSUB_ACU_NODE 0x1F

/* RMN Monitor */
#define rmassRMNMON_NODE      0x21

/* RMN Analysis WS. TPH 20150630 */
#define rmassRMNANALYSIS_NODE 0x22

/* MIDI */
#define rmassMILCU_NODE       0x30

/* VINCI */
#define rmassWVNDC_NODE       0x40
#define rmassVNLCU_NODE       0x41  /* not connected */

/* MACAO */
#define rmassMACAO_UT1_NODE   0x51
#define rmassMACAO_UT2_NODE   0x52
#define rmassMACAO_UT3_NODE   0x53
#define rmassMACAO_UT4_NODE   0x54

/* Nodes 0x55-60 reserved */

/* MANHATTAN2 */
#define rmassMANHATTAN_UT1_NODE   0x61
#define rmassMANHATTAN_UT2_NODE   0x62
#define rmassMANHATTAN_UT3_NODE   0x63
#define rmassMANHATTAN_UT4_NODE   0x64

/* PIONIER */
#define rmassPIONIER_NODE   0x70


/* GRAVITY */
#define rmassGRAV_METROLOGY_NODE   0x80
```

```
#define rmassGRAV_FDDL_NODE        0x81
#define rmassGRAV_PHASENSOR_NODE   0x82
#define rmassGRAV_OPDC_NODE        0x83
#define rmassGRAV_KALMAN_NODE      0x84
#define rmassGRAV_TTP_NODE         0x85

#define rmassGRAV_RMNREC_NODE      0x8D

/* MATISSE */
#define rmassMATISSE_WS_NODE      0x90
#define rmassMATISSE1_NODE        0x91
#define rmassMATISSE2_NODE        0x92

/* Indentifier of instrument Using the delay offset for Fringe Tracking*/
#define rmassFTKSENS_NONE         0
#define rmassFTKSENS_GRAVITY      1
#define rmassFTKSENS_MATISSE      2



/*
 * Please put the LCUs in this list in the order in which they appear
 * in the new Rm ring.
 * Extracted and to be updated from VLT-SPE-ESO-17100-3439, issue 5.0.
 */

rmassNODE_TYPE rmnNodes[] = {
/*  {"lvgmon",  rmassRMNMON_NODE, 0, 0.0},
    {"ldlvib4", rmassMANHATTAN_UT4_NODE, 0, 0.0},
    {"ldl6",    rmassDL6_NODE, 0, 0.0},
    {"ldl5",    rmassDL5_NODE, 0, 0.0},
    {"ldl4",    rmassDL4_NODE, 0, 0.0},
    {"ldlfadu", rmassFINITO_NODE, 0, 0.0},
    {"ldlfacu", rmassFINITO_NODE+1, 0, 0.0},
    {"lmiics1", rmassMILCU_NODE, 0, 0.0},
    {"ldlvib3", rmassMANHATTAN_UT3_NODE, 0, 0.0},
    {"ldlopdc", rmassOPDC_NODE, 0, 0.0},
    {"lvgrec",  rmassRMNREC_NODE, 0, 0.0},
    {"ldlopdm", rmassOPDM_NODE, 0, 0.0},
    {"ldl3",    rmassDL3_NODE, 0, 0.0},
    {"ldl2",    rmassDL2_NODE, 0, 0.0},
    {"ldl1",    rmassDL1_NODE, 0, 0.0},
    {"ldlvib2", rmassMANHATTAN_UT2_NODE, 0, 0.0},
```

```
    {"ldlvib1", rmassMANHATTAN_UT1_NODE, 0, 0.0},
*/  {"",        -1, 0, 0.0}
};

/*
 * Please put the LCUs in this list in the order in which they appear
 * in the new Rm ring.
 * Extracted and to be updated from VLT-SPE-ESO-17100-3439, issue 5.0.
 */

rmassNODE_TYPE rfmNodes[] = {
    {"lariris", rmassIRIS_NODE, 0, 0.0},
    {"ldlfacu", rmassFINITO_NODE+1, 0, 0.0},
    {"ldlfadu", rmassFINITO_NODE, 0, 0.0},

    {"lgvrec",  rmassGRAV_RMNREC_NODE, 0, 0.0},
    {"lgvttp",  rmassGRAV_TTP_NODE, 0, 0.0},
    {"lgvddl",  rmassGRAV_FDDL_NODE, 0, 0.0},
    {"lgvmet",  rmassGRAV_METROLOGY_NODE, 0, 0.0},
    {"wgvkalm", rmassGRAV_KALMAN_NODE, 0, 0.0},
    {"lgvft1",  rmassGRAV_PHASENSOR_NODE, 0, 0.0},
    {"lgvft2",  rmassGRAV_OPDC_NODE, 0, 0.0},

    {"ldlvib1", rmassMANHATTAN_UT1_NODE, 0, 0.0},
    {"ldlvib2", rmassMANHATTAN_UT2_NODE, 0, 0.0},
    {"ldlvib3", rmassMANHATTAN_UT3_NODE, 0, 0.0},
    {"ldlvib4", rmassMANHATTAN_UT4_NODE, 0, 0.0},

    {"ldlopdc", rmassOPDC_NODE, 0, 0.0},
    {"ldlopdm", rmassOPDM_NODE, 0, 0.0},
    {"lvgrec",  rmassRMNREC_NODE, 0, 0.0},
    {"lvgmon",  rmassRMNMON_NODE, 0, 0.0},

    {"ldl1",    rmassDL1_NODE, 0, 0.0},
    {"ldl2",    rmassDL2_NODE, 0, 0.0},
    {"ldl3",    rmassDL3_NODE, 0, 0.0},
    {"ldl4",    rmassDL4_NODE, 0, 0.0},
    {"ldl5",    rmassDL5_NODE, 0, 0.0},
    {"ldl6",    rmassDL6_NODE, 0, 0.0},

    {"lvbacq",  rmassVIBMET_ACQ, 0, 0.0},
    {"wvbmet",  rmassVIBMET_WS,  0, 0.0},
```

```
/*  {"wmt",     rmassMATISSE_WS_NODE, 0, 0.0}, */
/*  {"lmtics1", rmassMATISSE1_NODE, 0, 0.0}, */
/*  {"lmtics2", rmassMATISSE2_NODE, 0, 0.0}, */

/*  {"wvgrmn",  rmassRMNANALYSIS_NODE, 0, 0.0}, */
/*  {"wpndcs",  rmassPIONIER_NODE, 0, 0.0}, */
    {"",       -1, 0, 0.0}
};

/* IMPORTANT:
 * - The token has to be unique!
 * - The list has to be ordered by incrasing memory offsets
 * - By agreement the tokens are grouped to messages which comprise of
 *   contigious fields which usually belong to a particular subsystem.
 *   The first fields of each message contain a timestamp

 */
const rmassRMN_LAYOUT rmassRmnTable[] = {
    {  "OPD DL1 Time sec",                "OPD1TS",    "",    0.5e-3,   rmassTIMESEC,  1 },
    {  "OPD DL1 Time usec",               "OPD1TUS",   "",    0.5e-3,   rmassTIMEUSEC, 2 },
    {  "OPD DL1 Rt Offset",               "OPD1OFF",   "",    0.5e-3,   rmassDOUBLE,   4 },
    {  "OPD DL1 Fringes detected",        "OPD1FDET",  "",    0.5e-3,   rmassINT32,    5 },
    {  "OPD DL1 Offset valid",            "OPD1OFFV",  "",    0.5e-3,   rmassINT32,    6 },

    {  "OPD DL2 Time sec",                "OPD2TS",    "",    0.5e-3,   rmassTIMESEC,  26 },
    {  "OPD DL2 Time usec",               "OPD2TUS",   "",    0.5e-3,   rmassTIMEUSEC, 27 },
    {  "OPD DL2 Rt Offset",               "OPD2OFF",   "",    0.5e-3,   rmassDOUBLE,   29 },
    {  "OPD DL2 Fringes detected",        "OPD2FDET",  "",    0.5e-3,   rmassINT32,    30 },
    {  "OPD DL2 Offset valid",            "OPD2OFFV",  "",    0.5e-3,   rmassINT32,    31 },

    {  "OPD DL3 Time sec",                "OPD3TS",    "",    0.5e-3,   rmassTIMESEC,  51 },
    {  "OPD DL3 Time usec",               "OPD3TUS",   "",    0.5e-3,   rmassTIMEUSEC, 52 },
    {  "OPD DL3 Rt Offset",               "OPD3OFF",   "",    0.5e-3,   rmassDOUBLE,   54 },
    {  "OPD DL3 Fringes detected",        "OPD3FDET",  "",    0.5e-3,   rmassINT32,    55 },
    {  "OPD DL3 Offset valid",            "OPD3OFFV",  "",    0.5e-3,   rmassINT32,    56 },

    {  "OPD DL4 Time sec",                "OPD4TS",    "",    0.5e-3,   rmassTIMESEC,  76 },
    {  "OPD DL4 Time usec",               "OPD4TUS",   "",    0.5e-3,   rmassTIMEUSEC, 77 },
    {  "OPD DL4 Rt Offset",               "OPD4OFF",   "",    0.5e-3,   rmassDOUBLE,   79 },
    {  "OPD DL4 Fringes detected",        "OPD4FDET",  "",    0.5e-3,   rmassINT32,    80 },
    {  "OPD DL4 Offset valid",            "OPD4OFFV",  "",    0.5e-3,   rmassINT32,    81 },

    {  "OPD DL5 Time sec",                "OPD5TS",    "",    0.5e-3,   rmassTIMESEC,  101 },
```

```
{  "OPD DL5 Time usec",              "OPD5TUS",   "",    0.5e-3,   rmassTIMEUSEC, 102 },
{  "OPD DL5 Rt Offset",              "OPD5OFF",   "",    0.5e-3,   rmassDOUBLE,   104 },
{  "OPD DL5 Fringes detected",       "OPD5FDET",  "",    0.5e-3,   rmassINT32,    105 },
{  "OPD DL5 Offset valid",           "OPD5OFFV",  "",    0.5e-3,   rmassINT32,    106 },

{  "OPD DL6 Time sec",               "OPD6TS",    "",    0.5e-3,   rmassTIMESEC,  126 },
{  "OPD DL6 Time usec",              "OPD6TUS",   "",    0.5e-3,   rmassTIMEUSEC, 127 },
{  "OPD DL6 Rt Offset",              "OPD6OFF",   "",    0.5e-3,   rmassDOUBLE,   129 },
{  "OPD DL6 Fringes detected",       "OPD6FDET",  "",    0.5e-3,   rmassINT32,    130 },
{  "OPD DL6 Offset valid",           "OPD6OFFV",  "",    0.5e-3,   rmassINT32,    131 },

{  "DL 1 timestamp sec",             "DL1TS",     "",    0.5e-3,   rmassTIMESEC,  251 },
{  "DL 1 timestamp usec",            "DL1TUS",    "",    0.5e-3,   rmassTIMEUSEC, 252 },
{  "DL 1 current position",          "DL1POS",    "",    0.5e-3,   rmassDOUBLE,   254 },
{  "DL 1 tracking OK flag",          "DL1TRK",    "",    0.5e-3,   rmassUINT32,   255 },
{  "DL 1 position error",            "DL1ERR",    "",    0.5e-3,   rmassDOUBLE,   256 },
{  "DL 1 position setpoint",         "DL1PSP",    "",    0.5e-3,   rmassDOUBLE,   257 },
{  "DL 1 ratelim position",          "DL1RLP",    "",    0.5e-3,   rmassDOUBLE,   258 },
{  "DL 1 ratelim active",            "DL1RLA",    "",    0.5e-3,   rmassINT32,    259 },

{  "DL 2 timestamp sec",             "DL2TS",     "",    0.5e-3,   rmassTIMESEC,  276 },
{  "DL 2 timestamp usec",            "DL2TUS",    "",    0.5e-3,   rmassTIMEUSEC, 277 },
{  "DL 2 current position",          "DL2POS",    "",    0.5e-3,   rmassDOUBLE,   279 },
{  "DL 2 tracking OK flag",          "DL2TRK",    "",    0.5e-3,   rmassUINT32,   280 },
{  "DL 2 position error",            "DL2ERR",    "",    0.5e-3,   rmassDOUBLE,   281 },
{  "DL 2 position setpoint",         "DL2PSP",    "",    0.5e-3,   rmassDOUBLE,   282 },
{  "DL 2 ratelim position",          "DL2RLP",    "",    0.5e-3,   rmassDOUBLE,   283 },
{  "DL 2 ratelim active",            "DL2RLA",    "",    0.5e-3,   rmassINT32,    284 },

{  "DL 3 timestamp sec",             "DL3TS",     "",    0.5e-3,   rmassTIMESEC,  301 },
{  "DL 3 timestamp usec",            "DL3TUS",    "",    0.5e-3,   rmassTIMEUSEC, 302 },
{  "DL 3 current position",          "DL3POS",    "",    0.5e-3,   rmassDOUBLE,   304 },
{  "DL 3 tracking OK flag",          "DL3TRK",    "",    0.5e-3,   rmassUINT32,   305 },
{  "DL 3 position error",            "DL3ERR",    "",    0.5e-3,   rmassDOUBLE,   306 },
{  "DL 3 position setpoint",         "DL3PSP",    "",    0.5e-3,   rmassDOUBLE,   307 },
{  "DL 3 ratelim position",          "DL3RLP",    "",    0.5e-3,   rmassDOUBLE,   308 },
{  "DL 3 ratelim active",            "DL3RLA",    "",    0.5e-3,   rmassINT32,    309 },

{  "DL 4 timestamp sec",             "DL4TS",     "",    0.5e-3,   rmassTIMESEC,  326 },
{  "DL 4 timestamp usec",            "DL4TUS",    "",    0.5e-3,   rmassTIMEUSEC, 327 },
{  "DL 4 current position",          "DL4POS",    "",    0.5e-3,   rmassDOUBLE,   329 },
{  "DL 4 tracking OK flag",          "DL4TRK",    "",    0.5e-3,   rmassUINT32,   330 },
{  "DL 4 position error",            "DL4ERR",    "",    0.5e-3,   rmassDOUBLE,   331 },
```

```
    {  "DL 4 position setpoint",            "DL4PSP",    "",    0.5e-3,   rmassDOUBLE,   332 },
    {  "DL 4 ratelim position",             "DL4RLP",    "",    0.5e-3,   rmassDOUBLE,   333 },
    {  "DL 4 ratelim active",               "DL4RLA",    "",    0.5e-3,   rmassINT32,    334 },

    {  "DL 5 timestamp sec",                "DL5TS",     "",    0.5e-3,   rmassTIMESEC,  351 },
    {  "DL 5 timestamp usec",               "DL5TUS",    "",    0.5e-3,   rmassTIMEUSEC, 352 },
    {  "DL 5 current position",             "DL5POS",    "",    0.5e-3,   rmassDOUBLE,   354 },
    {  "DL 5 tracking OK flag",             "DL5TRK",    "",    0.5e-3,   rmassUINT32,   355 },
    {  "DL 5 position error",               "DL5ERR",    "",    0.5e-3,   rmassDOUBLE,   356 },
    {  "DL 5 position setpoint",            "DL5PSP",    "",    0.5e-3,   rmassDOUBLE,   357 },
    {  "DL 5 ratelim position",             "DL5RLP",    "",    0.5e-3,   rmassDOUBLE,   358 },
    {  "DL 5 ratelim active",               "DL5RLA",    "",    0.5e-3,   rmassINT32,    359 },

    {  "DL 6 timestamp sec",                "DL6TS",     "",    0.5e-3,   rmassTIMESEC,  376 },
    {  "DL 6 timestamp usec",               "DL6TUS",    "",    0.5e-3,   rmassTIMEUSEC, 377 },
    {  "DL 6 current position",             "DL6POS",    "",    0.5e-3,   rmassDOUBLE,   379 },
    {  "DL 6 tracking OK flag",             "DL6TRK",    "",    0.5e-3,   rmassUINT32,   380 },
    {  "DL 6 position error",               "DL6ERR",    "",    0.5e-3,   rmassDOUBLE,   381 },
    {  "DL 6 position setpoint",            "DL6PSP",    "",    0.5e-3,   rmassDOUBLE,   382 },
    {  "DL 6 ratelim position",             "DL6RLP",    "",    0.5e-3,   rmassDOUBLE,   383 },
    {  "DL 6 ratelim active",               "DL6RLA",    "",    0.5e-3,   rmassINT32,    384 },

    {  "RMASS Aviso timestamp sec",         "RMASTS",    "",    0.0,      rmassTIMESEC,  876 },
    {  "RMASS Aviso timestamp usec",        "RMASTUS",   "",    0.0,      rmassTIMEUSEC, 877 },
    {  "RMASS Aviso version",               "RMASVER",   "",    0.0,      rmassDOUBLE,   878 },
    {  "RMASS Aviso RMN node",              "RMASRMND",  "",    0.0,      rmassINT32,    879 },
    {  "RMASS Aviso RFM node",              "RMASRFMD",  "",    0.0,      rmassINT32,    880 },
    {  "RMASS Aviso RMN node which sees no other",  "RMASRMN0",  "",    0.0,      rmassINT32,    882
},
    {  "RMASS Aviso RFM node which sees no other",  "RMASRFM0",  "",    0.0,      rmassINT32,    883
},
    { "RMASS VOID timestamp sec",           "VOIDTS",    "",    0.0,      rmassTIMESEC,  884 },
    { "RMASS VOID timestamp usec",          "VOIDTUS",   "",    0.0,      rmassTIMEUSEC, 885 },
    { "RMASS VOID (dummy) field  ",         "VOID",      "",    0.0,      rmassDOUBLE,   886 },

    /* rdembet : added new flag to know which fringe sensor is used */
    { "RMASSOP FTK_Sensor timestamp sec",   "FTKSTS",    "",    0.0,      rmassTIMESEC,  900 },
    { "RMASSOP FTK_Sensor timestamp usec",  "FTKSTUS",   "",    0.0,      rmassTIMEUSEC, 901 },
    { "RMASSOP FTK_Sensor value",           "FTKSENS",   "",    0.0,      rmassUINT32,   902 },

    {  "MACAO UT1 time sec",                "MAC1TS",    "",    2.381e-3,  rmassTIMESEC,  1251 },
    {  "MACAO UT1 time usec",               "MAC1TUS",   "",    2.381e-3,  rmassTIMEUSEC, 1252 },
    {  "MACAO UT1 wavefront error",         "MAC1WF",    "",    2.381e-3,  rmassDOUBLE,   1254 },
```

```
    {  "MACAO UT1 wavefront valid",         "MAC1WFV",   "",    2.381e-3,  rmassUINT32,   1255 },
    {  "MACAO UT1 tip",                     "MAC1TIP",   "",    2.381e-3,  rmassDOUBLE,   1256 },
    {  "MACAO UT1 tilt",                    "MAC1TILT",  "",    2.381e-3,  rmassDOUBLE,   1257 },

    {  "MACAO UT2 time sec",                "MAC2TS",    "",    2.381e-3,  rmassTIMESEC,  1276 },
    {  "MACAO UT2 time usec",               "MAC2TUS",   "",    2.381e-3,  rmassTIMEUSEC, 1277 },
    {  "MACAO UT2 wavefront error",         "MAC2WF",    "",    2.381e-3,  rmassDOUBLE,   1279 },
    {  "MACAO UT2 wavefront valid",         "MAC2WFV",   "",    2.381e-3,  rmassUINT32,   1280 },
    {  "MACAO UT2 tip",                     "MAC2TIP",   "",    2.381e-3,  rmassDOUBLE,   1281 },
    {  "MACAO UT2 tilt",                    "MAC2TILT",  "",    2.381e-3,  rmassDOUBLE,   1282 },

    {  "MACAO UT3 time sec",                "MAC3TS",    "",    2.381e-3,  rmassTIMESEC,  1301 },
    {  "MACAO UT3 time usec",               "MAC3TUS",   "",    2.381e-3,  rmassTIMEUSEC, 1302 },
    {  "MACAO UT3 wavefront error",         "MAC3WF",    "",    2.381e-3,  rmassDOUBLE,   1304 },
    {  "MACAO UT3 wavefront valid",         "MAC3WFV",   "",    2.381e-3,  rmassUINT32,   1305 },
    {  "MACAO UT3 tip",                     "MAC3TIP",   "",    2.381e-3,  rmassDOUBLE,   1306 },
    {  "MACAO UT3 tilt",                    "MAC3TILT",  "",    2.381e-3,  rmassDOUBLE,   1307 },

    {  "MACAO UT4 time sec",                "MAC4TS",    "",    2.381e-3,  rmassTIMESEC,  1326 },
    {  "MACAO UT4 time usec",               "MAC4TUS",   "",    2.381e-3,  rmassTIMEUSEC, 1327 },
    {  "MACAO UT4 wavefront error",         "MAC4WF",    "",    2.381e-3,  rmassDOUBLE,   1329 },
    {  "MACAO UT4 wavefront valid",         "MAC4WFV",   "",    2.381e-3,  rmassUINT32,   1330 },
    {  "MACAO UT4 tip",                     "MAC4TIP",   "",    2.381e-3,  rmassDOUBLE,   1331 },
    {  "MACAO UT4 tilt",                    "MAC4TILT",  "",    2.381e-3,  rmassDOUBLE,   1332 },

    {  "VIBMET Time sec",                   "VMETRTS",   "",    0.125e-3, rmassTIMESEC,  1501 },
    {  "VIBMET Time usec",                  "VMETRTUS",  "",    0.125e-3, rmassTIMEUSEC, 1502 },
    {  "VIBMET Delta",                      "VMETRD",    "",    0.125e-3, rmassDOUBLE,   1504 },
    {  "VIBMET Delta val",                  "VMETRDV",   "",    0.125e-3, rmassUINT32,   1505 },
    {  "VIBMET Status",                     "VMETRST",   "",    0.125e-3, rmassUINT32,   1506 },
    {  "VIBMET DC Probe 650k",              "VMETRP6",   "",    0.125e-3, rmassDOUBLE,   1507 },
    {  "VIBMET DC Probe 450k",              "VMETRP4",   "",    0.125e-3, rmassDOUBLE,   1508 },
    {  "VIBMET DC Ref 650k",                "VMETRR6",   "",    0.125e-3, rmassDOUBLE,   1509 },
    {  "VIBMET DC Ref 450k",                "VMETRR4",   "",    0.125e-3, rmassDOUBLE,   1510 },

/* RFR: Added accelerometer data to RMN for VIBMET project, re-using unused PRIMA RMN offsets */

    {  "Manhattan ACCEL1 sec",              "VMETTS1",    "",   0.25e-3,  rmassTIMESEC,  1526 },
    {  "Manhattan ACCEL1 usec",             "VMETTUS1",   "",   0.25e-3,  rmassTIMEUSEC, 1527 },
    {  "Manhattan ACCEL1 displace",         "VMETRD1",    "",   0.25e-3,  rmassDOUBLE,   1529 },

    {  "Manhattan ACCEL2 sec",              "VMETTS2",    "",   0.25e-3,  rmassTIMESEC,  1551 },
    {  "Manhattan ACCEL2 usec",             "VMETTUS2",   "",   0.25e-3,  rmassTIMEUSEC, 1552 },
```

```
{  "Manhattan ACCEL2 displace",        "VMETRD2",   "",    0.25e-3,  rmassDOUBLE,   1554 },

{  "Manhattan ACCEL3 sec",             "VMETTS3",    "",   0.25e-3,  rmassTIMESEC,  1576 },
{  "Manhattan ACCEL3 usec",            "VMETTUS3",   "",   0.25e-3,  rmassTIMEUSEC, 1577 },
{  "Manhattan ACCEL3 displace",        "VMETRD3",   "",    0.25e-3,  rmassDOUBLE,   1579 },

{  "Manhattan ACCEL4 sec",             "VMETTS4",    "",   0.25e-3,  rmassTIMESEC,  1601 },
{  "Manhattan ACCEL4 usec",            "VMETTUS4",   "",   0.25e-3,  rmassTIMEUSEC, 1602 },
{  "Manhattan ACCEL4 displace",        "VMETRD4",   "",    0.25e-3,  rmassDOUBLE,   1604 },

{  "Manhattan DL1 sec",                "VIB1TS",    "",    0.25e-3,  rmassTIMESEC,  1751 },
{  "Manhattan DL1 usec",               "VIB1TUS",   "",    0.25e-3,  rmassTIMEUSEC, 1752 },
{  "Manhattan DL1 datachk",            "VIB1CHK",   "",    0.25e-3,  rmassUINT32,   1753 },
{  "Manhattan DL1 accel",              "VIB1ACC",   "",    0.25e-3,  rmassDOUBLE,   1754 },
{  "Manhattan DL1 displace",           "VIB1DPL",   "",    0.25e-3,  rmassDOUBLE,   1755 },
{  "Manhattan DL1 test",               "VIB1TST",   "",    0.25e-3,  rmassDOUBLE,   1756 },

{  "Manhattan DL2 sec",                "VIB2TS",    "",    0.25e-3,  rmassTIMESEC,  1776 },
{  "Manhattan DL2 usec",               "VIB2TUS",   "",    0.25e-3,  rmassTIMEUSEC, 1777 },
{  "Manhattan DL2 datachk",            "VIB2CHK",   "",    0.25e-3,  rmassUINT32,   1778 },
{  "Manhattan DL2 accel",              "VIB2ACC",   "",    0.25e-3,  rmassDOUBLE,   1779 },
{  "Manhattan DL2 displace",           "VIB2DPL",   "",    0.25e-3,  rmassDOUBLE,   1780 },
{  "Manhattan DL2 test",               "VIB2TST",   "",    0.25e-3,  rmassDOUBLE,   1781 },

{  "Manhattan DL3 sec",                "VIB3TS",    "",    0.25e-3,  rmassTIMESEC,  1801 },
{  "Manhattan DL3 usec",               "VIB3TUS",   "",    0.25e-3,  rmassTIMEUSEC, 1802 },
{  "Manhattan DL3 datachk",            "VIB3CHK",   "",    0.25e-3,  rmassUINT32,   1803 },
{  "Manhattan DL3 accel",              "VIB3ACC",   "",    0.25e-3,  rmassDOUBLE,   1804 },
{  "Manhattan DL3 displace",           "VIB3DPL",   "",    0.25e-3,  rmassDOUBLE,   1805 },
{  "Manhattan DL3 test",               "VIB3TST",   "",    0.25e-3,  rmassDOUBLE,   1806 },

{  "Manhattan DL4 sec",                "VIB4TS",    "",    0.25e-3,  rmassTIMESEC,  1826 },
{  "Manhattan DL4 usec",               "VIB4TUS",   "",    0.25e-3,  rmassTIMEUSEC, 1827 },
{  "Manhattan DL4 datachk",            "VIB4CHK",   "",    0.25e-3,  rmassUINT32,   1828 },
{  "Manhattan DL4 accel",              "VIB4ACC",   "",    0.25e-3,  rmassDOUBLE,   1829 },
{  "Manhattan DL4 displace",           "VIB4DPL",   "",    0.25e-3,  rmassDOUBLE,   1830 },
{  "Manhattan DL4 test",               "VIB4TST",   "",    0.25e-3,  rmassDOUBLE,   1831 },

{  "Manhattan DL5 sec",                "VIB5TS",    "",    0.25e-3,  rmassTIMESEC,  1851 },
{  "Manhattan DL5 usec",               "VIB5TUS",   "",    0.25e-3,  rmassTIMEUSEC, 1852 },
{  "Manhattan DL5 datachk",            "VIB5CHK",   "",    0.25e-3,  rmassUINT32,   1853 },
{  "Manhattan DL5 accel",              "VIB5ACC",   "",    0.25e-3,  rmassDOUBLE,   1854 },
{  "Manhattan DL5 displace",           "VIB5DPL",   "",    0.25e-3,  rmassDOUBLE,   1855 },
```

```
{  "Manhattan DL5 test",               "VIB5TST",    "",    0.25e-3,  rmassDOUBLE,   1856 },

{  "Manhattan DL6 sec",                "VIB6TS",     "",    0.25e-3,  rmassTIMESEC,  1876 },
{  "Manhattan DL6 usec",               "VIB6TUS",    "",    0.25e-3,  rmassTIMEUSEC, 1877 },
{  "Manhattan DL6 datachk",            "VIB6CHK",    "",    0.25e-3,  rmassUINT32,   1878 },
{  "Manhattan DL6 accel",              "VIB6ACC",    "",    0.25e-3,  rmassDOUBLE,   1879 },
{  "Manhattan DL6 displace",           "VIB6DPL",    "",    0.25e-3,  rmassDOUBLE,   1880 },
{  "Manhattan DL6 test",               "VIB6TST",    "",    0.25e-3,  rmassDOUBLE,   1881 },

{  "FINITO Ch1 Times sec",             "FNT1TS",     "",    0.5e-3,   rmassTIMESEC,  2001 },
{  "FINITO Ch1 Times usec",            "FNT1TUS",    "",    0.5e-3,   rmassTIMEUSEC, 2002 },
{  "FINITO Ch1 Data check",            "FNT1CHK",    "",    0.5e-3,   rmassUINT32,   2003 },
{  "FINITO Ch1 Coherence",             "FNT1CO",     "",    0.5e-3,   rmassDOUBLE,   2004 },
{  "FINITO Ch1 Coherence valid",       "FNT1COV",    "",    0.5e-3,   rmassUINT32,   2005 },
{  "FINITO Ch1 Phase",                 "FNT1PH",     "",    0.5e-3,   rmassDOUBLE,   2006 },
{  "FINITO Ch1 Phase valid",           "FNT1PHV",    "",    0.5e-3,   rmassUINT32,   2007 },
{  "FINITO Ch1 SNR",                   "FNT1SNR",    "",    0.5e-3,   rmassDOUBLE,   2008 },
{  "FINITO Ch1 Comb. Coherence",       "FNT1CMB",    "",    0.5e-3,   rmassDOUBLE,   2012 },
{  "FINITO Modulator scan",            "FNTMOD",     "",    0.5e-3,   rmassDOUBLE,   2013 },
{  "FINITO Detector Phot0",            "FNTFX0",     "",    0.5e-3,   rmassDOUBLE,   2014 },
{  "FINITO Detector Phot1",            "FNTFX1",     "",    0.5e-3,   rmassDOUBLE,   2015 },
{  "FINITO Detector ITF1A",            "FNTFX1A",    "",    0.5e-3,   rmassDOUBLE,   2016 },
{  "FINITO Detector ITF1B",            "FNTFX1B",    "",    0.5e-3,   rmassDOUBLE,   2017 },

{  "FINITO Ch2 Times sec",             "FNT2TS",     "",    0.5e-3,   rmassTIMESEC,  2026 },
{  "FINITO Ch2 Times usec",            "FNT2TUS",    "",    0.5e-3,   rmassTIMEUSEC, 2027 },
{  "FINITO Ch2 Data check",            "FNT2CHK",    "",    0.5e-3,   rmassUINT32,   2028 },
{  "FINITO Ch2 Coherence",             "FNT2CO",     "",    0.5e-3,   rmassDOUBLE,   2029 },
{  "FINITO Ch2 Coherence valid",       "FNT2COV",    "",    0.5e-3,   rmassUINT32,   2030 },
{  "FINITO Ch2 Phase",                 "FNT2PH",     "",    0.5e-3,   rmassDOUBLE,   2031 },
{  "FINITO Ch2 Phase valid",           "FNT2PHV",    "",    0.5e-3,   rmassUINT32,   2032 },
{  "FINITO Ch2 SNR",                   "FNT2SNR",    "",    0.5e-3,   rmassDOUBLE,   2033 },
{  "FINITO Ch2 Comb. Coherence",       "FNT2CMB",    "",    0.5e-3,   rmassDOUBLE,   2037 },
{  "FINITO Modulator scan Duplicate",  "FNTMODDU",   "",    0.5e-3,   rmassDOUBLE,   2038 },
{  "FINITO Detector Phot0 Duplicate",  "FNTFX0DU",   "",    0.5e-3,   rmassDOUBLE,   2039 },
{  "FINITO Detector Phot2",            "FNTFX2",     "",    0.5e-3,   rmassDOUBLE,   2040 },
{  "FINITO Detector ITF2A",            "FNTFX2A",    "",    0.5e-3,   rmassDOUBLE,   2041 },
{  "FINITO Detector ITF2B",            "FNTFX2B",    "",    0.5e-3,   rmassDOUBLE,   2042 },

/* TPH 20091126: new IRIS fields for PRIMA FSU test */

{  "IRIS Q1 Times sec",                "IRI1TS",     "",    1.0e-3,   rmassTIMESEC,  2251 },
{  "IRIS Q1 Times sec",                "IRI1TUS",    "",    1.0e-3,   rmassTIMEUSEC, 2252 },
```

```
{  "IRIS Q1 Data Check",              "IRI1CHK",   "",    1.0e-3,   rmassUINT32,   2253 },
{  "IRIS Q1 Offset X",                "IRI1X",     "",    1.0e-3,   rmassDOUBLE,   2254 },
{  "IRIS Q1 Offset Y",                "IRI1Y",     "",    1.0e-3,   rmassDOUBLE,   2255 },

{  "IRIS Q1 Flux",                    "IRI1FLUX",  "",    1.0e-3,   rmassDOUBLE,   2256 },
{  "IRIS Q1 Pixel 1",                 "IRI1PI1",   "",    1.0e-3,   rmassDOUBLE,   2257 },
{  "IRIS Q1 Pixel 1 X",               "IRI1PI1X",  "",    1.0e-3,   rmassDOUBLE,   2258 },
{  "IRIS Q1 Pixel 1 Y",               "IRI1PI1Y",  "",    1.0e-3,   rmassDOUBLE,   2259 },
{  "IRIS Q1 Pixel 2",                 "IRI1PI2",   "",    1.0e-3,   rmassDOUBLE,   2260 },
{  "IRIS Q1 Pixel 2 X",               "IRI1PI2X",  "",    1.0e-3,   rmassDOUBLE,   2261 },
{  "IRIS Q1 Pixel 2 Y",               "IRI1PI2Y",  "",    1.0e-3,   rmassDOUBLE,   2262 },
{  "IRIS Q1 Pixel 3",                 "IRI1PI3",   "",    1.0e-3,   rmassDOUBLE,   2263 },
{  "IRIS Q1 Pixel 3 X",               "IRI1PI3X",  "",    1.0e-3,   rmassDOUBLE,   2264 },
{  "IRIS Q1 Pixel 3 Y",               "IRI1PI3Y",  "",    1.0e-3,   rmassDOUBLE,   2265 },
{  "IRIS Q1 Pixel 4",                 "IRI1PI4",   "",    1.0e-3,   rmassDOUBLE,   2266 },
{  "IRIS Q1 Pixel 4 X",               "IRI1PI4X",  "",    1.0e-3,   rmassDOUBLE,   2267 },
{  "IRIS Q1 Pixel 4 Y",               "IRI1PI4Y",  "",    1.0e-3,   rmassDOUBLE,   2268 },

{  "IRIS Q2 Times sec",               "IRI2TS",    "",    1.0e-3,   rmassTIMESEC,  2276 },
{  "IRIS Q2 Times sec",               "IRI2TUS",   "",    1.0e-3,   rmassTIMEUSEC, 2277 },
{  "IRIS Q2 Data Check",              "IRI2CHK",   "",    1.0e-3,   rmassUINT32,   2278 },
{  "IRIS Q2 Offset X",                "IRI2X",     "",    1.0e-3,   rmassDOUBLE,   2279 },
{  "IRIS Q2 Offset Y",                "IRI2Y",     "",    1.0e-3,   rmassDOUBLE,   2280 },

{  "IRIS Q2 Flux",                    "IRI2FLUX",  "",    1.0e-3,   rmassDOUBLE,   2281 },
{  "IRIS Q2 Pixel 1",                 "IRI2PI1",   "",    1.0e-3,   rmassDOUBLE,   2282 },
{  "IRIS Q2 Pixel 1 X",               "IRI2PI1X",  "",    1.0e-3,   rmassDOUBLE,   2283 },
{  "IRIS Q2 Pixel 1 Y",               "IRI2PI1Y",  "",    1.0e-3,   rmassDOUBLE,   2284 },
{  "IRIS Q2 Pixel 2",                 "IRI2PI2",   "",    1.0e-3,   rmassDOUBLE,   2285 },
{  "IRIS Q2 Pixel 2 X",               "IRI2PI2X",  "",    1.0e-3,   rmassDOUBLE,   2286 },
{  "IRIS Q2 Pixel 2 Y",               "IRI2PI2Y",  "",    1.0e-3,   rmassDOUBLE,   2287 },
{  "IRIS Q2 Pixel 3",                 "IRI2PI3",   "",    1.0e-3,   rmassDOUBLE,   2288 },
{  "IRIS Q2 Pixel 3 X",               "IRI2PI3X",  "",    1.0e-3,   rmassDOUBLE,   2289 },
{  "IRIS Q2 Pixel 3 Y",               "IRI2PI3Y",  "",    1.0e-3,   rmassDOUBLE,   2290 },
{  "IRIS Q2 Pixel 4",                 "IRI2PI4",   "",    1.0e-3,   rmassDOUBLE,   2291 },
{  "IRIS Q2 Pixel 4 X",               "IRI2PI4X",  "",    1.0e-3,   rmassDOUBLE,   2292 },
{  "IRIS Q2 Pixel 4 Y",               "IRI2PI4Y",  "",    1.0e-3,   rmassDOUBLE,   2293 },

{  "IRIS Q3 Times sec",               "IRI3TS",    "",    1.0e-3,   rmassTIMESEC,  2301 },
{  "IRIS Q3 Times sec",               "IRI3TUS",   "",    1.0e-3,   rmassTIMEUSEC, 2302 },
{  "IRIS Q3 Data Check",              "IRI3CHK",   "",    1.0e-3,   rmassUINT32,   2303 },
{  "IRIS Q3 Offset X",                "IRI3X",     "",    1.0e-3,   rmassDOUBLE,   2304 },
{  "IRIS Q3 Offset Y",                "IRI3Y",     "",    1.0e-3,   rmassDOUBLE,   2305 },
```

```
{  "IRIS Q3 Flux",                  "IRI3FLUX",  "",    1.0e-3,   rmassDOUBLE,   2306 },
{  "IRIS Q3 Pixel 1",               "IRI3PI1",   "",    1.0e-3,   rmassDOUBLE,   2307 },
{  "IRIS Q3 Pixel 1 X",             "IRI3PI1X",  "",    1.0e-3,   rmassDOUBLE,   2308 },
{  "IRIS Q3 Pixel 1 Y",             "IRI3PI1Y",  "",    1.0e-3,   rmassDOUBLE,   2309 },
{  "IRIS Q3 Pixel 2",               "IRI3PI2",   "",    1.0e-3,   rmassDOUBLE,   2310 },
{  "IRIS Q3 Pixel 2 X",             "IRI3PI2X",  "",    1.0e-3,   rmassDOUBLE,   2311 },
{  "IRIS Q3 Pixel 2 Y",             "IRI3PI2Y",  "",    1.0e-3,   rmassDOUBLE,   2312 },
{  "IRIS Q3 Pixel 3",               "IRI3PI3",   "",    1.0e-3,   rmassDOUBLE,   2313 },
{  "IRIS Q3 Pixel 3 X",             "IRI3PI3X",  "",    1.0e-3,   rmassDOUBLE,   2314 },
{  "IRIS Q3 Pixel 3 Y",             "IRI3PI3Y",  "",    1.0e-3,   rmassDOUBLE,   2315 },
{  "IRIS Q3 Pixel 4",               "IRI3PI4",   "",    1.0e-3,   rmassDOUBLE,   2316 },
{  "IRIS Q3 Pixel 4 X",             "IRI3PI4X",  "",    1.0e-3,   rmassDOUBLE,   2317 },
{  "IRIS Q3 Pixel 4 Y",             "IRI3PI4Y",  "",    1.0e-3,   rmassDOUBLE,   2318 },

{  "IRIS Q4 Times sec",             "IRI4TS",    "",    1.0e-3,   rmassTIMESEC,  2326 },
{  "IRIS Q4 Times sec",             "IRI4TUS",   "",    1.0e-3,   rmassTIMEUSEC, 2327 },
{  "IRIS Q4 Data Check",            "IRI4CHK",   "",    1.0e-3,   rmassUINT32,   2328 },
{  "IRIS Q4 Offset X",              "IRI4X",     "",    1.0e-3,   rmassDOUBLE,   2329 },
{  "IRIS Q4 Offset Y",              "IRI4Y",     "",    1.0e-3,   rmassDOUBLE,   2330 },

{  "IRIS Q4 Flux",                  "IRI4FLUX",  "",    1.0e-3,   rmassDOUBLE,   2331 },
{  "IRIS Q4 Pixel 1",               "IRI4PI1",   "",    1.0e-3,   rmassDOUBLE,   2332 },
{  "IRIS Q4 Pixel 1 X",             "IRI4PI1X",  "",    1.0e-3,   rmassDOUBLE,   2333 },
{  "IRIS Q4 Pixel 1 Y",             "IRI4PI1Y",  "",    1.0e-3,   rmassDOUBLE,   2334 },
{  "IRIS Q4 Pixel 2",               "IRI4PI2",   "",    1.0e-3,   rmassDOUBLE,   2335 },
{  "IRIS Q4 Pixel 2 X",             "IRI4PI2X",  "",    1.0e-3,   rmassDOUBLE,   2336 },
{  "IRIS Q4 Pixel 2 Y",             "IRI4PI2Y",  "",    1.0e-3,   rmassDOUBLE,   2337 },
{  "IRIS Q4 Pixel 3",               "IRI4PI3",   "",    1.0e-3,   rmassDOUBLE,   2338 },
{  "IRIS Q4 Pixel 3 X",             "IRI4PI3X",  "",    1.0e-3,   rmassDOUBLE,   2339 },
{  "IRIS Q4 Pixel 3 Y",             "IRI4PI3Y",  "",    1.0e-3,   rmassDOUBLE,   2340 },
{  "IRIS Q4 Pixel 4",               "IRI4PI4",   "",    1.0e-3,   rmassDOUBLE,   2341 },
{  "IRIS Q4 Pixel 4 X",             "IRI4PI4X",  "",    1.0e-3,   rmassDOUBLE,   2342 },
{  "IRIS Q4 Pixel 4 Y",             "IRI4PI4Y",  "",    1.0e-3,   rmassDOUBLE,   2343 },


{  "BTK Beam 0 Times sec",          "BTK0TS",    "",    0.5e-3,   rmassTIMESEC,  2501 },
{  "BTK Beam 0 Times sec",          "BTK0TUS",   "",    0.5e-3,   rmassTIMEUSEC, 2502 },
{  "BTK Beam 0 Data check",         "BTK0CHK",   "",    0.5e-3,   rmassUINT32,   2503 },
{  "BTK Beam 0 Flux",               "BTK0FX",    "",    0.5e-3,   rmassDOUBLE,   2504 },

{  "BTK Beam 1 Times sec",          "BTK1TS",    "",    0.5e-3,   rmassTIMESEC,  2526 },
{  "BTK Beam 1 Times sec",          "BTK1TUS",   "",    0.5e-3,   rmassTIMEUSEC, 2527 },
```

```
{  "BTK Beam 1 Data check",          "BTK1CHK",    "",    0.5e-3,   rmassUINT32,   2528 },
{  "BTK Beam 1 Flux",                "BTK1FX",     "",    0.5e-3,   rmassDOUBLE,   2529 },

{  "BTK Beam 2 Times sec",           "BTK2TS",     "",    0.5e-3,   rmassTIMESEC,  2551 },
{  "BTK Beam 2 Times sec",           "BTK2TUS",    "",    0.5e-3,   rmassTIMEUSEC, 2552 },
{  "BTK Beam 2 Data check",          "BTK2CHK",    "",    0.5e-3,   rmassUINT32,   2553 },
{  "BTK Beam 2 Flux",                "BTK2FX",     "",    0.5e-3,   rmassDOUBLE,   2554 },


{  "Monitor Ch1 Index 1",            "MON1.1",     "",    0.0,      rmassDOUBLE,   2750 },
{  "Monitor Ch1 Index 2",            "MON1.2",     "",    0.0,      rmassDOUBLE,   2751 },
{  "Monitor Ch1 Index 3",            "MON1.3",     "",    0.0,      rmassDOUBLE,   2752 },
{  "Monitor Ch1 Index 4",            "MON1.4",     "",    0.0,      rmassDOUBLE,   2753 },
{  "Monitor Ch1 Index 5",            "MON1.5",     "",    0.0,      rmassDOUBLE,   2754 },
{  "Monitor Ch1 Index 6",            "MON1.6",     "",    0.0,      rmassDOUBLE,   2755 },
{  "Monitor Ch1 Index 7",            "MON1.7",     "",    0.0,      rmassDOUBLE,   2756 },
{  "Monitor Ch1 Index 8",            "MON1.8",     "",    0.0,      rmassDOUBLE,   2757 },
{  "Monitor Ch1 Index 9",            "MON1.9",     "",    0.0,      rmassDOUBLE,   2758 },
{  "Monitor Ch1 Index 10",           "MON1.10",    "",    0.0,      rmassDOUBLE,   2759 },

{  "Monitor Ch2 Index 1",            "MON2.1",     "",    0.0,      rmassDOUBLE,   2775 },
{  "Monitor Ch2 Index 2",            "MON2.2",     "",    0.0,      rmassDOUBLE,   2776 },
{  "Monitor Ch2 Index 3",            "MON2.3",     "",    0.0,      rmassDOUBLE,   2777 },
{  "Monitor Ch2 Index 4",            "MON2.4",     "",    0.0,      rmassDOUBLE,   2778 },
{  "Monitor Ch2 Index 5",            "MON2.5",     "",    0.0,      rmassDOUBLE,   2779 },
{  "Monitor Ch2 Index 6",            "MON2.6",     "",    0.0,      rmassDOUBLE,   2780 },
{  "Monitor Ch2 Index 7",            "MON2.7",     "",    0.0,      rmassDOUBLE,   2781 },
{  "Monitor Ch2 Index 8",            "MON2.8",     "",    0.0,      rmassDOUBLE,   2782 },
{  "Monitor Ch2 Index 9",            "MON2.9",     "",    0.0,      rmassDOUBLE,   2783 },
{  "Monitor Ch2 Index 10",           "MON2.10",    "",    0.0,      rmassDOUBLE,   2784 },

{  "Monitor Ch3 Index 1",            "MON3.1",     "",    0.0,      rmassDOUBLE,   2800 },
{  "Monitor Ch3 Index 2",            "MON3.2",     "",    0.0,      rmassDOUBLE,   2801 },
{  "Monitor Ch3 Index 3",            "MON3.3",     "",    0.0,      rmassDOUBLE,   2802 },
{  "Monitor Ch3 Index 4",            "MON3.4",     "",    0.0,      rmassDOUBLE,   2803 },
{  "Monitor Ch3 Index 5",            "MON3.5",     "",    0.0,      rmassDOUBLE,   2804 },
{  "Monitor Ch3 Index 6",            "MON3.6",     "",    0.0,      rmassDOUBLE,   2805 },
{  "Monitor Ch3 Index 7",            "MON3.7",     "",    0.0,      rmassDOUBLE,   2806 },
{  "Monitor Ch3 Index 8",            "MON3.8",     "",    0.0,      rmassDOUBLE,   2807 },
{  "Monitor Ch3 Index 9",            "MON3.9",     "",    0.0,      rmassDOUBLE,   2808 },
{  "Monitor Ch3 Index 10",           "MON3.10",    "",    0.0,      rmassDOUBLE,   2809 },

{  "Monitor Ch4 Index 1",            "MON4.1",     "",    0.0,      rmassDOUBLE,   2825 },
```

```
{  "Monitor Ch4 Index 2",              "MON4.2",    "",    0.0,      rmassDOUBLE,   2826 },
{  "Monitor Ch4 Index 3",              "MON4.3",    "",    0.0,      rmassDOUBLE,   2827 },
{  "Monitor Ch4 Index 4",              "MON4.4",    "",    0.0,      rmassDOUBLE,   2828 },
{  "Monitor Ch4 Index 5",              "MON4.5",    "",    0.0,      rmassDOUBLE,   2829 },
{  "Monitor Ch4 Index 6",              "MON4.6",    "",    0.0,      rmassDOUBLE,   2830 },
{  "Monitor Ch4 Index 7",              "MON4.7",    "",    0.0,      rmassDOUBLE,   2831 },
{  "Monitor Ch4 Index 8",              "MON4.8",    "",    0.0,      rmassDOUBLE,   2832 },
{  "Monitor Ch4 Index 9",              "MON4.9",    "",    0.0,      rmassDOUBLE,   2833 },
{  "Monitor Ch4 Index 10",             "MON4.10",   "",    0.0,      rmassDOUBLE,   2834 },

{  "Monitor Ch5 Index 1",              "MON5.1",    "",    0.0,      rmassDOUBLE,   2850 },
{  "Monitor Ch5 Index 2",              "MON5.2",    "",    0.0,      rmassDOUBLE,   2851 },
{  "Monitor Ch5 Index 3",              "MON5.3",    "",    0.0,      rmassDOUBLE,   2852 },
{  "Monitor Ch5 Index 4",              "MON5.4",    "",    0.0,      rmassDOUBLE,   2853 },
{  "Monitor Ch5 Index 5",              "MON5.5",    "",    0.0,      rmassDOUBLE,   2854 },
{  "Monitor Ch5 Index 6",              "MON5.6",    "",    0.0,      rmassDOUBLE,   2855 },
{  "Monitor Ch5 Index 7",              "MON5.7",    "",    0.0,      rmassDOUBLE,   2856 },
{  "Monitor Ch5 Index 8",              "MON5.8",    "",    0.0,      rmassDOUBLE,   2857 },
{  "Monitor Ch5 Index 9",              "MON5.9",    "",    0.0,      rmassDOUBLE,   2858 },
{  "Monitor Ch5 Index 10",             "MON5.10",   "",    0.0,      rmassDOUBLE,   2859 },

{  "OPDC Finito1 Time sec",            "OD1TS",     "",    0.5e-3,   rmassTIMESEC,  3251 },
{  "OPDC Finito1 Time usec",           "OD1TUS",    "",    0.5e-3,   rmassTIMEUSEC, 3252 },
{  "OPDC Finito1 Rt Offset",           "OD1OFF",    "",    0.5e-3,   rmassDOUBLE,   3254 },
{  "OPDC Finito1 Fringe det",          "OD1FDET",   "",    0.5e-3,   rmassUINT32,   3255 },
{  "OPDC Finito1 Rt Off val",          "OD1OFFV",   "",    0.5e-3,   rmassUINT32,   3256 },
{  "OPDC Finito1 State",               "OD1ST",     "",    0.5e-3,   rmassUINT32,   3257 },
{  "OPDC Finito1 unwr Phase",          "OD1UPH",    "",    0.5e-3,   rmassDOUBLE,   3258 },
{  "OPDC Finito1 full Off.",           "OD1FOFF",   "",    0.5e-3,   rmassDOUBLE,   3259 },
{  "OPDC Finito1 DL feedback",         "OD1DLFB",   "",    0.5e-3,   rmassDOUBLE,   3260 },
{  "OPDC Finito1 Stp Phase",           "OD1STPH",   "",    0.5e-3,   rmassUINT32,   3261 },

{  "OPDC Finito2 Time sec",            "OD2TS",     "",    0.5e-3,   rmassTIMESEC,  3276 },
{  "OPDC Finito2 Time usec",           "OD2TUS",    "",    0.5e-3,   rmassTIMEUSEC, 3277 },
{  "OPDC Finito2 Rt Offset",           "OD2OFF",    "",    0.5e-3,   rmassDOUBLE,   3279 },
{  "OPDC Finito2 Fringe det",          "OD2FDET",   "",    0.5e-3,   rmassUINT32,   3280 },
{  "OPDC Finito2 Rt Off val",          "OD2OFFV",   "",    0.5e-3,   rmassUINT32,   3281 },
{  "OPDC Finito2 State",               "OD2ST",     "",    0.5e-3,   rmassUINT32,   3282 },
{  "OPDC Finito2 unwr Phase",          "OD2UPH",    "",    0.5e-3,   rmassDOUBLE,   3283 },
{  "OPDC Finito2 full Off.",           "OD2FOFF",   "",    0.5e-3,   rmassDOUBLE,   3284 },
{  "OPDC Finito2 DL feedback",         "OD2DLFB",   "",    0.5e-3,   rmassDOUBLE,   3285 },
{  "OPDC Finito2 Stp Phase",           "OD2STPH",   "",    0.5e-3,   rmassUINT32,   3286 },
```

```
{  "OPDC Prima Time sec",              "ODPTS",     "",    0.5e-3,   rmassTIMESEC,  3301 },
{  "OPDC Prima Time usec",             "ODPTUS",    "",    0.5e-3,   rmassTIMEUSEC, 3302 },
{  "OPDC Prima Rt Offset",             "ODPOFF",    "",    0.5e-3,   rmassDOUBLE,   3304 },
{  "OPDC Prima Fringe det",            "ODPFDET",   "",    0.5e-3,   rmassUINT32,   3305 },
{  "OPDC Prima Rt Off val",            "ODPOFFV",   "",    0.5e-3,   rmassUINT32,   3306 },
{  "OPDC Prima State",                 "ODPST",     "",    0.5e-3,   rmassUINT32,   3307 },
{  "OPDC Prima unwr Phase",            "ODPUPH",    "",    0.5e-3,   rmassDOUBLE,   3308 },
{  "OPDC Prima full Off.",             "ODPFOFF",   "",    0.5e-3,   rmassDOUBLE,   3309 },
{  "OPDC Prima DL1 feedback",          "ODPDL1FB",  "",    0.5e-3,   rmassDOUBLE,   3310 },
{  "OPDC Prima DL2 feedback",          "ODPDL2FB",  "",    0.5e-3,   rmassDOUBLE,   3311 },
{  "OPDC Prima DL3 feedback",          "ODPDL3FB",  "",    0.5e-3,   rmassDOUBLE,   3312 },
{  "OPDC Prima DL4 feedback",          "ODPDL4FB",  "",    0.5e-3,   rmassDOUBLE,   3313 },
{  "OPDC Prima DL5 feedback",          "ODPDL5FB",  "",    0.5e-3,   rmassDOUBLE,   3314 },
{  "OPDC Prima DL6 feedback",          "ODPDL6FB",  "",    0.5e-3,   rmassDOUBLE,   3315 },
{  "Track DL position setpoint",       "ODPPSP",    "",    0.5e-3,   rmassDOUBLE,   3316 },
{  "Track DL ratelim position",        "ODPRLP",    "",    0.5e-3,   rmassDOUBLE,   3317 },
{  "OPDC Prima Stp Phase",             "ODPSTPH",   "",    0.5e-3,   rmassUINT32,   3318 },


/********************/
/* GRAVITY RMN AREA */
/********************/


/*
 * Gravity Fringe Sensor -> IMAGING_DATA_FT
 */
{  "GR Fringe Sensor Time sec",        "GRFSTS",    "",    0.125e-3,  rmassTIMESEC,  3701 },
{  "GR Fringe Sensor Time usec",       "GRFSTUS",   "",    0.125e-3,  rmassTIMEUSEC, 3702 },

/* 576 pixels all sectors between GRPIX1 and GRPIX576 are used (group rmass write) */
{  "GR Fringe Sensor raw pix 1",       "GRPIX1",    "",    0.125e-3,  rmassINT32,   3704 },
{  "GR Fringe Sensor raw pix 576",     "GRPIX576",  "",    0.125e-3,  rmassINT32,   4279 },

{  "GR Fringe Sensor pd base 1",       "GRFSPD1",   "",    0.125e-3,  rmassFLOAT,    4280 },
{  "GR Fringe Sensor pd base 2",       "GRFSPD2",   "",    0.125e-3,  rmassFLOAT,    4281 },
{  "GR Fringe Sensor pd base 3",       "GRFSPD3",   "",    0.125e-3,  rmassFLOAT,    4282 },
{  "GR Fringe Sensor pd base 4",       "GRFSPD4",   "",    0.125e-3,  rmassFLOAT,    4283 },
{  "GR Fringe Sensor pd base 5",       "GRFSPD5",   "",    0.125e-3,  rmassFLOAT,    4284 },
{  "GR Fringe Sensor pd base 6",       "GRFSPD6",   "",    0.125e-3,  rmassFLOAT,    4285 },

{  "GR Fringe Sensor gd base 1",       "GRFSGD1",   "",    0.125e-3,  rmassFLOAT,    4286 },
{  "GR Fringe Sensor gd base 2",       "GRFSGD2",   "",    0.125e-3,  rmassFLOAT,    4287 },
```

```
{  "GR Fringe Sensor gd base 3",        "GRFSGD3",   "",    0.125e-3,  rmassFLOAT,    4288 },
{  "GR Fringe Sensor gd base 4",        "GRFSGD4",   "",    0.125e-3,  rmassFLOAT,    4289 },
{  "GR Fringe Sensor gd base 5",        "GRFSGD5",   "",    0.125e-3,  rmassFLOAT,    4290 },
{  "GR Fringe Sensor gd base 6",        "GRFSGD6",   "",    0.125e-3,  rmassFLOAT,    4291 },

{  "GR Fringe Sensor noise base 1",     "GRFSNS1",   "",    0.125e-3,  rmassFLOAT,    4292 },
{  "GR Fringe Sensor noise base 2",     "GRFSNS2",   "",    0.125e-3,  rmassFLOAT,    4293 },
{  "GR Fringe Sensor noise base 3",     "GRFSNS3",   "",    0.125e-3,  rmassFLOAT,    4294 },
{  "GR Fringe Sensor noise base 4",     "GRFSNS4",   "",    0.125e-3,  rmassFLOAT,    4295 },
{  "GR Fringe Sensor noise base 5",     "GRFSNS5",   "",    0.125e-3,  rmassFLOAT,    4296 },
{  "GR Fringe Sensor noise base 6",     "GRFSNS6",   "",    0.125e-3,  rmassFLOAT,    4297 },

{  "GR Fringe Sensor SNR base 1",       "GRFSSNR1",  "",    0.125e-3,  rmassFLOAT,    4298 },
{  "GR Fringe Sensor SNR base 2",       "GRFSSNR2",  "",    0.125e-3,  rmassFLOAT,    4299 },
{  "GR Fringe Sensor SNR base 3",       "GRFSSNR3",  "",    0.125e-3,  rmassFLOAT,    4300 },
{  "GR Fringe Sensor SNR base 4",       "GRFSSNR4",  "",    0.125e-3,  rmassFLOAT,    4301 },
{  "GR Fringe Sensor SNR base 5",       "GRFSSNR5",  "",    0.125e-3,  rmassFLOAT,    4302 },
{  "GR Fringe Sensor SNR base 6",       "GRFSSNR6",  "",    0.125e-3,  rmassFLOAT,    4303 },

{  "GR Fringe Sensor Vis base 1",       "GRFSVIS1",  "",    0.125e-3,  rmassFLOAT,    4304 },
{  "GR Fringe Sensor Vis base 2",       "GRFSVIS2",  "",    0.125e-3,  rmassFLOAT,    4305 },
{  "GR Fringe Sensor Vis base 3",       "GRFSVIS3",  "",    0.125e-3,  rmassFLOAT,    4306 },
{  "GR Fringe Sensor Vis base 4",       "GRFSVIS4",  "",    0.125e-3,  rmassFLOAT,    4307 },
{  "GR Fringe Sensor Vis base 5",       "GRFSVIS5",  "",    0.125e-3,  rmassFLOAT,    4308 },
{  "GR Fringe Sensor Vis base 6",       "GRFSVIS6",  "",    0.125e-3,  rmassFLOAT,    4309 },

{  "GR Fringe Sensor flux T1",          "GRFSFLX1",  "",    0.125e-3,  rmassFLOAT,    4310 },
{  "GR Fringe Sensor flux T2",          "GRFSFLX2",  "",    0.125e-3,  rmassFLOAT,    4311 },
{  "GR Fringe Sensor flux T3",          "GRFSFLX3",  "",    0.125e-3,  rmassFLOAT,    4312 },
{  "GR Fringe Sensor flux T4",          "GRFSFLX4",  "",    0.125e-3,  rmassFLOAT,    4313 },

{  "GR Fringe Sensor clo phase PD 1",   "GRFSCLP1",  "",    0.125e-3,  rmassFLOAT,    4314 },
{  "GR Fringe Sensor clo phase PD 2",   "GRFSCLP2",  "",    0.125e-3,  rmassFLOAT,    4315 },
{  "GR Fringe Sensor clo phase PD 3",   "GRFSCLP3",  "",    0.125e-3,  rmassFLOAT,    4316 },
{  "GR Fringe Sensor clo phase PD 4",   "GRFSCLP4",  "",    0.125e-3,  rmassFLOAT,    4317 },

{  "GR Fringe Sensor clo phase GD 1",   "GRFSCLG1",  "",    0.125e-3,  rmassFLOAT,    4318 },
{  "GR Fringe Sensor clo phase GD 2",   "GRFSCLG2",  "",    0.125e-3,  rmassFLOAT,    4319 },
{  "GR Fringe Sensor clo phase GD 3",   "GRFSCLG3",  "",    0.125e-3,  rmassFLOAT,    4320 },
{  "GR Fringe Sensor clo phase GD 4",   "GRFSCLG4",  "",    0.125e-3,  rmassFLOAT,    4321 },


/*
```

```
 * Gravity FDDL controller
 */
{  "GR FDDL Time sec",                "GRDLTS",    "",    0.125e-3,  rmassTIMESEC,  4401 },
{  "GR FDDL Time usec",               "GRDLTUS",   "",    0.125e-3,  rmassTIMEUSEC, 4402 },

{  "GR FDDL FT position sensor 1",    "GRFTPOS1",  "",    0.125e-3,  rmassFLOAT,    4404 },
{  "GR FDDL FT position sensor 2",    "GRFTPOS2",  "",    0.125e-3,  rmassFLOAT,    4405 },
{  "GR FDDL FT position sensor 3",    "GRFTPOS3",  "",    0.125e-3,  rmassFLOAT,     4406 },
{  "GR FDDL FT position sensor 4",    "GRFTPOS4",  "",     0.125e-3,  rmassFLOAT,    4407 },

{  "GR FDDL SC position sensor 1",    "GRSCPOS1",  "",     0.125e-3,  rmassFLOAT,    4408 },
{  "GR FDDL SC position sensor 2",    "GRSCPOS2",  "",     0.125e-3,  rmassFLOAT,    4409 },
{  "GR FDDL SC position sensor 3",    "GRSCPOS3",  "",     0.125e-3,  rmassFLOAT,    4410 },
{  "GR FDDL SC position sensor 4",    "GRSCPOS4",  "",     0.125e-3,  rmassFLOAT,    4411 },

{  "GR Air OPL prediction  1",        "GRDISP1",   "",    0.125e-3,  rmassFLOAT,    4412 },
{  "GR Air OPL prediction  2",        "GRDISP2",   "",    0.125e-3,  rmassFLOAT,    4413 },
{  "GR Air OPL prediction  3",        "GRDISP3",   "",    0.125e-3,  rmassFLOAT,    4414 },
{  "GR Air OPL prediction  4",        "GRDISP4",   "",    0.125e-3,  rmassFLOAT,    4415 },

{  "GR FDDL FT FDDL command  1",      "GRFTDDL1",  "",    0.125e-3,  rmassFLOAT,    4416 },
{  "GR FDDL FT FDDL command  2",      "GRFTDDL2",  "",    0.125e-3,  rmassFLOAT,    4417 },
{  "GR FDDL FT FDDL command  3",      "GRFTDDL3",  "",    0.125e-3,  rmassFLOAT,    4418 },
{  "GR FDDL FT FDDL command  4",      "GRFTDDL4",  "",    0.125e-3,  rmassFLOAT,    4419 },

{  "GR FDDL SC FDDL command  1",      "GRSCDDL1",  "",    0.125e-3,  rmassFLOAT,    4420 },
{  "GR FDDL SC FDDL command  2",      "GRSCDDL2",  "",    0.125e-3,  rmassFLOAT,    4421 },
{  "GR FDDL SC FDDL command  3",      "GRSCDDL3",  "",    0.125e-3,  rmassFLOAT,    4422 },
{  "GR FDDL SC FDDL command  4",       "GRSCDDL4",  "",    0.125e-3,  rmassFLOAT,    4423 },


/*
 * Gravity OPD Controller
 */
{  "GR OPDC Time sec",                "GROPTS",    "",    0.125e-3,  rmassTIMESEC,  4501 },
{  "GR OPDC Time usec",               "GROPTUS",   "",    0.125e-3,  rmassTIMEUSEC, 4502 },

{  "GR OPDC Main State",              "GROPSTAT",  "",    0.125e-3,  rmassUINT32,   4504 },
{  "GR OPDC Modulation",              "GROPMOD",   "",    0.125e-3,  rmassUINT32,   4505 },
{  "GR OPDC System State",            "GROPSYS",   "",    0.125e-3,  rmassUINT32,   4506 },

{  "GR OPDC Piezo Offset 1",          "GROPPZ1",   "",    0.125e-3,  rmassFLOAT,    4507 },
{  "GR OPDC Piezo Offset 2",          "GROPPZ2",   "",    0.125e-3,  rmassFLOAT,    4508 },
```

```
{  "GR OPDC Piezo Offset 3",           "GROPPZ3",   "",    0.125e-3,  rmassFLOAT,    4509 },
{  "GR OPDC Piezo Offset 4",           "GROPPZ4",   "",    0.125e-3,  rmassFLOAT,    4510 },

{  "GR OPDC VLTI DL Offset 1",         "GROPVLT1",   "",    0.125e-3,  rmassFLOAT,    4511 },
{  "GR OPDC VLTI DL Offset 2",         "GROPVLT2",   "",    0.125e-3,  rmassFLOAT,    4512 },
{  "GR OPDC VLTI DL Offset 3",         "GROPVLT3",   "",    0.125e-3,  rmassFLOAT,    4513 },
{  "GR OPDC VLTI DL Offset 4",         "GROPVLT4",   "",    0.125e-3,  rmassFLOAT,    4514 },

{  "GR OPDC Piezo prediction 1",       "GROPKZ1",   "",    0.125e-3,  rmassFLOAT,    4515 },
{  "GR OPDC Piezo prediction 2",       "GROPKZ2",   "",    0.125e-3,  rmassFLOAT,    4516 },
{  "GR OPDC Piezo prediction 3",       "GROPKZ3",   "",    0.125e-3,  rmassFLOAT,    4517 },
{  "GR OPDC Piezo prediction 4",       "GROPKZ4",   "",    0.125e-3,  rmassFLOAT,    4518 },

{  "GR OPDC OPD phase 1",       "GROPPD1",   "",    0.125e-3,  rmassFLOAT,    4519 },
{  "GR OPDC OPD phase 2",              "GROPPD2",   "",    0.125e-3,  rmassFLOAT,    4520 },
{  "GR OPDC OPD phase 3",              "GROPPD3",   "",    0.125e-3,  rmassFLOAT,    4521 },
{  "GR OPDC OPD phase 4",              "GROPPD4",   "",    0.125e-3,  rmassFLOAT,    4522 },
{  "GR OPDC OPD phase 5",              "GROPPD5",   "",    0.125e-3,  rmassFLOAT,    4523 },
{  "GR OPDC OPD phase 6",              "GROPPD6",   "",    0.125e-3,  rmassFLOAT,    4524 },

{  "GR OPDC Kalman prediction 1",      "GROPPR1",   "",    0.125e-3,  rmassFLOAT,    4525 },
{  "GR OPDC Kalman prediction 2",      "GROPPR2",   "",    0.125e-3,  rmassFLOAT,    4526 },
{  "GR OPDC Kalman prediction 3",      "GROPPR3",   "",    0.125e-3,  rmassFLOAT,    4527 },
{  "GR OPDC Kalman prediction 4",      "GROPPR4",   "",    0.125e-3,  rmassFLOAT,    4528 },
{  "GR OPDC Kalman prediction 5",      "GROPPR5",   "",    0.125e-3,  rmassFLOAT,    4529 },
{  "GR OPDC Kalman prediction 6",      "GROPPR6",   "",    0.125e-3,  rmassFLOAT,    4530 },

{  "GR OPDC FDDL Offset 1",            "GROPDL1",   "",    0.125e-3,  rmassFLOAT,    4531 },
{  "GR OPDC FDDL Offset 2",            "GROPDL2",   "",    0.125e-3,  rmassFLOAT,    4532 },
{  "GR OPDC FDDL Offset 3",            "GROPDL3",   "",    0.125e-3,  rmassFLOAT,    4533 },
{  "GR OPDC FDDL Offset 4",            "GROPDL4",   "",    0.125e-3,  rmassFLOAT,    4534 },

{  "GR OPDC OGD phase 1",       "GROPGD1",   "",    0.125e-3,  rmassFLOAT,    4535 },
{  "GR OPDC OGD phase 2",              "GROPGD2",   "",    0.125e-3,  rmassFLOAT,    4536 },
{  "GR OPDC OGD phase 3",              "GROPGD3",   "",    0.125e-3,  rmassFLOAT,    4537 },
{  "GR OPDC OGD phase 4",              "GROPGD4",   "",    0.125e-3,  rmassFLOAT,    4538 },
{  "GR OPDC OGD phase 5",              "GROPGD5",   "",    0.125e-3,  rmassFLOAT,    4539 },
{  "GR OPDC OGD phase 6",              "GROPGD6",   "",    0.125e-3,  rmassFLOAT,    4540 },

{  "GR OPDC OGD closure 1",             "GROPGDC1",   "",    0.125e-3,  rmassFLOAT,    4541 },
{  "GR OPDC OGD closure 2",            "GROPGDC2",   "",    0.125e-3,  rmassFLOAT,    4542 },
{  "GR OPDC OGD closure 3",            "GROPGDC3",   "",    0.125e-3,  rmassFLOAT,    4543 },
{  "GR OPDC OGD closure 4",            "GROPGDC4",   "",    0.125e-3,  rmassFLOAT,    4544 },
```

```
{  "GR OPDC OGD closure 5",          "GROPGDC5",   "",    0.125e-3,  rmassFLOAT,    4545 },
{  "GR OPDC OGD closure 6",          "GROPGDC6",   "",    0.125e-3,  rmassFLOAT,    4546 },

{  "GR OPDC Reference PD 1",         "GROPRPD1",   "",    0.125e-3,  rmassFLOAT,    4547 },
{  "GR OPDC Reference PD 2",         "GROPRPD2",   "",    0.125e-3,  rmassFLOAT,    4548 },
{  "GR OPDC Reference PD 3",         "GROPRPD3",   "",    0.125e-3,  rmassFLOAT,    4549 },
{  "GR OPDC Reference PD 4",         "GROPRPD4",   "",    0.125e-3,  rmassFLOAT,    4550 },

{  "GR OPDC Flux Instant 1",         "GROPFLX1",   "",    0.125e-3,  rmassFLOAT,    4551 },
{  "GR OPDC Flux Instant 2",         "GROPFLX2",   "",    0.125e-3,  rmassFLOAT,    4552 },
{  "GR OPDC Flux Instant 3",         "GROPFLX3",   "",    0.125e-3,  rmassFLOAT,    4553 },
{  "GR OPDC Flux Instant 4",         "GROPFLX4",   "",    0.125e-3,  rmassFLOAT,    4554 },

{  "GR OPDC SNR Instant 1",          "GROPSNR1",   "",    0.125e-3,  rmassFLOAT,    4555 },
{  "GR OPDC SNR Instant 2",          "GROPSNR2",   "",    0.125e-3,  rmassFLOAT,    4556 },
{  "GR OPDC SNR Instant 3",          "GROPSNR3",   "",    0.125e-3,  rmassFLOAT,    4557 },
{  "GR OPDC SNR Instant 4",          "GROPSNR4",   "",    0.125e-3,  rmassFLOAT,    4558 },
{  "GR OPDC SNR Instant 5",          "GROPSNR5",   "",    0.125e-3,  rmassFLOAT,    4559 },
{  "GR OPDC SNR Instant 6",          "GROPSNR6",   "",    0.125e-3,  rmassFLOAT,    4560 },

{  "GR OPDC Kalman weights 1",       "GROPWE1",    "",    0.125e-3,  rmassFLOAT,    4561 },
{  "GR OPDC Kalman weights 2",       "GROPWE2",    "",    0.125e-3,  rmassFLOAT,    4562 },
{  "GR OPDC Kalman weights 3",       "GROPWE3",    "",    0.125e-3,  rmassFLOAT,    4563 },
{  "GR OPDC Kalman weights 4",       "GROPWE4",    "",    0.125e-3,  rmassFLOAT,    4564 },
{  "GR OPDC Kalman weights 5",       "GROPWE5",    "",    0.125e-3,  rmassFLOAT,    4565 },
{  "GR OPDC Kalman weights 6",       "GROPWE6",    "",    0.125e-3,  rmassFLOAT,    4566 },

{  "GR OPDC Flux Smoothed 1",        "GROPFLS1",   "",    0.125e-3,  rmassFLOAT,    4567 },
{  "GR OPDC Flux Smoothed 2",        "GROPFLS2",   "",    0.125e-3,  rmassFLOAT,    4568 },
{  "GR OPDC Flux Smoothed 3",        "GROPFLS3",   "",    0.125e-3,  rmassFLOAT,    4569 },
{  "GR OPDC Flux Smoothed 4",        "GROPFLS4",   "",    0.125e-3,  rmassFLOAT,    4570 },

{  "GR OPDC DL position 1",          "GROPDLP1",   "",    0.125e-3,  rmassFLOAT,    4571 },
{  "GR OPDC DL position 2",          "GROPDLP2",   "",    0.125e-3,  rmassFLOAT,    4572 },
{  "GR OPDC DL position 3",          "GROPDLP3",   "",    0.125e-3,  rmassFLOAT,    4573 },
{  "GR OPDC DL position 4",          "GROPDLP4",   "",    0.125e-3,  rmassFLOAT,    4574 },

{  "GR OPDC Flux Threshold 1",       "GROPFLT1",   "",    0.125e-3,  rmassFLOAT,    4575 },
{  "GR OPDC Flux Threshold 2",       "GROPFLT2",   "",    0.125e-3,  rmassFLOAT,    4576 },
{  "GR OPDC Flux Threshold 3",       "GROPFLT3",   "",    0.125e-3,  rmassFLOAT,    4577 },
{  "GR OPDC Flux Threshold 4",       "GROPFLT4",   "",    0.125e-3,  rmassFLOAT,    4578 },

{  "GR OPDC SNR Smoothed 1",         "GROPSNS1",   "",    0.125e-3,  rmassFLOAT,   4579 },
```

```
{  "GR OPDC SNR Smoothed 2",          "GROPSNS2",   "",    0.125e-3,  rmassFLOAT,     4580 },
{  "GR OPDC SNR Smoothed 3",          "GROPSNS3",   "",    0.125e-3,  rmassFLOAT,     4581 },
{  "GR OPDC SNR Smoothed 4",          "GROPSNS4",   "",    0.125e-3,  rmassFLOAT,     4582 },
{  "GR OPDC SNR Smoothed 5",          "GROPSNS5",   "",    0.125e-3,  rmassFLOAT,     4583 },
{  "GR OPDC SNR Smoothed 6",          "GROPSNS6",   "",    0.125e-3,  rmassFLOAT,     4584 },

{  "GR OPDC SNR Threshold 1",         "GROPSNT1",   "",    0.125e-3,  rmassFLOAT,   4585 },
{  "GR OPDC SNR Threshold 2",         "GROPSNT2",   "",    0.125e-3,  rmassFLOAT,     4586 },
{  "GR OPDC SNR Threshold 3",         "GROPSNT3",   "",    0.125e-3,  rmassFLOAT,     4587 },
{  "GR OPDC SNR Threshold 4",         "GROPSNT4",   "",    0.125e-3,  rmassFLOAT,     4588 },
{  "GR OPDC SNR Threshold 5",         "GROPSNT5",   "",    0.125e-3,  rmassFLOAT,     4589 },
{  "GR OPDC SNR Threshold 6",         "GROPSNT6",   "",    0.125e-3,  rmassFLOAT,     4590 },

{  "GR OPDC SNR Background 1",        "GROPSNB1",   "",    0.125e-3,  rmassFLOAT,   4591 },
{  "GR OPDC SNR Background 2",        "GROPSNB2",   "",    0.125e-3,  rmassFLOAT,     4592 },
{  "GR OPDC SNR Background 3",        "GROPSNB3",   "",    0.125e-3,  rmassFLOAT,     4593 },
{  "GR OPDC SNR Background 4",        "GROPSNB4",   "",    0.125e-3,  rmassFLOAT,     4594 },
{  "GR OPDC SNR Background 5",        "GROPSNB5",   "",    0.125e-3,  rmassFLOAT,     4595 },
{  "GR OPDC SNR Background 6",        "GROPSNB6",   "",    0.125e-3,  rmassFLOAT,     4596 },

{  "GR OPDC Scan Amplitude",          "GROPSCAN",   "",    0.125e-3,  rmassFLOAT,     4597 },


/*
 * Gravity Metrology
 */
{  "GR MET Times sec",                "GRTS",       "",    0.125e-3,  rmassTIMESEC,  4601 },
{  "GR MET Times usec",               "GRTUS",      "",    0.125e-3,  rmassTIMEUSEC, 4602 },

{  "GR MET Data check",               "GRCHK",      "",    0.125e-3,  rmassUINT32,   4604 },

{  "GR MET Volt T1 D1 sin FT",        "GRMV11SF",   "",    0.125e-3,  rmassFLOAT,    4605 },
{  "GR MET Volt T1 D1 cos FT",        "GRMV11CF",   "",    0.125e-3,  rmassFLOAT,    4606 },
{  "GR MET Volt T1 D2 sin FT",        "GRMV12SF",   "",    0.125e-3,  rmassFLOAT,    4607 },
{  "GR MET Volt T1 D2 cos FT",        "GRMV12CF",   "",    0.125e-3,  rmassFLOAT,    4608 },
{  "GR MET Volt T1 D3 sin FT",        "GRMV13SF",   "",    0.125e-3,  rmassFLOAT,    4609 },
{  "GR MET Volt T1 D3 cos FT",        "GRMV13CF",   "",    0.125e-3,  rmassFLOAT,    4610 },
{  "GR MET Volt T1 D4 sin FT",        "GRMV14SF",   "",    0.125e-3,  rmassFLOAT,    4611 },
{  "GR MET Volt T1 D4 cos FT",        "GRMV14CF",   "",    0.125e-3,  rmassFLOAT,    4612 },

{  "GR MET Volt T2 D1 sin FT",        "GRMV21SF",   "",    0.125e-3,  rmassFLOAT,    4613 },
{  "GR MET Volt T2 D1 cos FT",        "GRMV21CF",   "",    0.125e-3,  rmassFLOAT,    4614 },
{  "GR MET Volt T2 D2 sin FT",        "GRMV22SF",   "",    0.125e-3,  rmassFLOAT,    4615 },
```

```
{  "GR MET Volt T2 D2 cos FT",          "GRMV22CF",  "",    0.125e-3,  rmassFLOAT,    4616 },
{  "GR MET Volt T2 D3 sin FT",          "GRMV23SF",  "",    0.125e-3,  rmassFLOAT,    4617 },
{  "GR MET Volt T2 D3 cos FT",          "GRMV23CF",  "",    0.125e-3,  rmassFLOAT,    4618 },
{  "GR MET Volt T2 D4 sin FT",          "GRMV24SF",  "",    0.125e-3,  rmassFLOAT,    4619 },
{  "GR MET Volt T2 D4 cos FT",          "GRMV24CF",  "",    0.125e-3,  rmassFLOAT,    4620 },

{  "GR MET Volt T3 D1 sin FT",          "GRMV31SF",  "",    0.125e-3,  rmassFLOAT,    4621 },
{  "GR MET Volt T3 D1 cos FT",          "GRMV31CF",  "",    0.125e-3,  rmassFLOAT,    4622 },
{  "GR MET Volt T3 D2 sin FT",          "GRMV32SF",  "",    0.125e-3,  rmassFLOAT,    4623 },
{  "GR MET Volt T3 D2 cos FT",          "GRMV32CF",  "",    0.125e-3,  rmassFLOAT,    4624 },
{  "GR MET Volt T3 D3 sin FT",          "GRMV33SF",  "",    0.125e-3,  rmassFLOAT,    4625 },
{  "GR MET Volt T3 D3 cos FT",          "GRMV33CF",  "",    0.125e-3,  rmassFLOAT,    4626 },
{  "GR MET Volt T3 D4 sin FT",          "GRMV34SF",  "",    0.125e-3,  rmassFLOAT,    4627 },
{  "GR MET Volt T3 D4 cos FT",          "GRMV34CF",  "",    0.125e-3,  rmassFLOAT,    4628 },

{  "GR MET Volt T4 D1 sin FT",          "GRMV41SF",  "",    0.125e-3,  rmassFLOAT,    4629 },
{  "GR MET Volt T4 D1 cos FT",          "GRMV41CF",  "",    0.125e-3,  rmassFLOAT,    4630 },
{  "GR MET Volt T4 D2 sin FT",          "GRMV42SF",  "",    0.125e-3,  rmassFLOAT,    4631 },
{  "GR MET Volt T4 D2 cos FT",          "GRMV42CF",  "",    0.125e-3,  rmassFLOAT,    4632 },
{  "GR MET Volt T4 D3 sin FT",          "GRMV43SF",  "",    0.125e-3,  rmassFLOAT,    4633 },
{  "GR MET Volt T4 D3 cos FT",          "GRMV43CF",  "",    0.125e-3,  rmassFLOAT,    4634 },
{  "GR MET Volt T4 D4 sin FT",          "GRMV44SF",  "",    0.125e-3,  rmassFLOAT,    4635 },
{  "GR MET Volt T4 D4 cos FT",          "GRMV44CF",  "",    0.125e-3,  rmassFLOAT,    4636 },

{  "GR MET Volt T1 D1 sin SC",          "GRMV11SS",  "",    0.125e-3,  rmassFLOAT,    4637 },
{  "GR MET Volt T1 D1 cos SC",          "GRMV11CS",  "",    0.125e-3,  rmassFLOAT,    4638 },
{  "GR MET Volt T1 D2 sin SC",          "GRMV12SS",  "",    0.125e-3,  rmassFLOAT,    4639 },
{  "GR MET Volt T1 D2 cos SC",          "GRMV12CS",  "",    0.125e-3,  rmassFLOAT,    4640 },
{  "GR MET Volt T1 D3 sin SC",          "GRMV13SS",  "",    0.125e-3,  rmassFLOAT,    4641 },
{  "GR MET Volt T1 D3 cos SC",          "GRMV13CS",  "",    0.125e-3,  rmassFLOAT,    4642 },
{  "GR MET Volt T1 D4 sin SC",          "GRMV14SS",  "",    0.125e-3,  rmassFLOAT,    4643 },
{  "GR MET Volt T1 D4 cos SC",          "GRMV14CS",  "",    0.125e-3,  rmassFLOAT,    4644 },

{  "GR MET Volt T2 D1 sin SC",          "GRMV21SS",  "",    0.125e-3,  rmassFLOAT,    4645 },
{  "GR MET Volt T2 D1 cos SC",          "GRMV21CS",  "",    0.125e-3,  rmassFLOAT,    4646 },
{  "GR MET Volt T2 D2 sin SC",          "GRMV22SS",  "",    0.125e-3,  rmassFLOAT,    4647 },
{  "GR MET Volt T2 D2 cos SC",          "GRMV22CS",  "",    0.125e-3,  rmassFLOAT,    4648 },
{  "GR MET Volt T2 D3 sin SC",          "GRMV23SS",  "",    0.125e-3,  rmassFLOAT,    4649 },
{  "GR MET Volt T2 D3 cos SC",          "GRMV23CS",  "",    0.125e-3,  rmassFLOAT,    4650 },
{  "GR MET Volt T2 D4 sin SC",          "GRMV24SS",  "",    0.125e-3,  rmassFLOAT,    4651 },
{  "GR MET Volt T2 D4 cos SC",          "GRMV24CS",  "",    0.125e-3,  rmassFLOAT,    4652 },

{  "GR MET Volt T3 D1 sin SC",          "GRMV31SS",  "",    0.125e-3,  rmassFLOAT,    4653 },
```

```
{  "GR MET Volt T3 D1 cos SC",          "GRMV31CS",  "",    0.125e-3,  rmassFLOAT,    4654 },
{  "GR MET Volt T3 D2 sin SC",          "GRMV32SS",  "",    0.125e-3,  rmassFLOAT,    4655 },
{  "GR MET Volt T3 D2 cos SC",          "GRMV32CS",  "",    0.125e-3,  rmassFLOAT,    4656 },
{  "GR MET Volt T3 D3 sin SC",          "GRMV33SS",  "",    0.125e-3,  rmassFLOAT,    4657 },
{  "GR MET Volt T3 D3 cos SC",          "GRMV33CS",  "",    0.125e-3,  rmassFLOAT,    4658 },
{  "GR MET Volt T3 D4 sin SC",          "GRMV34SS",  "",    0.125e-3,  rmassFLOAT,    4659 },
{  "GR MET Volt T3 D4 cos SC",          "GRMV34CS",  "",    0.125e-3,  rmassFLOAT,    4660 },

{  "GR MET Volt T4 D1 sin SC",          "GRMV41SS",  "",    0.125e-3,  rmassFLOAT,    4661 },
{  "GR MET Volt T4 D1 cos SC",          "GRMV41CS",  "",    0.125e-3,  rmassFLOAT,    4662 },
{  "GR MET Volt T4 D2 sin SC",          "GRMV42SS",  "",    0.125e-3,  rmassFLOAT,    4663 },
{  "GR MET Volt T4 D2 cos SC",          "GRMV42CS",  "",    0.125e-3,  rmassFLOAT,    4664 },
{  "GR MET Volt T4 D3 sin SC",          "GRMV43SS",  "",    0.125e-3,  rmassFLOAT,    4665 },
{  "GR MET Volt T4 D3 cos SC",          "GRMV43CS",  "",    0.125e-3,  rmassFLOAT,    4666 },
{  "GR MET Volt T4 D4 sin SC",          "GRMV44SS",  "",    0.125e-3,  rmassFLOAT,    4667 },
{  "GR MET Volt T4 D4 cos SC",          "GRMV44CS",  "",    0.125e-3,  rmassFLOAT,    4668 },

{  "GR MET Volt FC1 sin FT",            "GRMV51SF",  "",     0.125e-3,  rmassFLOAT,    4669 },
{  "GR MET Volt FC1 cos FT",            "GRMV51CF",  "",     0.125e-3,  rmassFLOAT,    4670 },
{  "GR MET Volt FC2 sin FT",            "GRMV52SF",  "",     0.125e-3,  rmassFLOAT,    4671 },
{  "GR MET Volt FC2 cos FT",            "GRMV52CF",  "",     0.125e-3,  rmassFLOAT,    4672 },
{  "GR MET Volt FC3 sin FT",            "GRMV53SF",  "",     0.125e-3,  rmassFLOAT,    4673 },
{  "GR MET Volt FC3 cos FT",            "GRMV53CF",  "",     0.125e-3,  rmassFLOAT,    4674 },
{  "GR MET Volt FC4 sin FT",            "GRMV54SF",  "",     0.125e-3,  rmassFLOAT,    4675 },
{  "GR MET Volt FC4 cos FT",            "GRMV54CF",  "",     0.125e-3,  rmassFLOAT,    4676 },

{  "GR MET Volt FC1 sin SC",            "GRMV51SS",  "",     0.125e-3,  rmassFLOAT,    4677 },
{  "GR MET Volt FC1 cos SC",            "GRMV51CS",  "",     0.125e-3,  rmassFLOAT,    4678 },
{  "GR MET Volt FC2 sin SC",            "GRMV52SS",  "",     0.125e-3,  rmassFLOAT,    4679 },
{  "GR MET Volt FC2 cos SC",            "GRMV52CS",  "",     0.125e-3,  rmassFLOAT,    4680 },
{  "GR MET Volt FC3 sin SC",            "GRMV53SS",  "",     0.125e-3,  rmassFLOAT,    4681 },
{  "GR MET Volt FC3 cos SC",            "GRMV53CS",  "",     0.125e-3,  rmassFLOAT,    4682 },
{  "GR MET Volt FC4 sin SC",            "GRMV54SS",  "",     0.125e-3,  rmassFLOAT,    4683 },
{  "GR MET Volt FC4 cos SC",            "GRMV54CS",  "",     0.125e-3,  rmassFLOAT,    4684 },

{  "GR MET Flag T1 D1 FT",              "GRMF11F",   "",     0.125e-3,  rmassUINT32,   4685 },
{  "GR MET Flag T1 D2 FT",              "GRMF12F",   "",     0.125e-3,  rmassUINT32,   4686 },
{  "GR MET Flag T1 D3 FT",              "GRMF13F",   "",     0.125e-3,  rmassUINT32,   4687 },
{  "GR MET Flag T1 D4 FT",              "GRMF14F",   "",     0.125e-3,  rmassUINT32,   4688 },
{  "GR MET Flag T2 D1 FT",              "GRMF21F",   "",     0.125e-3,  rmassUINT32,   4689 },
{  "GR MET Flag T2 D2 FT",              "GRMF22F",   "",     0.125e-3,  rmassUINT32,   4690 },
{  "GR MET Flag T2 D3 FT",              "GRMF23F",   "",     0.125e-3,  rmassUINT32,   4691 },
{  "GR MET Flag T2 D4 FT",              "GRMF24F",   "",     0.125e-3,  rmassUINT32,   4692 },
```

```
{  "GR MET Flag T3 D1 FT",              "GRMF31F",   "",     0.125e-3,  rmassUINT32,   4693 },
{  "GR MET Flag T3 D2 FT",              "GRMF32F",   "",     0.125e-3,  rmassUINT32,   4694 },
{  "GR MET Flag T3 D3 FT",              "GRMF33F",   "",     0.125e-3,  rmassUINT32,   4695 },
{  "GR MET Flag T3 D4 FT",              "GRMF34F",   "",     0.125e-3,  rmassUINT32,   4696 },
{  "GR MET Flag T4 D1 FT",              "GRMF41F",   "",     0.125e-3,  rmassUINT32,   4697 },
{  "GR MET Flag T4 D2 FT",              "GRMF42F",   "",     0.125e-3,  rmassUINT32,   4698 },
{  "GR MET Flag T4 D3 FT",              "GRMF43F",   "",     0.125e-3,  rmassUINT32,   4699 },
{  "GR MET Flag T4 D4 FT",              "GRMF44F",   "",     0.125e-3,  rmassUINT32,   4700 },

{  "GR MET Flag T1 D1 SC",              "GRMF11S",   "",     0.125e-3,  rmassUINT32,   4701 },
{  "GR MET Flag T1 D2 SC",              "GRMF12S",   "",     0.125e-3,  rmassUINT32,   4702 },
{  "GR MET Flag T1 D3 SC",              "GRMF13S",   "",     0.125e-3,  rmassUINT32,   4703 },
{  "GR MET Flag T1 D4 SC",              "GRMF14S",   "",     0.125e-3,  rmassUINT32,   4704 },
{  "GR MET Flag T2 D1 SC",              "GRMF21S",   "",     0.125e-3,  rmassUINT32,   4705 },
{  "GR MET Flag T2 D2 SC",              "GRMF22S",   "",     0.125e-3,  rmassUINT32,   4706 },
{  "GR MET Flag T2 D3 SC",              "GRMF23S",   "",     0.125e-3,  rmassUINT32,   4707 },
{  "GR MET Flag T2 D4 SC",              "GRMF24S",   "",     0.125e-3,  rmassUINT32,   4708 },
{  "GR MET Flag T3 D1 SC",              "GRMF31S",   "",     0.125e-3,  rmassUINT32,   4709 },
{  "GR MET Flag T3 D2 SC",              "GRMF32S",   "",     0.125e-3,  rmassUINT32,   4710 },
{  "GR MET Flag T3 D3 SC",              "GRMF33S",   "",     0.125e-3,  rmassUINT32,   4711 },
{  "GR MET Flag T3 D4 SC",              "GRMF34S",   "",     0.125e-3,  rmassUINT32,   4712 },
{  "GR MET Flag T4 D1 SC",              "GRMF41S",   "",     0.125e-3,  rmassUINT32,   4713 },
{  "GR MET Flag T4 D2 SC",              "GRMF42S",   "",     0.125e-3,  rmassUINT32,   4714 },
{  "GR MET Flag T4 D3 SC",              "GRMF43S",   "",     0.125e-3,  rmassUINT32,   4715 },
{  "GR MET Flag T4 D4 SC",              "GRMF44S",   "",     0.125e-3,  rmassUINT32,   4716 },

{  "GR MET Flag FC1 FT",                "GRMF51F",    "",    0.125e-3,  rmassUINT32,   4717 },
{  "GR MET Flag FC2 FT",                "GRMF52F",    "",    0.125e-3,  rmassUINT32,   4718 },
{  "GR MET Flag FC3 FT",                "GRMF53F",    "",    0.125e-3,  rmassUINT32,   4719 },
{  "GR MET Flag FC4 FT",                "GRMF54F",    "",    0.125e-3,  rmassUINT32,   4720 },

{  "GR MET Flag FC1 SC",                "GRMF51S",    "",    0.125e-3,  rmassUINT32,   4721 },
{  "GR MET Flag FC2 SC",                "GRMF52S",    "",    0.125e-3,  rmassUINT32,   4722 },
{  "GR MET Flag FC3 SC",                "GRMF53S",    "",    0.125e-3,  rmassUINT32,   4723 },
{  "GR MET Flag FC4 SC",                "GRMF54S",    "",    0.125e-3,  rmassUINT32,   4724 },

{  "GR MET Unwrapped Phase T1 D1 FT",   "GRMP11F",   "",    0.125e-3,  rmassFLOAT,    4725 },
{  "GR MET Unwrapped Phase T1 D2 FT",   "GRMP12F",   "",    0.125e-3,  rmassFLOAT,    4726 },
{  "GR MET Unwrapped Phase T1 D3 FT",   "GRMP13F",   "",    0.125e-3,  rmassFLOAT,    4727 },
{  "GR MET Unwrapped Phase T1 D4 FT",   "GRMP14F",   "",    0.125e-3,  rmassFLOAT,    4728 },
{  "GR MET Unwrapped Phase T2 D1 FT",   "GRMP21F",   "",    0.125e-3,  rmassFLOAT,    4729 },
{  "GR MET Unwrapped Phase T2 D2 FT",   "GRMP22F",   "",    0.125e-3,  rmassFLOAT,    4730 },
{  "GR MET Unwrapped Phase T2 D3 FT",   "GRMP23F",   "",    0.125e-3,  rmassFLOAT,    4731 },
```

```
{  "GR MET Unwrapped Phase T2 D4 FT",   "GRMP24F",   "",    0.125e-3,  rmassFLOAT,    4732 },
{  "GR MET Unwrapped Phase T3 D1 FT",   "GRMP31F",   "",    0.125e-3,  rmassFLOAT,    4733 },
{  "GR MET Unwrapped Phase T3 D2 FT",   "GRMP32F",   "",    0.125e-3,  rmassFLOAT,    4734 },
{  "GR MET Unwrapped Phase T3 D3 FT",   "GRMP33F",   "",    0.125e-3,  rmassFLOAT,    4735 },
{  "GR MET Unwrapped Phase T3 D4 FT",   "GRMP34F",   "",    0.125e-3,  rmassFLOAT,    4736 },
{  "GR MET Unwrapped Phase T4 D1 FT",   "GRMP41F",   "",    0.125e-3,  rmassFLOAT,    4737 },
{  "GR MET Unwrapped Phase T4 D2 FT",   "GRMP42F",   "",    0.125e-3,  rmassFLOAT,    4738 },
{  "GR MET Unwrapped Phase T4 D3 FT",   "GRMP43F",   "",    0.125e-3,  rmassFLOAT,    4739 },
{  "GR MET Unwrapped Phase T4 D4 FT",   "GRMP44F",   "",    0.125e-3,  rmassFLOAT,    4740 },

{  "GR MET Unwrapped Phase T1 D1 SC",   "GRMP11S",   "",    0.125e-3,  rmassFLOAT,    4741 },
{  "GR MET Unwrapped Phase T1 D2 SC",   "GRMP12S",   "",    0.125e-3,  rmassFLOAT,    4742 },
{  "GR MET Unwrapped Phase T1 D3 SC",   "GRMP13S",   "",    0.125e-3,  rmassFLOAT,    4743 },
{  "GR MET Unwrapped Phase T1 D4 SC",   "GRMP14S",   "",    0.125e-3,  rmassFLOAT,    4744 },
{  "GR MET Unwrapped Phase T2 D1 SC",   "GRMP21S",   "",    0.125e-3,  rmassFLOAT,    4745 },
{  "GR MET Unwrapped Phase T2 D2 SC",   "GRMP22S",   "",    0.125e-3,  rmassFLOAT,    4746 },
{  "GR MET Unwrapped Phase T2 D3 SC",   "GRMP23S",   "",    0.125e-3,  rmassFLOAT,    4747 },
{  "GR MET Unwrapped Phase T2 D4 SC",   "GRMP24S",   "",    0.125e-3,  rmassFLOAT,    4748 },
{  "GR MET Unwrapped Phase T3 D1 SC",   "GRMP31S",   "",    0.125e-3,  rmassFLOAT,    4749 },
{  "GR MET Unwrapped Phase T3 D2 SC",   "GRMP32S",   "",    0.125e-3,  rmassFLOAT,    4750 },
{  "GR MET Unwrapped Phase T3 D3 SC",   "GRMP33S",   "",    0.125e-3,  rmassFLOAT,    4751 },
{  "GR MET Unwrapped Phase T3 D4 SC",   "GRMP34S",   "",    0.125e-3,  rmassFLOAT,    4752 },
{  "GR MET Unwrapped Phase T4 D1 SC",   "GRMP41S",   "",    0.125e-3,  rmassFLOAT,    4753 },
{  "GR MET Unwrapped Phase T4 D2 SC",   "GRMP42S",   "",    0.125e-3,  rmassFLOAT,    4754 },
{  "GR MET Unwrapped Phase T4 D3 SC",   "GRMP43S",   "",    0.125e-3,  rmassFLOAT,    4755 },
{  "GR MET Unwrapped Phase T4 D4 SC",   "GRMP44S",   "",    0.125e-3,  rmassFLOAT,    4756 },

{  "GR MET Unwrapped Phase FC1 FT",     "GRMP51F",    "",    0.125e-3,  rmassFLOAT,    4757 },
{  "GR MET Unwrapped Phase FC2 FT",     "GRMP52F",    "",    0.125e-3,  rmassFLOAT,    4758 },
{  "GR MET Unwrapped Phase FC3 FT",     "GRMP53F",    "",    0.125e-3,  rmassFLOAT,    4759 },
{  "GR MET Unwrapped Phase FC4 FT",     "GRMP54F",    "",    0.125e-3,  rmassFLOAT,    4760 },

{  "GR MET Unwrapped Phase FC1 SC",     "GRMP51S",    "",    0.125e-3,  rmassFLOAT,    4761 },
{  "GR MET Unwrapped Phase FC2 SC",     "GRMP52S",    "",    0.125e-3,  rmassFLOAT,    4762 },
{  "GR MET Unwrapped Phase FC3 SC",     "GRMP53S",    "",    0.125e-3,  rmassFLOAT,    4763 },
{  "GR MET Unwrapped Phase FC4 SC",     "GRMP54S",    "",    0.125e-3,  rmassFLOAT,    4764 },

{  "GR MET Laser Power in mV",          "GRMLPO",     "",    0.125e-3,  rmassFLOAT,    4765 },
{  "GR MET Laser Wavelength",           "GRMLWAVE",   "",    0.125e-3,  rmassFLOAT,    4766 },

{  "GR MET OPL T1",                      "GRMOPT1",    "",    0.125e-3,  rmassDOUBLE,   4767 },
{  "GR MET OPL T2",                      "GRMOPT2",    "",    0.125e-3,  rmassDOUBLE,   4768 },
{  "GR MET OPL T3",                      "GRMOPT3",    "",    0.125e-3,  rmassDOUBLE,   4769 },
```

```
{  "GR MET OPL T4",                    "GRMOPT4",    "",    0.125e-3,  rmassDOUBLE,   4770 },
{  "GR MET OPL FC1",            "GRMOPF1",    "",    0.125e-3,  rmassDOUBLE,   4771 },
{  "GR MET OPL FC2",            "GRMOPF2",    "",    0.125e-3,  rmassDOUBLE,   4772 },
{  "GR MET OPL FC3",            "GRMOPF3",    "",    0.125e-3,  rmassDOUBLE,   4773 },
{  "GR MET OPL FC4",            "GRMOPF4",    "",    0.125e-3,  rmassDOUBLE,   4774 },


/*
 * Gravity Kalman workstation
 */
{  "GR Kalman Time sec" ,              "GRKALTS" ,  "",    0.125e-3,  rmassTIMESEC,  4801 },
{  "GR Kalman Time usec",              "GRKALTUS",  "",    0.125e-3,  rmassTIMEUSEC, 4802 },

{  "GR Kalman State",                  "GRKAST",    "",    0.125e-3,  rmassUINT32,   4804 },

{  "GR Kalman turbulence TF    1",     "GRKAA1",    "",    0.125e-3,  rmassFLOAT,    4805 },
{  "GR Kalman turbulence TF    31",    "GRKAA31",   "",    0.125e-3,  rmassFLOAT,    4835 },
{  "GR Kalman turbulence TF    61",    "GRKAA61",   "",    0.125e-3,  rmassFLOAT,    4865 },
{  "GR Kalman turbulence TF    91",    "GRKAA91",   "",    0.125e-3,  rmassFLOAT,    4895 },
{  "GR Kalman turbulence TF    121",   "GRKAA121",  "",    0.125e-3,  rmassFLOAT,    4925 },
{  "GR Kalman turbulence TF    151",   "GRKAA151",  "",    0.125e-3,  rmassFLOAT,    4955 },
{  "GR Kalman turbulence TF    180",   "GRKAA180",  "",    0.125e-3,  rmassFLOAT,    4984 },

{  "GR Kalman turb feedback   1",      "GRKAF1",    "",    0.125e-3,  rmassFLOAT,    4985 },
{  "GR Kalman turb feedback   31",     "GRKAF31",   "",    0.125e-3,  rmassFLOAT,    5015 },
{  "GR Kalman turb feedback   61",     "GRKAF61",   "",    0.125e-3,  rmassFLOAT,    5045 },
{  "GR Kalman turb feedback   91",     "GRKAF91",   "",    0.125e-3,  rmassFLOAT,    5075 },
{  "GR Kalman turb feedback   121",    "GRKAF121",  "",    0.125e-3,  rmassFLOAT,    5105 },
{  "GR Kalman turb feedback   151",    "GRKAF151",  "",    0.125e-3,  rmassFLOAT,    5135 },
{  "GR Kalman turb feedback   180",    "GRKAF180",  "",    0.125e-3,  rmassFLOAT,    5164 },

{  "GR Kalman turb gain 1",            "GRKAG1",    "",    0.125e-3,  rmassFLOAT,    5165 },
{  "GR Kalman turb gain 31",           "GRKAG31",   "",    0.125e-3,  rmassFLOAT,    5195 },
{  "GR Kalman turb gain 61",           "GRKAG61",   "",    0.125e-3,  rmassFLOAT,    5225 },
{  "GR Kalman turb gain 91",           "GRKAG91",   "",    0.125e-3,  rmassFLOAT,    5255 },
{  "GR Kalman turb gain 121",          "GRKAG121",  "",    0.125e-3,  rmassFLOAT,    5285 },
{  "GR Kalman turb gain 151",          "GRKAG151",  "",    0.125e-3,  rmassFLOAT,    5315 },
{  "GR Kalman turb gain 180",          "GRKAG180",  "",    0.125e-3,  rmassFLOAT,    5344 },

{  "GR Kalman piezo TF  1",            "GRKAC1",    "",    0.125e-3,  rmassFLOAT,    5345 },
{  "GR Kalman piezo TF 20",            "GRKAC20",   "",    0.125e-3,  rmassFLOAT,    5364 },
```

```
/*
 * Gravity Tip Tilt Piston LCU
 */
/* rabuter added for Timing Tests*/
{  "GR TTP Time sec" ,                "GRTTPTS" ,  "",    0.125e-3,  rmassTIMESEC,  5601 },
{  "GR TTP Time usec",                "GRTTPUS" ,  "",    0.125e-3,  rmassTIMEUSEC, 5602 },

{  "GR TTP T1 Tip",                   "GRTTPX1" ,  "",    0.125e-3,  rmassFLOAT,    5604 },
{  "GR TTP T1 Tilt",                  "GRTTPY1" ,  "",    0.125e-3,  rmassFLOAT,    5605 },
{  "GR TTP T1 Piston",                "GRTTPZ1" ,  "",    0.125e-3,  rmassFLOAT,    5606 },

{  "GR TTP T2 Tip",                   "GRTTPX2" ,  "",    0.125e-3,  rmassFLOAT,    5607 },
{  "GR TTP T2 Tilt",                  "GRTTPY2" ,  "",    0.125e-3,  rmassFLOAT,    5608 },
{  "GR TTP T2 Piston",                "GRTTPZ2" ,  "",    0.125e-3,  rmassFLOAT,    5609 },

{  "GR TTP T3 Tip",                   "GRTTPX3" ,  "",    0.125e-3,  rmassFLOAT,    5610 },
{  "GR TTP T3 Tilt",                  "GRTTPY3" ,  "",    0.125e-3,  rmassFLOAT,    5611 },
{  "GR TTP T3 Piston",                "GRTTPZ3" ,  "",    0.125e-3,  rmassFLOAT,    5612 },

{  "GR TTP T4 Tip",                   "GRTTPX4" ,  "",    0.125e-3,  rmassFLOAT,    5613 },
{  "GR TTP T4 Tilt",                  "GRTTPY4" ,  "",    0.125e-3,  rmassFLOAT,    5614 },
{  "GR TTP T4 Piston",                "GRTTPZ4" ,  "",    0.125e-3,  rmassFLOAT,    5615 },
/* rabuter added for Timing Tests*/

/* tott added for Laser Guiding Tests */
{  "GR TTP T1 PSD X",                  "GRPSDX1" ,  "",    0.125e-3,  rmassFLOAT,    5616 },
{  "GR TTP T1 PSD Y",                  "GRPSDY1" ,  "",    0.125e-3,  rmassFLOAT,    5617 },
{  "GR TTP T1 PSD sum",                "GRPSDS1" ,  "",    0.125e-3,  rmassFLOAT,    5618 },

{  "GR TTP T2 PSD X",                  "GRPSDX2" ,  "",    0.125e-3,  rmassFLOAT,    5619 },
{  "GR TTP T2 PSD Y",                  "GRPSDY2" ,  "",    0.125e-3,  rmassFLOAT,    5620 },
{  "GR TTP T2 PSD sum",                "GRPSDS2" ,  "",    0.125e-3,  rmassFLOAT,    5621 },

{  "GR TTP T3 PSD X",                  "GRPSDX3" ,  "",    0.125e-3,  rmassFLOAT,    5622 },
{  "GR TTP T3 PSD Y",                  "GRPSDY3" ,  "",    0.125e-3,  rmassFLOAT,    5623 },
{  "GR TTP T3 PSD sum",                "GRPSDS3" ,  "",    0.125e-3,  rmassFLOAT,    5624 },

{  "GR TTP T4 PSD X",                  "GRPSDX4" ,  "",    0.125e-3,  rmassFLOAT,    5625 },
{  "GR TTP T4 PSD Y",                  "GPSDY4" ,   "",    0.125e-3,  rmassFLOAT,    5626 },
{  "GR TTP T4 PSD sum",                "GRPSDS4" ,  "",    0.125e-3,  rmassFLOAT,    5627 },
/* tott added for Laser Guiding Tests */
```

```
    /********************/
    /* MATISSE RMN AREA */
    /********************/


    /*
     * MATISSE L-band
     */
    { "MATISSE L-band Times sec",           "MTLTS",      "",   1e-2,      rmassTIMESEC, 8001 },
    { "MATISSE L-band Times microsec",      "MTLTUS",     "",   1e-2,      rmassTIMEUSEC,      8002
},
    { "MATISSE L-band Frame index",         "MTLFRX",     "",   1e-2,      rmassINT32,     8003 },
    { "MATISSE L-band Trk-OK-flag DL bm 1", "MTLTRK1",    "",   1e-2,      rmassUINT32,   8004 },
    { "MATISSE L-band Trk-OK-flag DL bm 2", "MTLTRK2",    "",   1e-2,      rmassUINT32,   8005 },
    { "MATISSE L-band Trk-OK-flag DL bm 3", "MTLTRK3",    "",   1e-2,      rmassUINT32,   8006 },
    { "MATISSE L-band Trk-OK-flag DL bm 4", "MTLTRK4",    "",   1e-2,      rmassUINT32,  8007 },
    { "MATISSE L-band State-machine",       "MTLFSM",     "",   1e-2,      rmassUINT32,   8008 },
    { "MATISSE L-band Offset to DL bm 1",   "MTLOFFS1",   "",   1e-2,      rmassDOUBLE,   8009 },
    { "MATISSE L-band Offset to DL bm 2",   "MTLOFFS2",   "",   1e-2,      rmassDOUBLE,   8010 },
    { "MATISSE L-band Offset to DL bm 3",   "MTLOFFS3",   "",   1e-2,      rmassDOUBLE,   8011 },
    { "MATISSE L-band Offset to DL bm 4",   "MTLOFFS4",   "",   1e-2,      rmassDOUBLE,   8012 },
    { "MATISSE L-band DL pos beam 1",       "MTLDLPS1",   "",   1e-2,      rmassDOUBLE,   8013 },
    { "MATISSE L-band DL pos beam 2",       "MTLDLPS2",   "",   1e-2,      rmassDOUBLE,   8014 },
    { "MATISSE L-band DL pos beam 3",       "MTLDLPS3",   "",   1e-2,      rmassDOUBLE,   8015 },
    { "MATISSE L-band DL pos beam 4",       "MTLDLPS4",   "",   1e-2,      rmassDOUBLE,   8016 },
    { "MATISSE L-band Piston baseline 1",   "MTLPIS1",    "",   1e-2,      rmassDOUBLE,   8017 },
    { "MATISSE L-band Piston baseline 2",   "MTLPIS2",    "",   1e-2,      rmassDOUBLE,   8018 },
    { "MATISSE L-band Piston baseline 3",   "MTLPIS3",    "",   1e-2,      rmassDOUBLE,   8019 },
    { "MATISSE L-band Piston baseline 4",   "MTLPIS4",    "",   1e-2,      rmassDOUBLE,   8020 },
    { "MATISSE L-band Piston baseline 5",   "MTLPIS5",    "",   1e-2,      rmassDOUBLE,   8021 },
    { "MATISSE L-band Piston baseline 6",   "MTLPIS6",    "",   1e-2,      rmassDOUBLE,   8022 },
    { "MATISSE L-band SNR baseline 1",      "MTLSNR1",    "",   1e-2,      rmassDOUBLE,   8023 },
    { "MATISSE L-band SNR baseline 2",      "MTLSNR2",    "",   1e-2,      rmassDOUBLE,   8024 },
    { "MATISSE L-band SNR baseline 3",      "MTLSNR3",    "",   1e-2,      rmassDOUBLE,   8025 },
    { "MATISSE L-band SNR baseline 4",      "MTLSNR4",    "",   1e-2,      rmassDOUBLE,   8026 },
    { "MATISSE L-band SNR baseline 5",      "MTLSNR5",    "",   1e-2,      rmassDOUBLE,   8027 },
    { "MATISSE L-band SNR baseline 6",      "MTLSNR6",    "",   1e-2,      rmassDOUBLE,   8028 },
    { "MATISSE L-band IRIS bm 1 offset X",  "MTLIR1X",    "",   1e-2,      rmassDOUBLE,   8029 },
    { "MATISSE L-band IRIS bm 1 offset Y",  "MTLIR1Y",    "",   1e-2,      rmassDOUBLE,   8030 },
    { "MATISSE L-band IRIS bm 2 offset X",  "MTLIR2X",    "",   1e-2,      rmassDOUBLE,    8031 },
    { "MATISSE L-band IRIS bm 2 offset Y",  "MTLIR2Y",    "",   1e-2,      rmassDOUBLE,   8032 },
    { "MATISSE L-band IRIS bm 3 offset X",  "MTLIR3X",    "",   1e-2,      rmassDOUBLE,   8033 },
    { "MATISSE L-band IRIS bm 3 offset Y",  "MTLIR3Y",    "",   1e-2,      rmassDOUBLE,   8034 },
```

```
    { "MATISSE L-band IRIS bm 4 offset X",  "MTLIR4X",    "",   1e-2,      rmassDOUBLE,   8035 },
    { "MATISSE L-band IRIS bm 4 offset Y",  "MTLIR4Y",    "",   1e-2,      rmassDOUBLE,   8036 },
    { "MATISSE L-band MACAO WF error UT1",  "MTLMCW1",    "",   1e-2,      rmassDOUBLE,   8037 },
    { "MATISSE L-band MACAO WF valid UT1",  "MTLMCWV1",   "",   1e-2,      rmassUINT32,   8038 },
    { "MATISSE L-band MACAO WF error UT2",  "MTLMCW2",    "",   1e-2,      rmassDOUBLE,   8039 },
    { "MATISSE L-band MACAO WF valid UT2",  "MTLMCWV2",   "",   1e-2,      rmassUINT32,   8040 },
    { "MATISSE L-band MACAO WF error UT3",  "MTLMCW3",    "",   1e-2,      rmassDOUBLE,   8041 },
    { "MATISSE L-band MACAO WF valid UT3",  "MTLMCWV3",   "",   1e-2,      rmassUINT32,   8042 },
    { "MATISSE L-band MACAO WF error UT4",  "MTLMCW4",    "",   1e-2,      rmassDOUBLE,   8043 },
    { "MATISSE L-band MACAO WF valid UT4",  "MTLMCWV4",   "",   1e-2,      rmassUINT32,   8044 },

    /*
     * MATISSE N-band
     */
    { "MATISSE N-band Times sec",           "MTNTS",      "",   1e-2,      rmassTIMESEC, 8101 },
    { "MATISSE N-band Times microsec",      "MTNTUS",     "",   1e-2,      rmassTIMEUSEC,      8102
},
    { "MATISSE N-band Frame index",         "MTNFRX",     "",   1e-2,      rmassINT32,     8103 },
    { "MATISSE N-band Trk-OK-flag DL bm 1", "MTNTRK1",    "",   1e-2,      rmassUINT32,   8104 },
    { "MATISSE N-band Trk-OK-flag DL bm 2", "MTNTRK2",    "",   1e-2,      rmassUINT32,   8105 },
    { "MATISSE N-band Trk-OK-flag DL bm 3", "MTNTRK3",    "",   1e-2,      rmassUINT32,   8106 },
    { "MATISSE N-band Trk-OK-flag DL bm 4", "MTNTRK4",    "",   1e-2,      rmassUINT32,  8107 },
    { "MATISSE N-band State-machine",       "MTNFSM",     "",   1e-2,      rmassUINT32,   8108 },
    { "MATISSE N-band Offset to DL bm 1",   "MTNOFFS1",   "",   1e-2,      rmassDOUBLE,   8109 },
    { "MATISSE N-band Offset to DL bm 2",   "MTNOFFS2",   "",   1e-2,      rmassDOUBLE,   8110 },
    { "MATISSE N-band Offset to DL bm 3",   "MTNOFFS3",   "",   1e-2,      rmassDOUBLE,   8111 },
    { "MATISSE N-band Offset to DL bm 4",   "MTNOFFS4",   "",   1e-2,      rmassDOUBLE,   8112 },
    { "MATISSE N-band DL pos beam 1",       "MTNDLPS1",   "",   1e-2,      rmassDOUBLE,   8113 },
    { "MATISSE N-band DL pos beam 2",       "MTNDLPS2",   "",   1e-2,      rmassDOUBLE,   8114 },
    { "MATISSE N-band DL pos beam 3",       "MTNDLPS3",   "",   1e-2,      rmassDOUBLE,   8115 },
    { "MATISSE N-band DL pos beam 4",       "MTNDLPS4",   "",   1e-2,      rmassDOUBLE,   8116 },
    { "MATISSE N-band Piston baseline 1",   "MTNPIS1",    "",   1e-2,      rmassDOUBLE,   8117 },
    { "MATISSE N-band Piston baseline 2",   "MTNPIS2",    "",   1e-2,      rmassDOUBLE,   8118 },
    { "MATISSE N-band Piston baseline 3",   "MTNPIS3",    "",   1e-2,      rmassDOUBLE,   8119 },
    { "MATISSE N-band Piston baseline 4",   "MTNPIS4",    "",   1e-2,      rmassDOUBLE,   8120 },
    { "MATISSE N-band Piston baseline 5",   "MTNPIS5",    "",   1e-2,      rmassDOUBLE,   8121 },
    { "MATISSE N-band Piston baseline 6",   "MTNPIS6",    "",   1e-2,      rmassDOUBLE,   8122 },
    { "MATISSE N-band SNR baseline 1",      "MTNSNR1",    "",   1e-2,      rmassDOUBLE,   8123 },
    { "MATISSE N-band SNR baseline 2",      "MTNSNR2",    "",   1e-2,      rmassDOUBLE,   8124 },
    { "MATISSE N-band SNR baseline 3",      "MTNSNR3",    "",   1e-2,      rmassDOUBLE,   8125 },
    { "MATISSE N-band SNR baseline 4",      "MTNSNR4",    "",   1e-2,      rmassDOUBLE,   8126 },
    { "MATISSE N-band SNR baseline 5",      "MTNSNR5",    "",   1e-2,      rmassDOUBLE,   8127 },
    { "MATISSE N-band SNR baseline 6",      "MTNSNR6",    "",   1e-2,      rmassDOUBLE,   8128 },
```

```
    { "MATISSE N-band IRIS bm 1 offset X",  "MTNIR1X",    "",   1e-2,      rmassDOUBLE,   8129 },
    { "MATISSE N-band IRIS bm 1 offset Y",  "MTNIR1Y",    "",   1e-2,      rmassDOUBLE,   8130 },
    { "MATISSE N-band IRIS bm 2 offset X",  "MTNIR2X",    "",   1e-2,      rmassDOUBLE,    8131 },
    { "MATISSE N-band IRIS bm 2 offset Y",  "MTNIR2Y",    "",   1e-2,      rmassDOUBLE,   8132 },
    { "MATISSE N-band IRIS bm 3 offset X",  "MTNIR3X",    "",   1e-2,      rmassDOUBLE,   8133 },
    { "MATISSE N-band IRIS bm 3 offset Y",  "MTNIR3Y",    "",   1e-2,      rmassDOUBLE,   8134 },
    { "MATISSE N-band IRIS bm 4 offset X",  "MTNIR4X",    "",   1e-2,      rmassDOUBLE,   8135 },
    { "MATISSE N-band IRIS bm 4 offset Y",  "MTNIR4Y",    "",   1e-2,      rmassDOUBLE,   8136 },
    { "MATISSE N-band MACAO WF error UT1",  "MTNMCW1",    "",   1e-2,      rmassDOUBLE,   8137 },
    { "MATISSE N-band MACAO WF valid UT1",  "MTNMCWV1",   "",   1e-2,      rmassUINT32,   8138 },
    { "MATISSE N-band MACAO WF error UT2",  "MTNMCW2",    "",   1e-2,      rmassDOUBLE,   8139 },
    { "MATISSE N-band MACAO WF valid UT2",  "MTNMCWV2",   "",   1e-2,      rmassUINT32,   8140 },
    { "MATISSE N-band MACAO WF error UT3",  "MTNMCW3",    "",   1e-2,      rmassDOUBLE,   8141 },
    { "MATISSE N-band MACAO WF valid UT3",  "MTNMCWV3",   "",   1e-2,      rmassUINT32,   8142 },
    { "MATISSE N-band MACAO WF error UT4",  "MTNMCW4",    "",   1e-2,      rmassDOUBLE,   8143 },
    { "MATISSE N-band MACAO WF valid UT4",  "MTNMCWV4",   "",   1e-2,      rmassUINT32,   8144 },



    /* last Entry */
    { "", "", "", 0.0, rmassEND_OF_TABLE, 0 }
};

#endif /* RMASS_LAYOUT_H */
```

17. Annex D: statistics of the pupil motion due to hysteresis

Hysteresis is estimated once per week for each DL from Delirium data taken with the carriage moving in both directions. For 6 years of data we calculated the motion of the pupil due to hysteresis when the carriage is at 10 m (VCM with small curvature) in Figure 42 and 110 m (VCM with large curvature) in Figure 43.

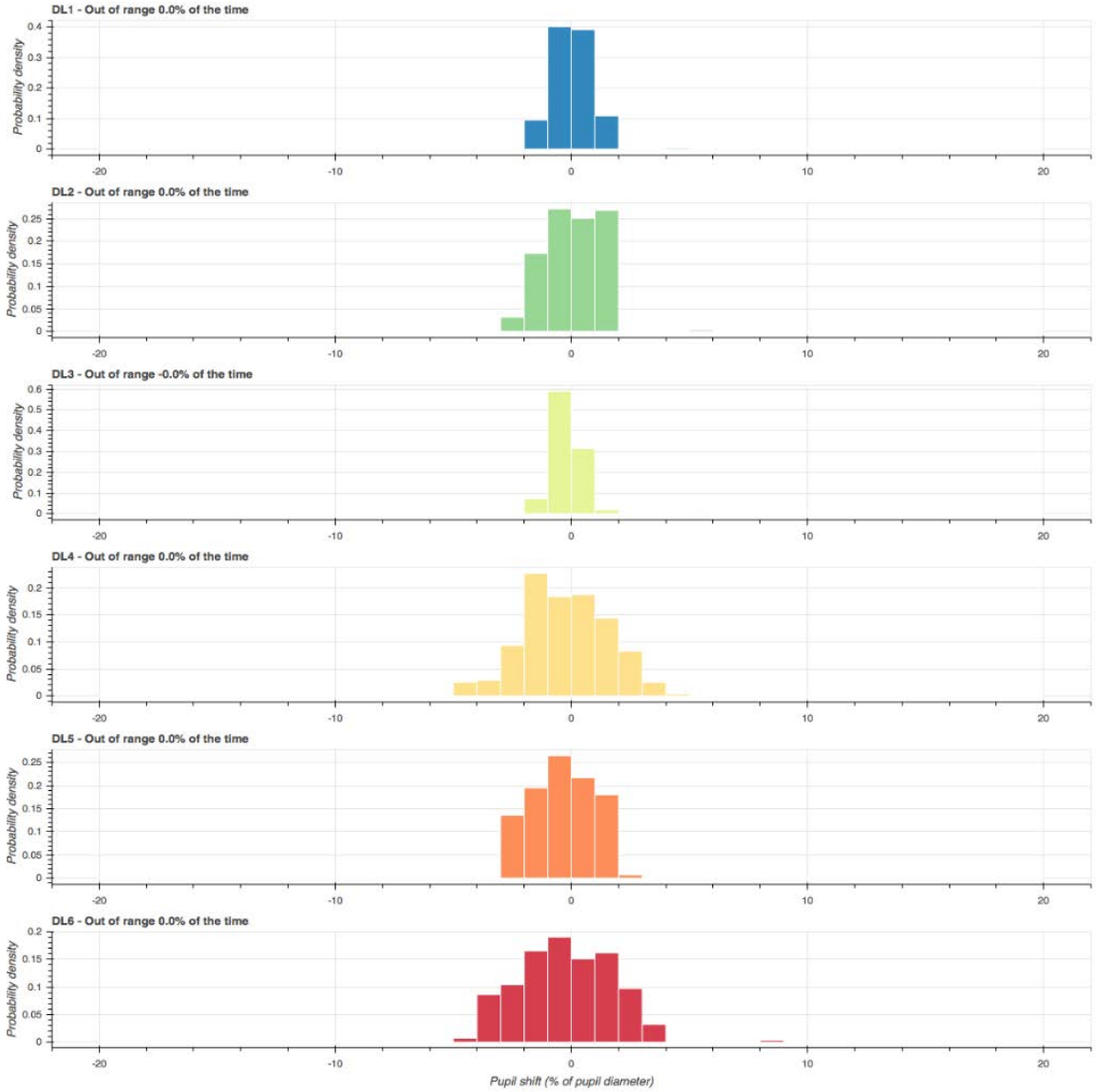

Figure 42: probability density of the pupil shift created by the hysteresis of the carriage for the carriage at 10 m OPL.

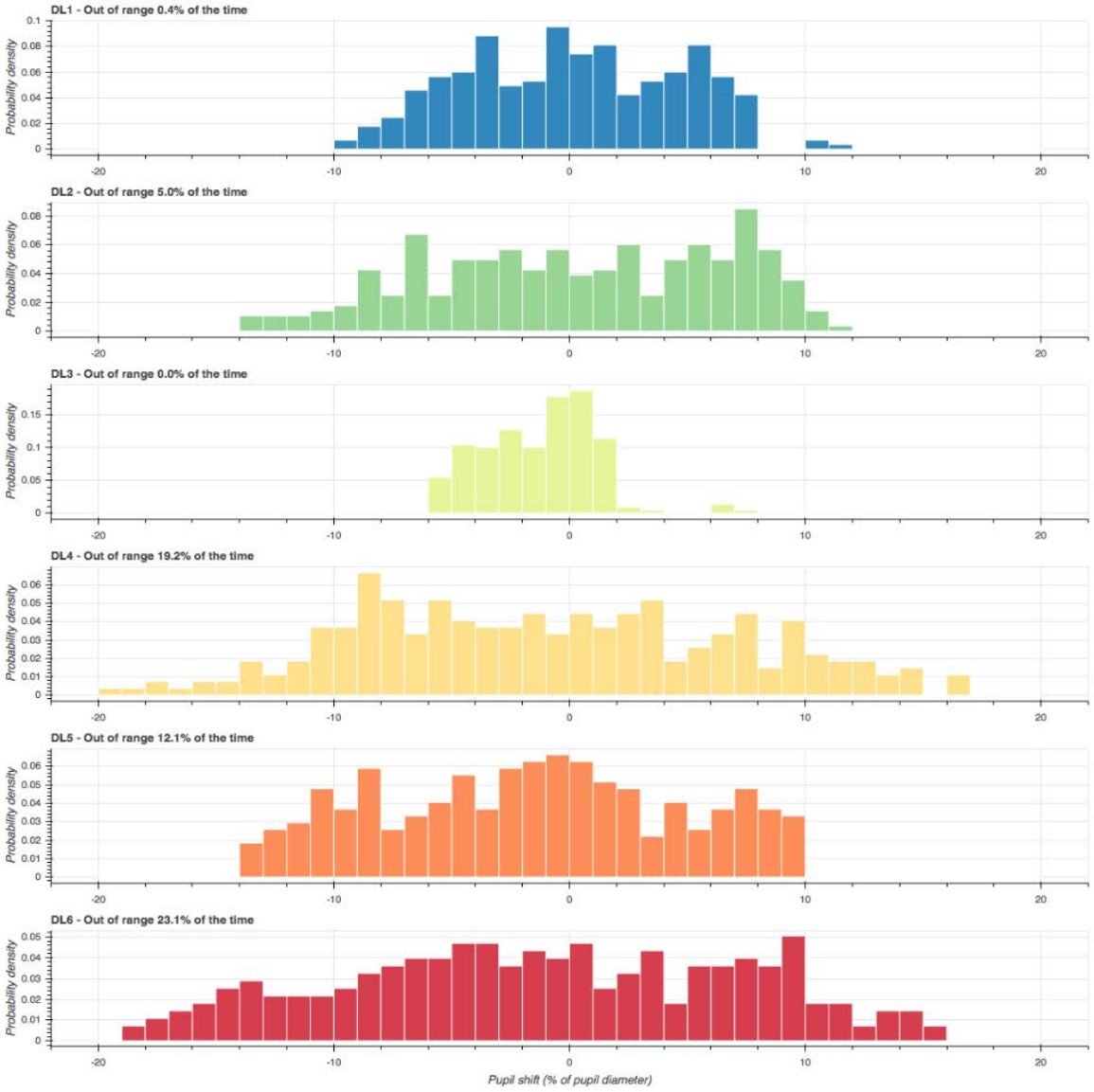

Figure 43: probability density of the pupil shift created by the hysteresis of the carriage for the carriage at 110 m OPL.

18. Annex E: Infrared transmission monitoring

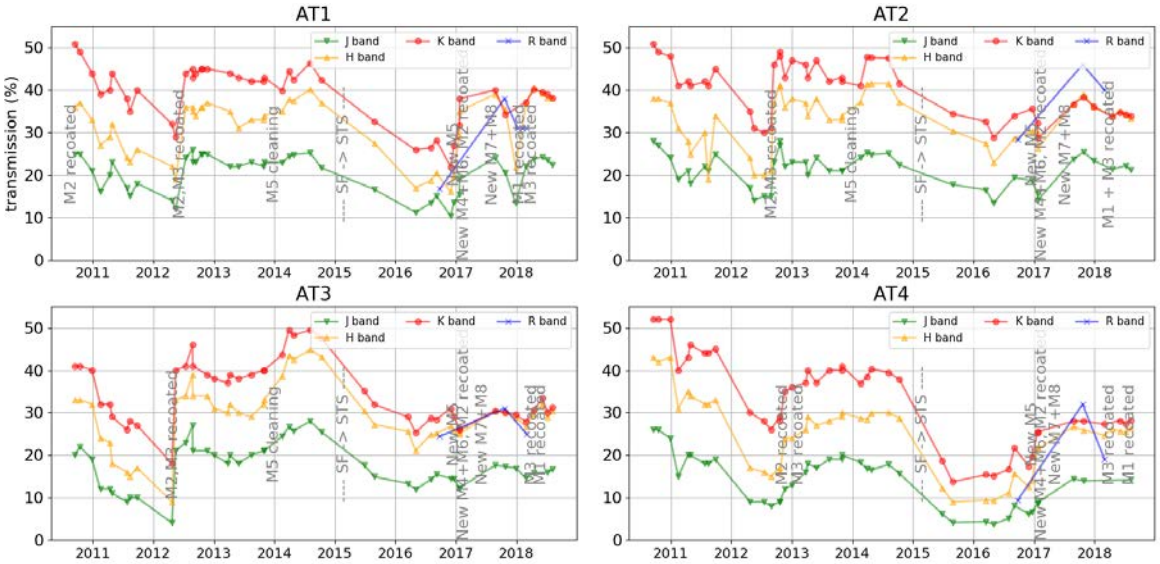

Table 67: infrared transmission of the VLTI with the ATs (ratio of photons after reflection on the switchyard to the number of photons reaching the AT M1).

VLTI arm configuration	J band	H band	K band
UT1-DL5-Q2	0.173 ± 0.023	0.314 ± 0.042	0.371 ± 0.041
UT2-DL2-Q1	0.165 ± 0.030	0.319 ± 0.048	0.365 ± 0.049
UT3-DL3-Q3	0.134 ± 0.014	0.259 ± 0.024	0.307 ± 0.017
UT4-DL4-Q4	0.193 ± 0.043	0.359 ± 0.051	0.390 ± 0.041

Table 68: last measurement of the UT infrared transmission (ratio of photons after reflection on the switchyard to the number of photons reaching the UT M1).

19. Annex F: coolant datasheet

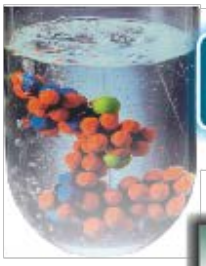

Biochemical

www.biochemical.cl

BIOCOOLANT HVAC-MA

REFRIGERANTE Y FLUIDO DE TRANSFERENCIA DE CALOR CON ACCIÓN MICROBIOCIDA Y ALGUICIDA

BIOCOOLANT HVAC-MA es un refrigerante industrial y fluido de transferencia de calor y frío base glicol que incorpora un paquete de inhibidores de corrosión y biocidas para la protección de las superficies de transferencia de calor manteniéndolas libre de fouling, depósitos de sales y al ataque de. la corrosión.

BIOCOOLANT HVAC-MA es el fluido refrigerante que satisface los requerimientos de protección frente al ataque corrosivo a los metales, a la deposición de sales, a daños por cavitación y erosión de sistemas que trabajan con agua para la: calefacción, refrigeración, ventilación cerrada, compresores, calentadores, aire acondicionado, sistema HVAC, etc.

BIOCOOLANT HVAC-MA provee un excelente medio a la transferencia del calor

- Aumenta el punto de ebullición de la mezcla refrigerante disminuyendo la posibilidad de recalentamiento.
- Baja el punto de congelación, evitando en invierno las posibilidades de roturas de cañerías, radiadores, etc.

BIOCOOLANT HVAC-MA tiene un rango de operación de temperaturas entre –50°C (-60°F) y 120°C (250°F)

VENTAJAS

- Excelente protección al congelamiento y ebullición.
- Excelente protección a la corrosión de los metales: bronce, cobre, acero, hierro, aluminio, y otros metales comúnmente encontrados en sistemas acuosos de calefacción y refrigeración.
- Evita la formación de incrustaciones debido a aguas duras .
- Mantiene las superficies de transferencia de calor limpias y protegidas a la corrosión y el fouling.
- Larga vida del fluido y bajos costos de mantencion.
- Análisis de control producto.

VALPARAISO: G. Escala 1077 - 14 - Fono: (32) 2287096 • **ANTOFAGASTA • RANCAGUA • CONCEPCION**

--- End of document ---